

GEOLOGY OF THE BLOODY BASIN:  
CENTRAL ARIZONA'S TRANSITION ZONE

by

Gwyn Rhys-Evans

A Thesis Presented in Partial Fulfillment  
Of the Requirements for the Degree  
Master of Science

ARIZONA STATE UNIVERSITY

DECEMBER 2006

GEOLOGY OF THE BLOODY BASIN:  
CENTRAL ARIZONA'S TRANSITION ZONE

by

Gwyn Rhys-Evans

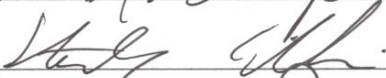
has been approved

September 2006

APPROVED:



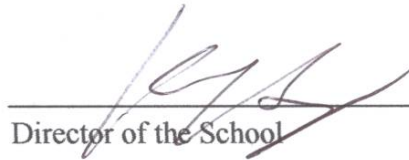
\_\_\_\_\_, Chair





Supervisory Committee

ACCEPTED:



\_\_\_\_\_  
Director of the School



\_\_\_\_\_  
Dean, Division of Graduate Studies

## ABSTRACT

New geologic mapping in the Bloody Basin of central Arizona's Transition Zone reveals two distinct sets of normal faults that have a nearly 90° orientation with respect to one another. Miocene Hickey basalt unconformably overlies the Verde River granite that together makes a sequence of rocks that has been dissected into a series of tilted fault blocks. Regionally anomalous, northeast-striking normal faulting resulted in a synthetic array of half-grabens that are locally filled with a volcanoclastic conglomerate grading into a granite-rich conglomerate. These northeast-striking faults are thought to be influenced by a preexisting Precambrian structure that has been defined by aeromagnetic studies as the Holbrook lineament. This lineament projects directly through the Bloody Basin and would explain, at least in part, the origin of these anomalously oriented faults. Following this northwest-southeast directed extension, a dominant northeast-southwest extension direction resulted in a more regionally pervasive pattern of northwest-striking normal faults, including the Verde fault that cross-cuts the previously formed set. The least principal stress direction required for development of these extensional features is that which currently exists within the Colorado Plateau, northeast-southwest directed. The resultant thinned upper crust due to this extension gave way to the emplacement of a suite of mafic dikes that intruded basin-filling material shed during the first tectonic event.

Timing of the first event is constrained to between 13.5 and 8 Ma, the age of tilted Hickey basalt and Miocene movement along the cross-cutting Verde fault, respectively. This timing is coeval with the Basin and Range Disturbance; however, characteristics that help to define this event do not wholly agree with what is observed in the Bloody Basin.

A pulse of local northwest-southeast directed extension may have swept through the area giving rise to the infant Bloody Basin, which was then cut short by extension created possibly by crustal buoyancy forces related to the Colorado Plateau.

Because the Bloody Basin lacks detailed geologic mapping, a nexus is provided that connects previous studies in the region. A synthesis of these studies has led to a better understanding of extensional tectonic events and how they are manifested in the Transition Zone of central Arizona. Continued efforts into filling voids through detailed geologic mapping such as this, will provide a better understanding as to the fundamental framework of such a unique region.

## ACKNOWLEDGMENTS

I would like to thank my advisor Dr. Edmund Stump for suggesting what amounted to be a rewarding and challenging project, shrouded by the ominous name: The Bloody Basin. I had many unique and branding experiences in the Bloody Basin and I have Ed to thank for these. I would also like to express my gratitude towards him for partially funding this project. I would also like to thank my supervisory committee, Dr. Stephen J. Reynolds and Dr. Stan Williams for their time and efforts. Special thanks to Dr. Williams for his determination and willingness to see me through last minute issues. Special thanks also goes to Doug Greene for putting together and leading an adventurous trip down the 'wild' stretch of the Verde River. Without his generosity, some parts of this country would have never been seen by myself. Additionally, I would like to thank Patty Fetter of the US Forest Service for the many insights during the river trip and also for playing a major role in use of equipment. I would also like to thank Marivel Linares of the US Forest Service for her patience and helpfulness in allowing me to use and acquire the air-photos of the Bloody Basin, this saved many long hours of hiking. I would also like to thank the Department of Geology (now the School of Earth and Space Exploration) at ASU for partial funding of this project. Special thanks to my friends and family for all of their support. Finally, I would like to thank my wife for allowing me to pursue this goal in my life and for supporting me throughout thick and thin, and with an extraordinary amount of support.

## TABLE OF CONTENTS

	Page
LIST OF FIGURES.....	vii
LIST OF PLATES.....	x
INTRODUCTION .....	1
METHOD OF STUDY.....	6
GEOLOGIC SETTING .....	8
Regional.....	8
Local .....	10
PREVIOUS STUDIES.....	12
MAP UNIT DESCRIPTIONS .....	16
Stratigraphy .....	17
Precambrian Units .....	18
Tertiary Units.....	22
Quaternary Units.....	45
PETROGRAPHY .....	48
Sample Locations .....	49
Precambrian Units .....	50
Tertiary Units.....	54
Summary Table.....	64
STRUCTURE .....	65
Precambrian.....	65
Tertiary .....	67

Northeast Trending Faults .....	68
Amount of Extension .....	77
Timing.....	77
Northwest Trending Faults.....	78
Verde Fault.....	83
Amount of Extension .....	88
Timing.....	88
Reverse and Strike-slip Faulting .....	89
Timing.....	91
Dikes.....	91
Timing.....	93
Tertiary Dome .....	93
DISCUSSION.....	95
Least Principal Stress Direction .....	95
Fault Orientation and Regional Considerations.....	99
Fault-Block Widths.....	106
Relations to Basin and Range Disturbance.....	108
Conclusions .....	109
TERTIARY HISTORY .....	112
REFERENCES .....	116

## LIST OF FIGURES

Figure	Page
1. Physiographic provinces of Arizona.....	2
2. Location of study area.....	4
3. 2004 ASTER satellite image of the Bloody Basin and vicinity.....	7
4. Map showing locations of previous studies conducted in the vicinity of the Bloody Basin .....	13
5. Representative stratigraphy from four locations in the Bloody Basin.....	17
6. Field photographs of Precambrian chlorite-mica schist.....	19
7. Field photograph of Precambrian Verde granite.....	21
8. Field photograph of Tertiary volcanics overlying older conglomerate (Toc).....	24
9. Field photograph of confined Tertiary older conglomerate (Toc).....	25
10. Field photograph of regionally tilted Tertiary volcanics .....	28
11. Field photograph of Tertiary mudstone .....	30
12. Field photograph of Tertiary tuff overlying Tertiary conglomerate .....	32
13. Field photograph of Tertiary conglomerate (Tc <sub>1</sub> ).....	34
14. Field photograph of Tertiary conglomerate (Tc <sub>2</sub> ).....	36
15. Field photograph of Tertiary younger sediments.....	38
16. Field photograph of Tertiary granite conglomerate .....	40
17. Field photograph of angular unconformity showing horizontal basin fill overlying gently dipping Tertiary volcanics .....	41
18. Field photographs of Tertiary dome; including brecciated margins and flow banding .....	43

19. Field photograph of steeply dipping Tertiary dike .....	46
20. Map showing locations of sample collections for petrographic analysis .....	49
21. Photomicrograph of Precambrian chlorite-mica schist.....	51
22. Photomicrograph of Precambrian Verde River granite .....	53
23. Photomicrographs of interlocking aggregate and trachytic textures observed in Tertiary volcanics.....	56
24. Photomicrograph of Tertiary tuff.....	58
25. Photomicrograph of Tertiary mudstone .....	60
26. Photomicrograph of representative Tertiary dike .....	62
27. Photomicrograph of Tertiary dome.....	63
28. Map showing locations of structures observed in the Bloody Basin.....	66
29. Field photographs showing vertical trace of Pine Mountain fault and a segment displaying the steeply dipping nature .....	70
30. Field photograph of northeast-striking fault intersected by a northwest-striking fault .....	71
31. Field photograph of volcanic breccia at the Marble Mine.....	71
32. Field photographs of North Red Creek fault with striations along the plane .....	73
33. Stereogram of data for northeast-striking faults .....	76
34. Field photograph of offset northwest striking fault along Forest Service Road 24...	79
35. Simplified cross-section from B to B' .....	81
36. Field photograph of mineral lineations on granite footwall of Red Creek fault.....	82
37. Field photographs of Verde fault .....	84
38. Field photograph of steeply dipping Precambrian bedding .....	86

39. Stereogram of data for northwest-striking faults .....	87
40. Field photographs of strike-slip faulting in the Bloody Basin; including lineations .	90
41. Stereogram of data for dike orientations.....	92
42. Map showing synthesis of faults in the area from past studies.....	101
43. Stereogram showing the combination of data for northwest and northeast-striking faults.....	103
44. Map showing general locations of magnetic anomalies on the Colorado Plateau...	105
45. Map showing locations of basins in the Transition Zone .....	107
46. Diagrammatic summary of the Tertiary history of the Bloody Basin .....	115

## LIST OF PLATES

Plate

1. Geologic map of the Bloody Basin

## INTRODUCTION

Central Arizona is a topographically and geologically diverse region within a transition zone that crosses the State of Arizona between two other physiographically distinct provinces: the northern Colorado Plateau and the southern and western Basin and Range (Figure 1). The Colorado Plateau occupies portions of four southwestern states; Arizona, Utah, Colorado, and New Mexico. In Arizona, the Colorado Plateau is broadly characterized by relatively flat-lying, Paleozoic and Mesozoic sedimentary strata with relatively little structural deformation (Reynolds, 1988). The Basin and Range, spanning much of the western United States and vast portions of southern and western Arizona, is characterized regionally by block-faulted mountains (Eberly and Stanley, 1978) that are discontinuous and generally trend northwest- to northeast. The ranges developed due to this block faulting have been subsequently isolated by sediment filled basins (Menges and Pearthree, 1989). The Transition Zone, that separates the two, is generally characterized by horst-block mountain ranges, volcanic mountains, grabens, half-graben basins (Hendricks and Plescia, 1991), and plateau remnants (Menges and Pearthree, 1989). It is a zone that qualifies as a legitimate transition, because it contains features that characterize the other two provinces.

Detailed geologic mapping and petrographic analysis of areas in the Transition Zone are greatly limited and subsequently hinder our ability to fully understand this region. Although geophysical surveys have been conducted across this northwest-trending swath (e.g., West et al., 2004; Parsons et al., 1996; Warren, 1969) for understanding crustal thicknesses and isostatic equilibrium of the plateau, these studies need to be supplemented by detailed bedrock mapping and structural analysis to broaden

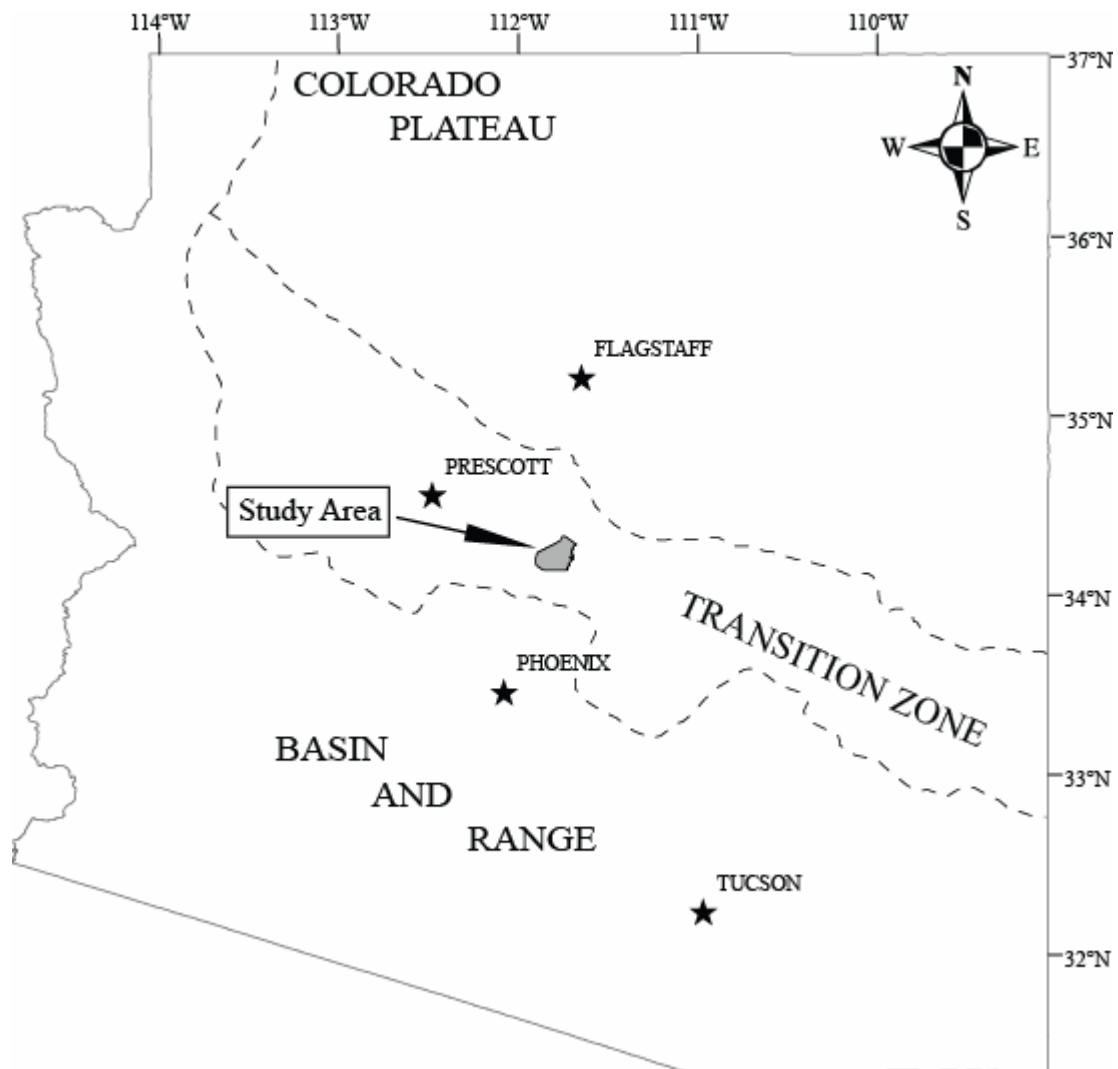


**Figure 1. General map of the State of Arizona showing the approximate extent of the three main physiographic provinces that are recognized.**

our understanding as to the evolution of the region. With these types of studies, such questions as how this region has responded to tectonic stress interaction between the relatively coherent Colorado Plateau and the highly extended Basin and Range can be answered. Additionally, detailed studies may offer insight as to the extent of deformational events such as the Basin and Range disturbance or even the Mid-Tertiary orogeny. Because of these needs, new geologic mapping has been completed in the Bloody Basin and vicinity of the central Transition Zone (Figure 1).

The Bloody Basin study area is located within the Tonto National Forest and is approximately 100 km north of Phoenix, Arizona in Yavapai County (Figure 2). This area referred to as the central Transition Zone by Leighty (1997), lies on the southwest margin of the Colorado Plateau and is locally bounded to the north by the Pine Mountain Wilderness area and to the east by the Mazatzal Wilderness area (Figure 2). The focus of the geologic mapping and accompanying research was concentrated on Tertiary evolution of the basin proper and surrounding area; however, Precambrian rocks are well exposed in the area and undoubtedly aided in the breadth of understanding. In addition to a new geologic map, a link has been provided to other geologic maps (see Previous Work Section) that have been previously constructed in the surrounding areas, such as Pine Mountain Wilderness (Canney et al. 1967), Mazatzal Wilderness (Wrucke and Conway, 1987) and the Rover Peak quadrangle (Brand, 2005). Brand's (2005) study linked geologic maps in the New River Mesa, Humboldt Mountain, and Horseshoe Dam quadrangle's (see Ferguson et al., 1998; Gilbert et al., 1998; and Ferguson et al., 1999; respectively). This new study, in concert with those just mentioned provides the

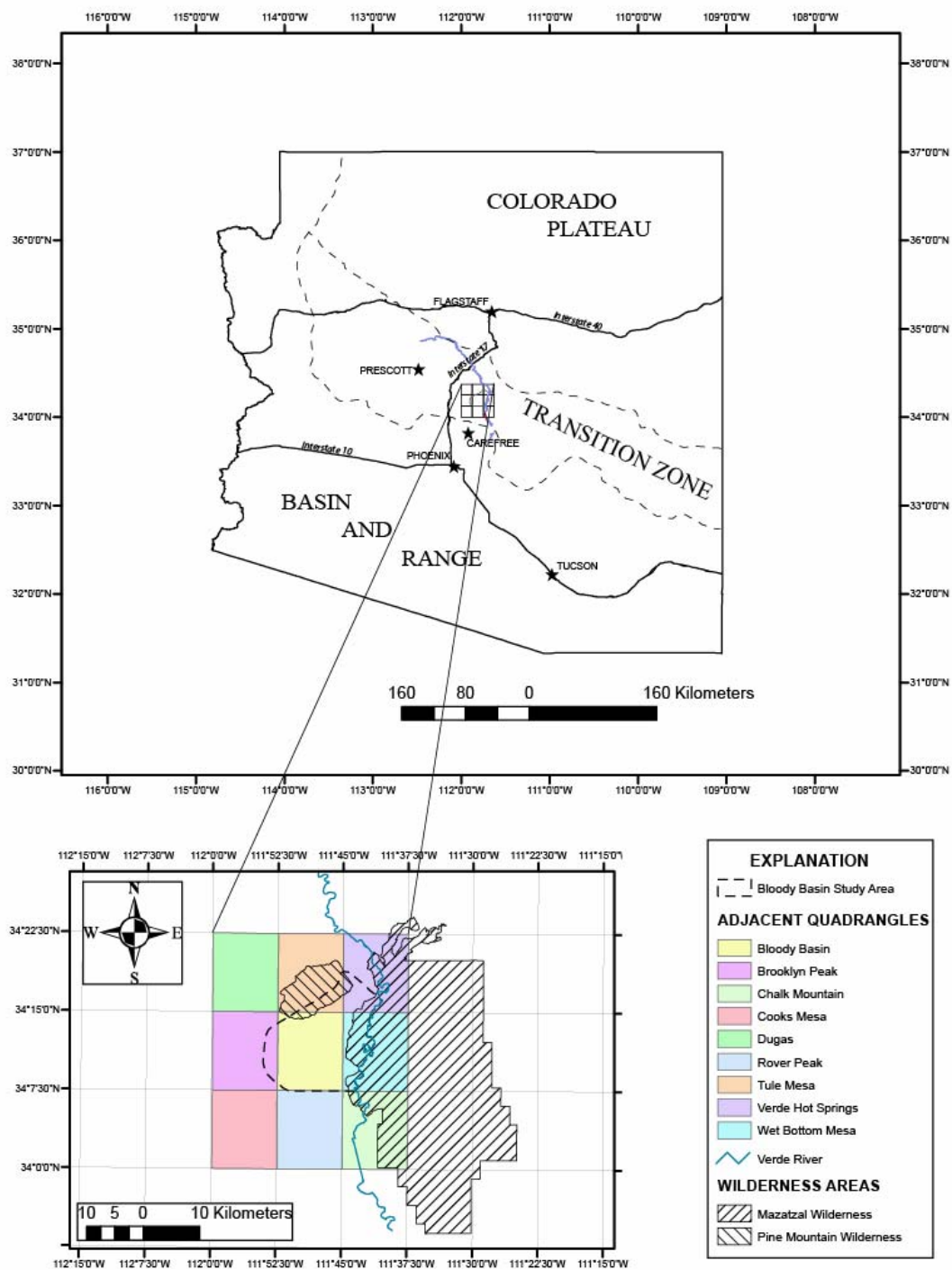


**Figure 2. Location map of the Bloody Basin study area. Note the study area is within the central Transition Zone.**

foundation for a broader tectonic understanding of the central Transition Zone that should lead to more insight into the evolution of this diverse region.

## **METHOD OF STUDY**

The following is a brief description of the methods used during the course of research conducted in the Bloody Basin:

1. The primary research effort was to construct an approximately 200 km<sup>2</sup> geologic map of the Bloody Basin area at a scale of 1:24,000. Some complicated areas required mapping at 1:10,000 for better understanding. Base topographic maps used were 1:24,000 USGS, 7.5' quadrangles: Bloody Basin, Brooklyn Peak, Tule Mesa, and Wet Bottom Mesa. The completed field maps were compiled using ArcMap 9.1.
2. Field mapping was supported with satellite image interpretation (Figure 3). 1:24,000 color aerial photographs which were provided by the United States Forest Service provided stereoscopic coverage of the area.
3. A six day kayak trip on the Verde River through the Mazatzal Wilderness was required to access portions of the Roadless area in the wilderness, that otherwise were inaccessible.
4. Thirty thin-sections from representative geologic units were used for petrographic identification.

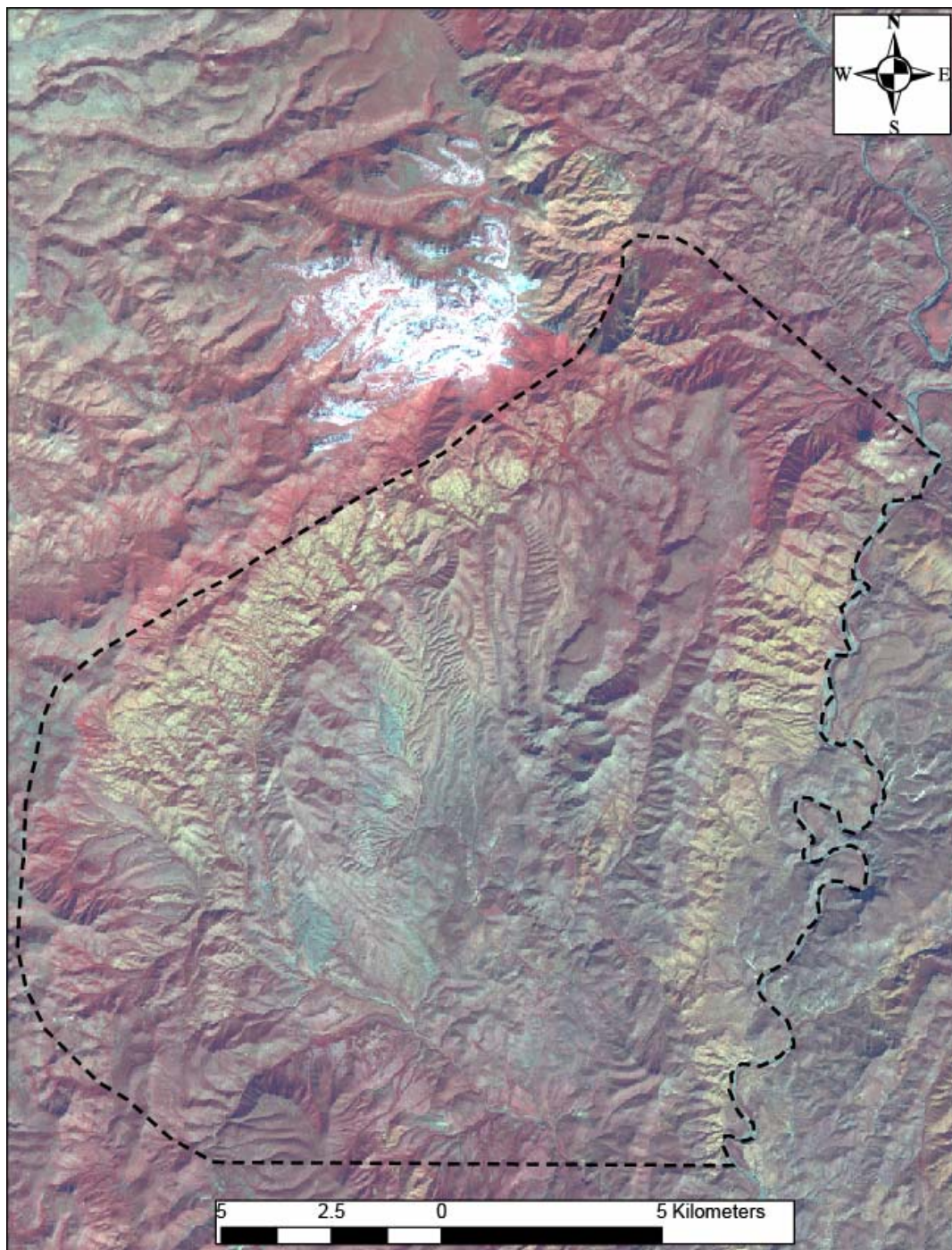


**Figure 3.** 2004 ASTER image used for coarse interpretation then supported by field reconnaissance. Yellow bands are granite bodies that subsequently helped delineate faulting in the area. Verde fault is well-recognized as the linear expression cutting across the northeast corner of the image. Dashed line is the approximate boundary of the study area. Source: [www.geoinformaticsnetwork.org/swgeonet/](http://www.geoinformaticsnetwork.org/swgeonet/)

## **GEOLOGIC SETTING**

### *Regional Overview*

As previously noted, Arizona contains portions of three physiographic provinces that make up the landscape of the American southwest (see Figure 1); Basin and Range, Colorado Plateau and Transition Zone. The Basin and Range and Colorado Plateau contain unique characteristics that distinguish each as a separate province. The Transition Zone contains characteristics of both the Basin and Range and Colorado Plateau and therefore offers a unique insight in regards to the interaction of the bounding provinces.

The Arizona Basin and Range physiography is due partly to the Basin and Range Disturbance (Menges and Pearthree, 1989), an event that resulted in extensional block faulting between 14 – 5 Ma ( Shafiqullah et al., 1980) and possibly beginning as young as 13 – 12 Ma (Eberly and Stanley, 1978). This event is now manifested by northwest trending pediment ranges, bounded by moderate to high angle normal faults and separated by deep valley alluvium (Eberly and Stanley, 1978). Range blocks that make up these pediments may be tilted as documented in Nevada (Stewart, 1981) although this characteristic is largely undocumented in Arizona (Menges and Pearthrees, 1989). Additionally, the fault zones that comprise these alluvial basins are generally structural boundaries of grabens or tilted half-grabens and fault block ranges (Stewart, 1998). Basin dimensions range from 10 km to locally up to 50 km wide with the amount of extension between 10 – 20% of original (Stewart, 1998).

The Colorado Plateau is described as a coherent block surrounded on three sides by the extensional block faulted regimes of the Basin and Range province and the Rio Grande Rift (Thompson and Zoback, 1979). This “coherent block” has elevations that range from 1200 m in its eroded center to 2600 m along several of its margins, with an average elevation of 2000 m (Chase et. al., 2002). Additionally, this elevation equates to approximately 1.2 km of uplift relative to the surrounding provinces (e.g. Chase et al., 2002). Geologically, the plateau consists of thick sequences of Paleozoic and Mesozoic strata that are generally flat-lying or sub-horizontal (Reynolds, 1988). The interior of the Arizona portion of the plateau is, for the most part, surficially structureless with some noted monoclines. Scarce northwest trending faults exist adjacent to the Colorado Plateau and Transition Zone boundary (Reynolds, 1988).

The Transition Zone, regionally speaking, is a zone of transitional structures as wide as 150 km between the Colorado Plateau and the Basin and Range province (Stewart, 1998). As seen on the state geologic map (Reynolds, 1988) the Transition Zone is roughly 70 to 80 km wide in central Arizona and trends northwest-southeast. The Transition Zone contains structures that are characteristic of both the Colorado Plateau and Basin and Range provinces (Stewart, 1998). The Bloody Basin lies within this Transition Zone.

### *Local Overview*

The Bloody Basin study area is just beyond the southern margin of the Pine Mountain Wilderness area, which is the south end of the Black Hills, a north- to northwest-trending footwall block of the Verde fault. The geology of the Black Hills has been studied extensively by Canney et al. (1968), Anderson and Creasy (1958) and from studies in the adjoining Verde Valley by Twenter and Metzger (1963). The geology of the southern Black Hills consist of Precambrian granites, gneisses, and metamorphic mafic rocks unconformably overlain by either Paleozoic sediments of Tapeats Sandstone, Martin Limestone, and remnant patches of Mississippian Redwall Limestone or directly overlain by Cenozoic volcanic rocks, whereby the Paleozoic have been stripped through erosion (Canney et al., 1968). The Black Hills are extensively faulted throughout and bounded to the east by the Verde fault zone and to the west by the Coyote/Shylock fault zones (Twenter and Metzger, 1963).

To the east of the study area lie the Mazatzal Mountains within the Mazatzal Wilderness area. The Mazatzal Wilderness is occupied by four stratified sequences of Proterozoic metasedimentary or metasedimentary and metavolcanic rocks, including the East Verde River Formation and the Tonto Basin Supergroup and, as Wrucke and Conway (1987) state, few areas in Arizona expose so many well preserved sections of layered Proterozoic rocks. These rocks are commonly intruded by the Gibson Creek Batholith and the Diamond Rim Intrusive Suite of various granite, aplite and intrusive rhyolite (Wrucke and Conway, 1987). These Proterozoic rocks record the folding and

thrusting from the Mazatzal orogeny originally mapped by Wilson (1939). The Mazatzal Wilderness also contains Paleozoic Tapeats Sandstone, Martin Formation, Mississippian Redwall Limestone and Naco Formation that overlie the Proterozoic basement described above. Tertiary sedimentary and volcanic rocks are exposed here in the Verde River valley and north of the East Verde River (Wrukke and Conway, 1987). Additionally, Wrukke and Conway (1987) note conspicuous north- and northwest-trending faults as well as the north-trending Verde River graben that overlaps into the current study.

To the south of the Bloody Basin, in the Rover Peak quadrangle, Precambrian basement granite and metamorphic rocks are overlain by Tertiary sediment and volcanic rocks (Brand, 2005) with no preserved Paleozoic rocks. Brand (2005) identified major north-northwest trending faults with east-side-down motion that were active later than 13.5 Ma, the  $^{40}\text{Ar}/^{39}\text{Ar}$  dates obtained from tilted basalts in the area. Additionally, Brand (2005) noted a younger flat-lying volcanic unit that caps these tilted basalts. Ages obtained from these rocks by  $^{40}\text{Ar}/^{39}\text{Ar}$  yielded ages around 6.4 Ma.

Finally, to the west of the study area is the Aqua Fria National Monument which can broadly be characterized as containing Precambrian granites and metamorphic rocks that are generally overlain by Tertiary sediment and volcanic rocks. It is worth noting that the western rim of the Bloody Basin is generally flat-lying to sub-horizontal and appears to be largely unextended.

## **PREVIOUS STUDIES**

New geologic mapping in the Bloody Basin area ties in three other geologic maps surrounding the project area (Figure 4). Mapping has been completed to the north within the Pine Mountains Wilderness (Canney et al., 1967), to the east within the Mazatzal Wilderness (Wrucke and Conway, 1987) and to the south within the Cedar Mountains (Brand, 2005). The western boundary remains unmapped at any significant detail. The Bloody Basin area has also received attention in terms of reconnaissance mapping and coarse stratigraphic correlations. (Leighty, 1997; Nations, 1982; Elston, 1984). The Verde River corridor bounds the project area to the east, and was mapped in terms of river terrace chronology by Pearthree (1993). The following is a brief overview of these studies.

Canney et al. (1967) studied the Pine Mountain Wilderness area (Figure 4) in order to evaluate the mineral potential. Their studies reveal Precambrian, Paleozoic and Tertiary rocks that occupy this location. Major northeast-trending, normal faults are observed here with offset noted between Tertiary and Precambrian rocks. They also reveal another set of faults with orthogonal orientation, including the Verde fault, and cite a separate faulting event responsible for this generation. The Pine Mountain Wilderness was studied and mapped at a scale of 1:31,680. Overlap of the current study and the Pine Mountain study occurs to the north of the Bloody Basin proper.

To the east, Wrucke and Conway (1987) mapped the adjacent Mazatzal Wilderness and Contiguous Roadless Area. Their efforts were focused on the mineral

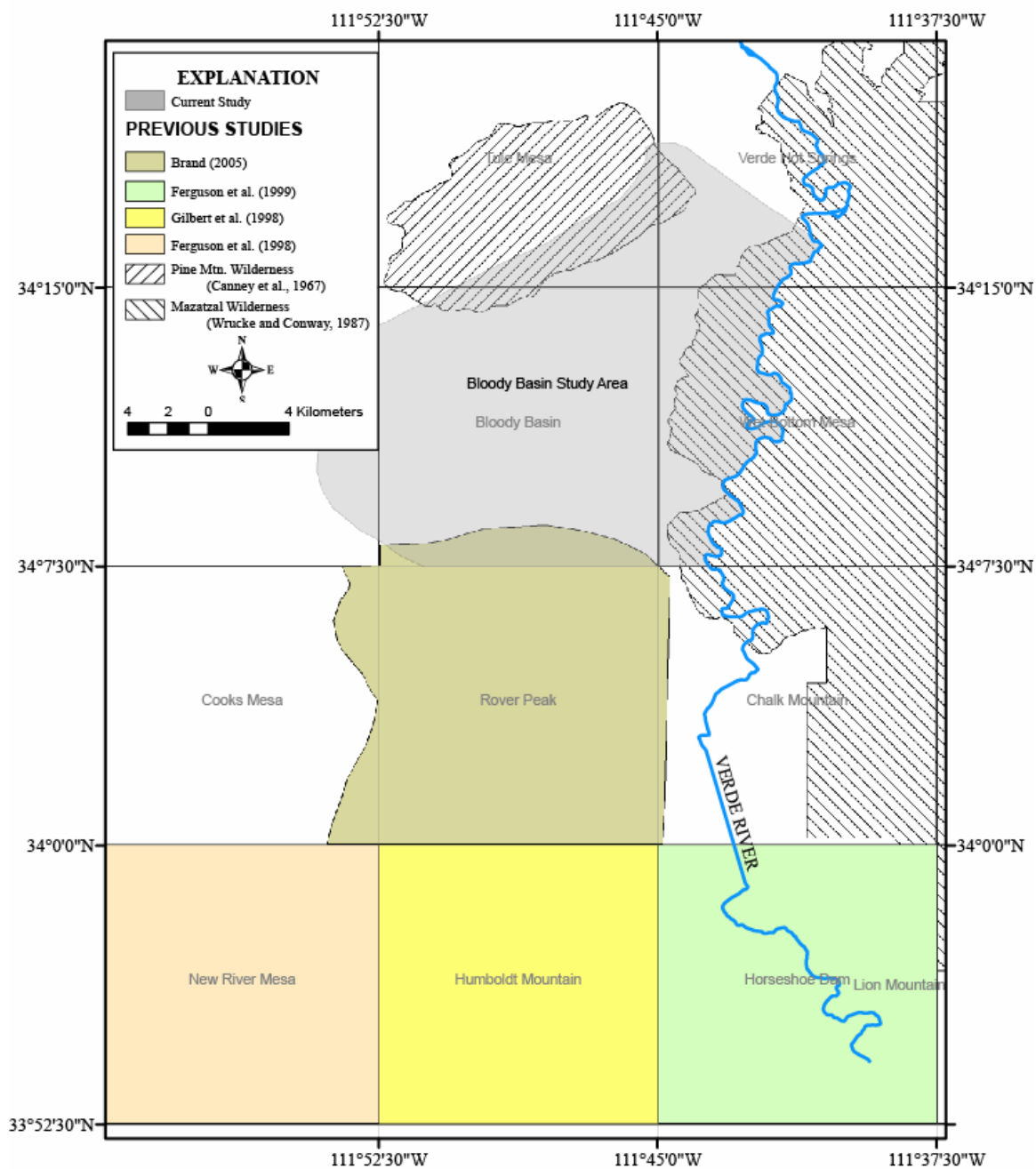


**Figure 4. Generalized map showing geographic locations of previously conducted studies around the Bloody Basin.**

resource potential in the wilderness area, which resulted in a geologic study that included detailed description and history of rocks from Precambrian through Tertiary. The Mazatzal Wilderness was studied and mapped at a scale of 1:48,000. The Mazatzal Wilderness and Bloody Basin study areas overlap slightly along the Verde River corridor (Figure 4).

Brand (2005) mapped the Cedar Mountains area to the south of the present study. His efforts included geologic mapping, history, tectonic interpretation, and  $^{40}\text{Ar}/^{39}\text{Ar}$  dating to constrain timing of faulting in the area. Precambrian and Tertiary volcanics found in the Cedar Mountains are similar and correlative with units in the Bloody Basin; however, the Tertiary Chalk Canyon Formation (Gomez, 1979) that Brand (2005) observed does not appear to continue from the Cedar Mountains area further on to the north. Brand (2005) completed geologic mapping at a scale of 1:24,000.

Leighty (1997) conducted an extraordinary study with the focus of Neogene tectonism and magmatism across the Basin and Range, specifically in central Arizona, that included, but was not limited to, reconnaissance-style geologic mapping, petrographic analysis, and tectonic stress field orientation. Leighty's (1997) work contains information regarding faulting and petrographic analysis of the Bloody Basin and surrounding areas.

Nations et al. (1982) conducted a review of the locations and chronology of Tertiary sedimentary deposits in Arizona. Although mention of the Bloody Basin is included in this study with respect to correlating stratigraphy, any in-depth details regarding the general history of the area are lacking.

Elston (1984) conducted a broad overview of central Arizona landscape development with regional correlation of rocks and timing of events responsible for present day landscapes of central Arizona. Specifically, Elston (1984) correlates a conglomerate found in the Bloody Basin (Bloody Basin conglomerate) with that found near Cave Creek. Elston (1984) also lists a detailed summary and time table of how tectonic and depositional events in central Arizona transpired over the last 38 m.y.

Pearthree (1993) conducted a study along the Verde River from Sullivan Lake to Horseshoe Reservoir with a focus primarily of the ages and correlations of terrace deposits along the Verde River corridor. This study, although detailed in terms of project objective, lacks any information regarding faulting that occurred along this corridor.

## MAP UNIT DESCRIPTIONS

For this study, the rocks in the Bloody Basin were divided into 19 different units based on lithology, composition, and relative age. Of these 19 units, 3 are defined as Precambrian, 11 are defined as Tertiary (Miocene), and the remaining 4 are Quaternary. The Miocene designation is based on dates yielded from similar volcanics to the south in the Cedar Mountains where an age of 13.5 Ma was obtained (Brand, 2005). These volcanics, as well as the volcanics in the study area have subsequently been correlated with the widespread Hickey Basalt Formation of central Arizona. This correlation is based on ages of nearby deposits, composition, and stratigraphic position. The Precambrian designation is from the past work of Anderson (1989). The granite observed in the Bloody Basin is correlated with the Verde River Granite Batholith, which has similar composition and is dated at approximately 1700 Ma, based on relative age relations to isotopically dated rocks (Anderson, 1989). Quaternary units are mapped primarily from active fluvial systems in the Bloody Basin and the Verde River drainage.

Figure 5 illustrates the generalized stratigraphy as represented by four localities in the study area that will help in understanding the extent and thickness of the volcanic and sedimentary units present. As Figure 5 shows, some of the sedimentary units in the area are discontinuous. Other units, such as the volcanics, are widespread and relatively uniform in thickness. Each unit description consists of observations followed by interpretation.

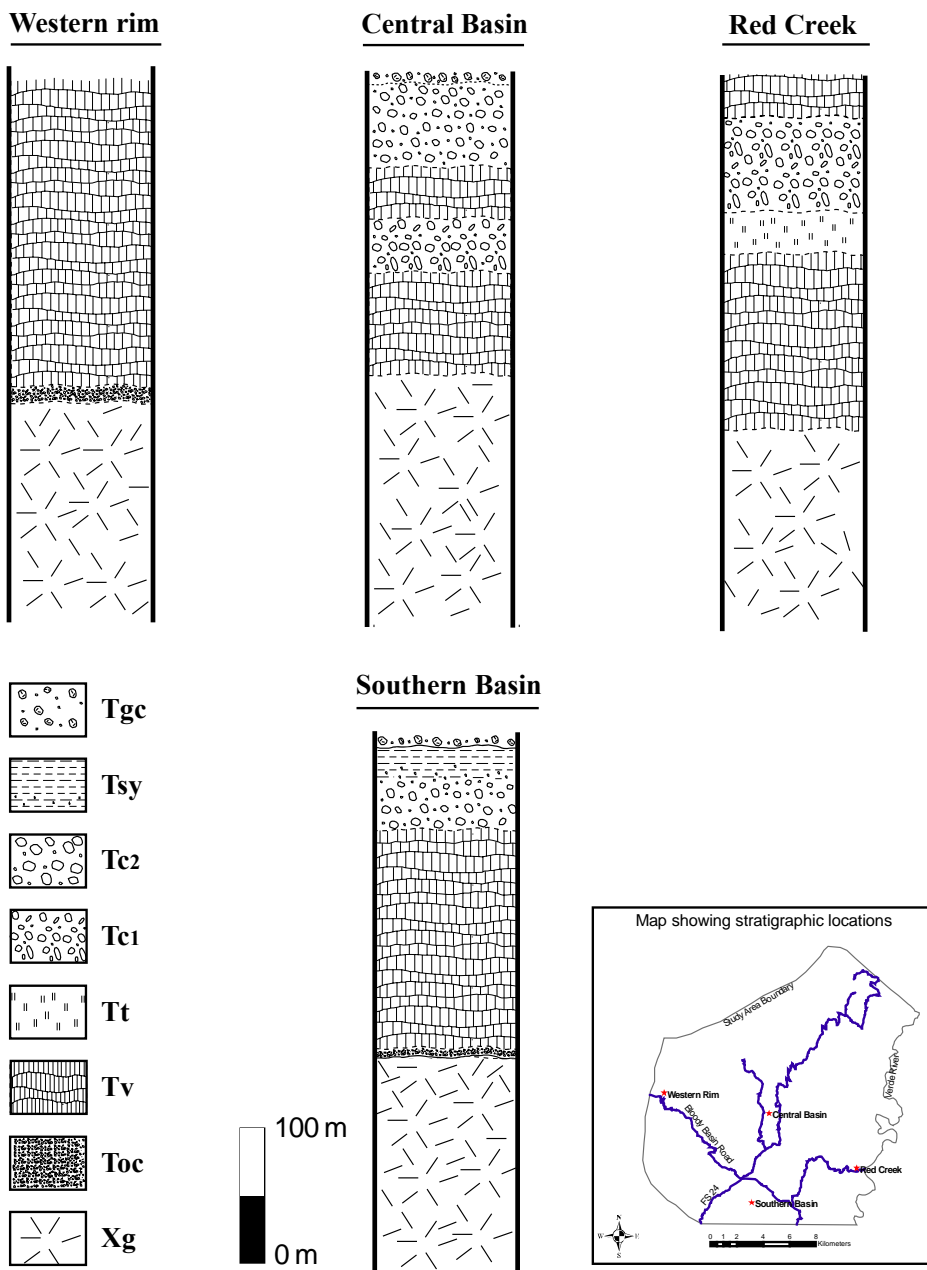


**Figure 5. Generalized stratigraphy representing four localities in the Bloody Basin study area. Note the discontinuous nature of Tc<sub>1</sub> to the west and Toc to the east. See text for details on symbols used and unit descriptions.**

## PRECAMBRIAN UNITS

### *Precambrian chlorite-mica schist (Xcms)*

Precambrian chlorite-mica schist (Xcms) is observed as a north-south trending body in the southwest portion of the study area (Plate 1). This unit is orange to tan on weathered surfaces, and locally black to dark brown. On fresh surfaces this unit displays a pinkish-orange and greenish hue. It generally has a corroded appearance displaying moderately eroded slopes, with local more resistant, cliff-forming outcrops. In hand sample, this unit is composed of muscovite (40%), chlorite (40%), and quartz (20%). Xcms has an intrusive contact with a feldspathic granite, Xg (Figure 6a) and locally is overlain by a coarse-grained conglomerate, Toc. Contacts with other units are faults (Plate 1). Muscovite + chlorite and quartz define a weak to moderate foliation as seen in thin-section, but this characteristic is hard to recognize in hand-sample. A weak lineation defined by the alignment of quartz is locally seen in hand sample. This unit also displays local mesoscopic folds and contains abundant west- southwest to east- southeast, ~1 m wide quartz veins. Figure 6b is a typical outcrop of Xcms.

Based on the presence of chlorite + muscovite + quartz, this unit is interpreted as having derived from an argillaceous sandstone, that has undergone moderate deformation manifested as the weak foliation and mesoscopic folding. The age of this unit is constrained by the intrusive contact with Xg, suggesting Xcms is the oldest unit in the study area.

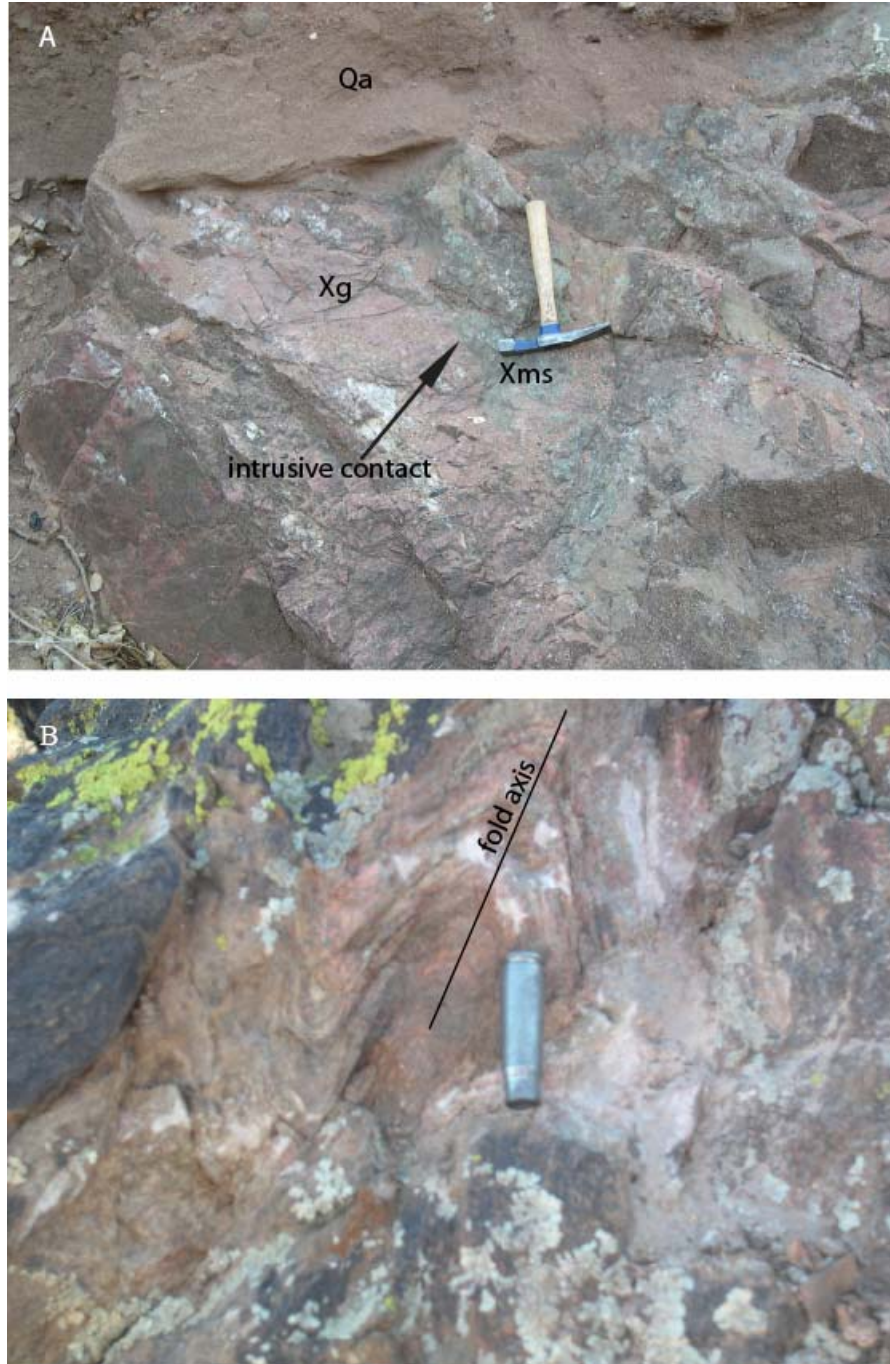


**Figure 6. Precambrian chlorite-mica schist (Xcms) found in the Bloody Basin. A) a picture showing an intrusive contact between feldspathic granite (Xg) and Xcms. Picture looking  $210^\circ$ . Qa contact is a local unconformity. Hammer is 29 cm long, and B) photograph of Xcms showing mesoscopic folding in a typical outcrop. Fold axis is oriented  $70 \rightarrow 190$ . Photograph looking  $175^\circ$ . Shell casing is 4 cm long.**

*Precambrian granite (Xg) (Verde River Granite)*

Precambrian granite (Xg) is the most widespread Precambrian unit in the study area and is observed mainly in three northeast trending swaths, with a local outcrop in the south-central portion of the field area. This unit is orange to burnt orange on weathered and fresh surfaces and typically weathers to subdued slopes. It is primarily composed of 60 - 70%, 5-10 mm, euhedral K-feldspar, 20 – 25%, 2-5 mm euhedral quartz, and 5 – 20% biotite flakes. Xg is unconformably overlain by the coarse-grained conglomerate, Toc (Figure 7), in the west and the northwest and also unconformably overlain by Tertiary volcanics (Tv), in the western portion of the study area. Additionally, this unit intrudes Xcms as noted above (see Figure 6a). Xg is typically massive but locally contains irregular joints and fractures as well as local dikes and sills of similar composition. Figure 7 is a field photograph of a typical outcrop.

The Xg unit in the Bloody Basin is correlated to the Verde River Granite Batholith (Anderson, 1989) on the basis of location and composition. This batholith occupies 1200 km<sup>2</sup> of the lower Verde River and extends from the New River-Cave Creek volcanic belt to the Mazatzal Mountains (see Figure 8, Anderson, 1989). Relative timing of this unit is thought to be post-deformation of Xcms, as Xg is not observed to have undergone a penetrative deformation, lacking foliation and any linear structures. However, because of the magnitude of this batholith, this interpretation should be considered local and preliminary.



**Figure 7. Field photograph of Precambrian granite (Xg) outcrop unconformably overlain by a coarse-grained conglomerate, Toc (see text for details). Photograph is looking 310°. Staff is 1.3 m.**

*Precambrian granite undifferentiated (Xgu)*

This unit was mapped in a reconnaissance fashion in the far northeast portion of the study area (Plate 1). Within this undifferentiated unit, there is a red to burgundy conglomerate that contains sub-angular to sub-rounded clast with < 10% well-rounded softball size lithophysae. Wrucke and Conway (1987) interpreted this as a rhyolite ash flow tuff. Also within this undifferentiated unit is a granodiorite that contains 60 – 70% euhedral biotite, approximately 20% quartz and < 10% feldspar. Additionally, and adjacent to the Verde River is a hematite bearing unit that contains possibly epidote veining 2 – 4 mm wide. For a more comprehensive description of this area the reader is referred to Wrucke and Conway (1987).

## **TERTIARY UNITS**

*Tertiary older conglomerate (Toc)*

Tertiary older conglomerate (Toc) is primarily located in a northeast trending swath on the northwest side of the study area and is mainly absent to the west (Plate 1). This unit is red to orange on fresh and weathered surfaces. It tends to form subtle slopes in the southern exposures and more moderate to steep slopes in the northern part of the study area. Toc is primarily composed of angular, 1 to 8 cm, granitic clasts, but may also locally contain metamorphic clasts (Leighty, 1997). Locally it displays crude horizontal

to sub-horizontal bedding 0.5 to 1.5 m thick. This unit is in sharp contact with the underlying Xg unit (Figure 7) and in sharp contact with the overlying Tv (Figure 8). It ranges in thickness from 50 to 250 m (see Figure 5).

Brand (2005) observed a similar unit to the south, describing a granite rich pre-volcanic conglomerate overlying Precambrian rocks. Leighty (1997) also describes a unit with similar characteristics which he interpreted to be a fanglomerate found in local troughs or depressions in the Bloody Basin and Cave Creek areas. Wrucke and Conway (1987) describe an older conglomerate similar to Toc in the central and northeastern parts of the Mazatzal Wilderness Area. Elston (1984) describes a “red fanglomerate” near Cave Creek that underlies a tuff containing an early Oligocene fossil that he correlates with this Bloody Basin unit, which he uses the name “Bloody Basin fanglomerate”. He also suggests these deposits were the result of strong regional uplift. The discontinuous, but widespread nature of this unit is suggestive of local basins receiving locally derived material prior to volcanism. Figure 9 shows what is interpreted to represent one of these local basins prior to volcanism in the region. The picture is taken looking to the south and shows a confining ridge of Xcms/Tv surrounding the margins of this unit. Timing of this unit is constrained to be no younger than early Oligocene based on Elston’s (1984) correlation.

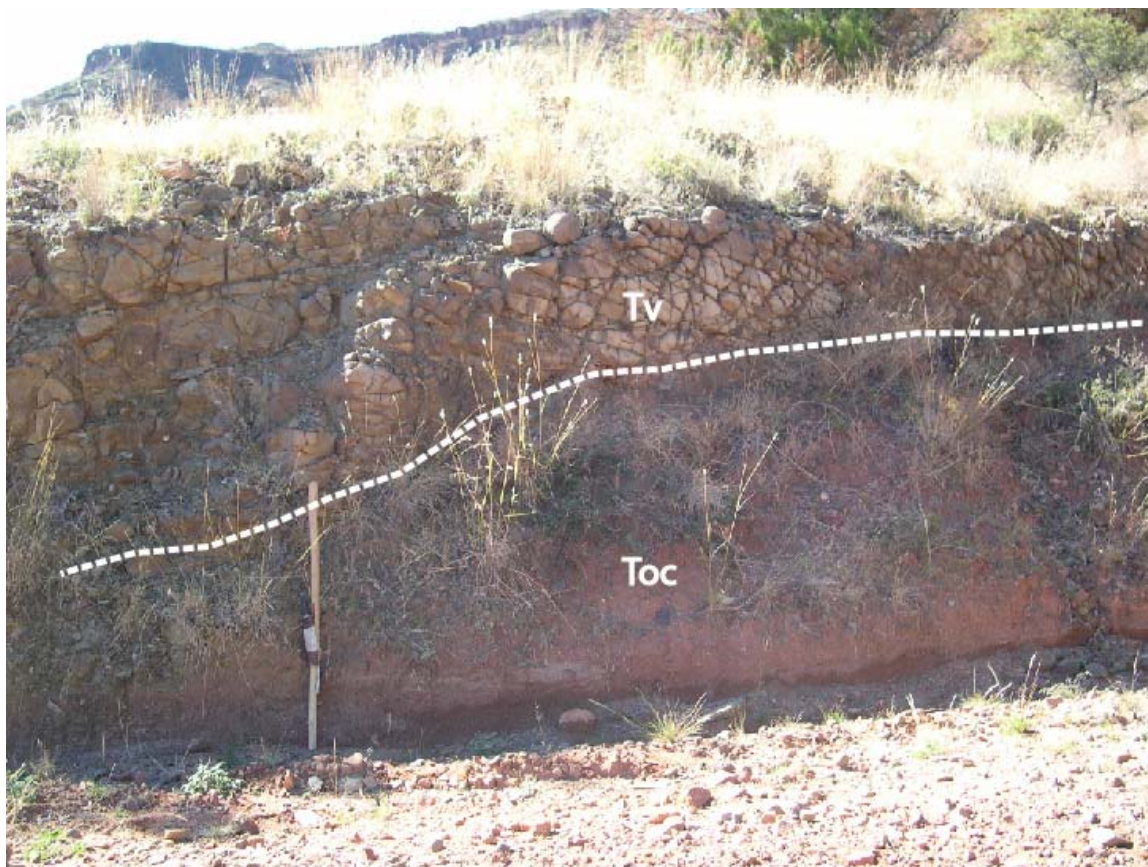


**Figure 8. Photograph of Tertiary volcanic unit (Tv) overlying older conglomerate (Toc). Picture looking 240°. Staff is 1.3 m.**



**Figure 9. Photograph of interpreted closed basin prior to regional volcanism. Note the highlands surrounding the margins of the Toc. Xcms is chlorite-mica schist. Photo is looking south from the western rim of the study area on Forest Service Road 269.**

*Tertiary volcanics (Tv) (Hickey Formation Basalt)*

Tertiary volcanics (Tv) is the most widespread unit of Tertiary rock in the study area (Plate 1). It was mapped as one unit, although it is noted that there are probably many individual flows in the region that could be distinguished and mapped separately if a detailed study were undertaken. Broadly, the volcanics consist of basaltic flows and agglomerate. The basalts are black to brown on weathered surfaces and grey to black when fresh. The agglomerates are typically burgundy on weathered surfaces and reddish brown to burgundy when fresh. These volcanics erode primarily to bench-slope topography, with more resistant benches possibly indicating individual flows. In hand sample, primary phenocrysts are commonly olivine and plagioclase with olivine phenocrysts typically altered to a brownish - yellow iddingsite (see Petrography section for further detail). Additionally, the basalts are commonly vesicular and secondary mineralization of calcite is widespread.

Unit Tv locally displays a mesoscopic, trachytic texture, defined as the parallel alignment of plagioclase laths with local olivine phenocrysts. In thin-section, this type of texture is very apparent and quite common. Outcrops displaying this characteristic can be found on top of Hardscramble Tank and North Pass Tank No. 1. Tv overlies Xg in the eastern portion of the field area and Toc in the west. As stated above, Tv is overlain in the central portion of the study area by units Tsy, Tc, and Tgc. Tv also contains interbedded red beds that are generally volcanoclastic sandstone that can be up to 2 m thick, as well as local interbedded, volcanoclastic conglomerate (Tc<sub>1</sub>) and tuffs. Tv has

been tilted  $10^{\circ}$  –  $30^{\circ}$  mainly westward, throughout the study area (Figure 10). The flat-lying volcanics (4 – 6 Ma) that aided in constraining timing of tilted fault blocks in the Rover Peak quadrangle to the south (Brand, 2005) are not observed in the Bloody Basin.

T<sub>v</sub> ranges in thickness from 450 to 600 m (Plate 1). This is consistent with observations by others in the region: Brand (2005) ~600m; Leighty (1997) > 450 m; Wrucke and Conway (1987) > 700 m; and Anderson and Creasy (1958), 0 – 400 m in the nearby Black Hills.

As indicated earlier, the volcanics in this region have been correlated with the Hickey Formation on the basis of geographic location and composition. The Hickey Formation ranges in age from 14.6 Ma to 10.1 Ma (McKee and Anderson, 1971). Brand (2005) obtained a confident age of 13.5 Ma from the top of the volcanic sequence at Cook's Mesa just to the south of the Bloody Basin in the Rover Peak quadrangle. Additionally, a younger sequence of Tertiary volcanics has been documented in central Arizona, including the Verde Valley (McKee and Anderson, 1971), Mazatzal Wilderness Area (Wrucke and Conway, 1987) and the Cedar Mountains (Brand, 2005), consisting of 7 to 4 Ma basalt flows (McKee and Anderson, 1971). At least in the Mazatzal Wilderness area and Cedar Mountains, these volcanics are flat-lying and cap a gently to moderately-tilted older sequence of the Hickey Formation. However, flat-lying volcanics were not observed in the Bloody Basin.



**Figure 10. Photograph of moderate, west-dipping Tertiary volcanics (Tv). Picture looking north from atop Dugan Peak (Plate 1).**

*Tertiary basalt undifferentiated (Tbu)*

Undifferentiated Tertiary basalt was mapped in reconnaissance fashion in the northeastern portion of the field area. This area contains basalts similar to those described above, as well as some thin, interbedded tuffaceous and sedimentary units.

*Tertiary mudstone (Tm)*

Tertiary mudstone (Tm) is observed only in the southern portion of the study area and is limited in aerial exposure (Plate 1). It is bluish to aqua on weathered surfaces and light green when fresh. Tm erodes as slopes and benches, with benches up to 25 cm thick. Tm is composed of fine-grain mud and more resistant layers of interbedded silt in hand sample. In thin-section however, this unit contains well-defined microcrystalline pods with curvilinear boundaries adjacent to regions that contain abundant, angular heterolithic fragments. The unit is overlain by Qc and Tv and is presumed to be interbedded within the Tv unit, although its base is not exposed. Tm contains local ripple marks and discoid shaped concretions that react vigorously with HCl. Also, this unit dips gently to the southwest at 10° and is at least 25 m thick. Figure 11 is a typical exposure of Tm.

Unit Tm may represent a local depression during volcanism in the region that was subsequently overlain by additional volcanics. The unique color and composition of this unit are not well understood, but the presence of ripple marks and strong calcification



**Figure 11. Photograph of typical exposure of Tertiary mudstone (Tm). Note more resistant silty layer outlined with white dashes, dipping gently to the southwest at  $10^\circ$  suggesting pre-tectonic deposition. Also note unique blue/green color. Outlined layer is  $\sim 25$  cm wide. Picture looking  $130^\circ$ .**

may be indicative of a low energy aqueous environment. Timing of this unit is not well constrained, but the fact that it is gently dipping suggests pre-tectonic deposition.

#### *Tertiary tuff (Tt)*

Tertiary tuff (Tt) is observed as a thin layer adjacent to the Verde River in the eastern portion of the study area (Plate 1). This unit is white to light tan on weathered and fresh surfaces and erodes as a cliff former. It is 70% composed of mm to 2 cm sized pumice fragments with additional and less abundant angular fragments composed of plagioclase, olivine, quartz, hornblende, and euhedral biotite less than 1 mm. This unit is in sharp contact with underlying Tv and Tc<sub>1</sub> and the overlying Tc<sub>1</sub>. It is typically massive; however, some joints and fractures are present locally. This unit is <75 m in thickness. Figure 12 is a typical exposure.

Timing of this unit can only be constrained to pre-tectonic as indicated by the moderate dip of the contact with the underlying unit, Tc<sub>1</sub> (Figure 12). Although local significance of this tuff is enigmatic, an interbedded tuff within a rather thick sequence of regionally abundant Hickey Formation is not unreasonable.

#### *Tertiary conglomerate (Tc<sub>1</sub>)*

Tertiary conglomerate (Tc<sub>1</sub>) is observed locally interbedded within the Tv unit (Plate 1) (Figure 5). Tc<sub>1</sub> is tan to light grey and erodes as a slope former unless incised



**Figure 12. Photograph of Tertiary tuff (Tt) overlying volcaniclastic conglomerate (Tc<sub>1</sub>) near the Verde River. Note massive appearance of Tt with some regular jointing. Contact is dipping to the west 30°. Picture looking due north. Staff is 1.3 m.**

by modern stream channels.  $Tc_1$  contains up to 30%, 5 – 8 cm, subangular to angular, reddish and black, volcanic clasts that are supported by a fine-grained volcanoclastic matrix. This unit is in sharp contact with underlying  $Tv$  and displays a 0.5 m wide alteration zone where  $Tv$  overlies this unit.  $Tc_1$  displays moderately defined bedding 0.5 – 1 m wide. This unit ranges in thickness from 25 to 180 m and appears to pinch out to the west, as it is not observed west of the Hutch Gulch. The thickest portion of this unit is along the Verde River where it contains an interbedded layer of  $Tv$ , whereas to the west  $Tv$  is interbedded with  $Tc_1$  (see Figure 5). Figure 13 is a typical exposure of  $Tc_1$  in the Bloody Basin.

Based on the lithology of angular volcanic clasts, suggesting local derivation, and the interbedded nature within  $Tv$ ,  $Tc_1$  is thought to represent a period of deposition associated with the onset of faulting in the region, subsequently concealed by continued volcanism. The fact that this unit is wedge shaped with the eastern exposures being the thickest indicates a source region somewhere other than the west, although paleotransport indicators were not observed. Timing of this unit can only be constrained to the age of the Hickey Formation, 14.6 to 10.1 Ma, and before movement occurred on the major northeast trending faults.

#### *Tertiary conglomerate ( $Tc_2$ )*

Tertiary conglomerate ( $Tc_2$ ) is mainly observed in the south-central portion of the study area and is typically absent in the north-northeast (Plate 1). This unit is generally a



**Figure 13. Typical outcrop of Tertiary conglomerate ( $Tc_1$ ) in the study area. Note layering within this unit. Picture looking due north. Staff is 1.3 m.**

defining grey on fresh and weathered surfaces, and typically erodes to subtle slopes unless observed adjacent to modern streams or drainages, in which case this unit is stable in cliff form. This unit is poorly sorted and contains clasts mm to 10's of cm's in size. Clasts are primarily black to grey, angular to sub-angular, volcanic rock, usually aphanitic but locally containing visible olivine and plagioclase. Clasts may also be highly vesicular with local infills of secondary calcite. Additionally, this unit locally contains clasts of reddish, agglomeritic volcanics and sub-angular marble clasts.  $Tc_2$  depositionally overlies  $Tv$  and is gradationally overlain locally by  $Tsy$  or  $Tgc$ . This unit may also be locally overlain by Quaternary colluvium ( $Qc$ ).  $Tc_2$  is crudely to moderately stratified with bedding planes 1-2 m apart and typically sub-horizontal. Fanning dips are observed in the west-central portion of the study area; however, this type of feature is an exception and not common in the Bloody Basin.  $Tc_2$  is 1 -180 m thick. Figure 14 is a typical exposure.

Based on angularity and composition of clasts that compose  $Tc_2$ , this unit is interpreted to be a locally derived basin fill that is a result of faulting in the Bloody Basin. The description by Brand (2005) of field relations and lithology of a similar unit in the Cedar Mountains area, suggests deposits resulting from similar mechanisms extend beyond this local basin.

Relative timing of this unit is constrained to syn to post-tectonic, based on the slight fanning dips and horizontal to subhorizontal nature of the unit. However, a fault gouge between  $Tc_2$  and  $Xcms$  is observed along the Bloody Basin Road, suggesting movement



**Figure 14. Photograph showing typical outcrop of Tertiary conglomerate (Tc<sub>2</sub>). Note the difference in clast size from Tc<sub>2</sub> (Figure 13) and Tc<sub>1</sub>. Also note absence of granite (see Tgc unit description for details). Photo looking 050°. Staff is 1.3 m.**

subsequent to deposition (see Fault section for further details). Tc<sub>2</sub> maintains sub-horizontal orientation in this locality.

*Tertiary younger sediments (Tsy)*

Tertiary younger sediment (Tsy), observed in the south-central portion of the study area (Plate 1), is light tan to brown on fresh and weathered surfaces. This unit is generally horizontal and topographically subdued with local incision by modern drainages. Tsy is primarily composed of a well sorted, silty-clay with interbedded gypsiferous layers that range in thickness from 2 – 20 cm. This unit positionally overlies Tv or gradationally overlies Tc<sub>2</sub>. Stratigraphically, it is overlain by a granite conglomerate, Tgc (see Figure 5). This unit also displays sub-horizontal to horizontal, thin laminae, 2-5 cm wide. Tsy is approximately 40 m thick. Figure 15 is a typical outcrop of Tsy.

Tsy could represent a lull or quiescent period without major faulting in the area based on the gradational nature from the underlying Tc<sub>2</sub> unit, which is considerably coarser and thought to represent active deposition due to faulting in the region. The reduced grain size may represent the lack of a major source for detritus, such as easily eroded, uplifting and fractured rock. It is clear then, that timing of this unit is constrained by its horizontal nature which suggests post-tectonic deposition. However, that this unit is stratigraphically overlain by Tgc (see Figure 5), suggests increased tectonism following



**Figure 15. Photograph showing sub-horizontal Tertiary younger sediment unit (Tsy). Picture looking 340° from the intersection of Bloody Basin Road and Forest Service Road 24.**

the deposition of this fine grain unit. Whether T<sub>sy</sub> is interbedded between T<sub>c2</sub> and T<sub>gc</sub> or is post-T<sub>gc</sub> is not clear. Contact between T<sub>gc</sub> and T<sub>sy</sub> was not observed.

#### *Tertiary granite conglomerate (Tgc)*

Tertiary granite conglomerate (T<sub>gc</sub>) is aurally exposed as an oblong body primarily in the central portion of the basin, but observed locally in the south (Plate 1). This unit is typically grey to tan on fresh and weathered surfaces and generally erodes as steep to moderate slopes. It is clast supported by 35-45%, 2-10 cm (locally up to 25 cm) angular to sub-angular granite clasts and 35-45%, 2-10 cm highly vesicular to massive volcanic clasts that may be composed of abundant olivine and plagioclase. T<sub>gc</sub> has a gradational contact with the underlying T<sub>c2</sub> unit and where T<sub>c2</sub> is absent, it directly overlies T<sub>v</sub>. T<sub>gc</sub> is generally massive in appearance but locally displays sub-horizontal planar structures up to 2 m wide. This unit is 1 to 120 m thick. Figure 16 is a typical outcrop of this unit.

This granite conglomerate is interpreted to be a locally derived, basin fill (Figure 17) resulting from the unroofing and deposition of the granite footwall of major faults in the study area. This interpretation is based on upward grading from a granite-poor section (T<sub>c2</sub>) into a conformable sequence of granite-rich material (T<sub>gc</sub>). The conformable sequence from the T<sub>c2</sub> into T<sub>gc</sub> (Figure 17) basin fill demonstrates the erosion exclusively of volcanics until granite is exposed and subsequently shed into the basin. Timing of this unit is then thought to be post-tectonic based on its relatively flat-



**Figure 16. Field photograph of Tertiary granite conglomerate (Tgc). Photo taken approximately mid-section of unit. Note greater percentage of volcanic clasts in photo and the less abundant sub-rounded granite clasts. Hammer handle is 29 cm long and is pointing to the north. Note: Locality of photograph is the floor of an ephemeral stream, giving rise to the sub-rounded appearance of some of the clasts.**

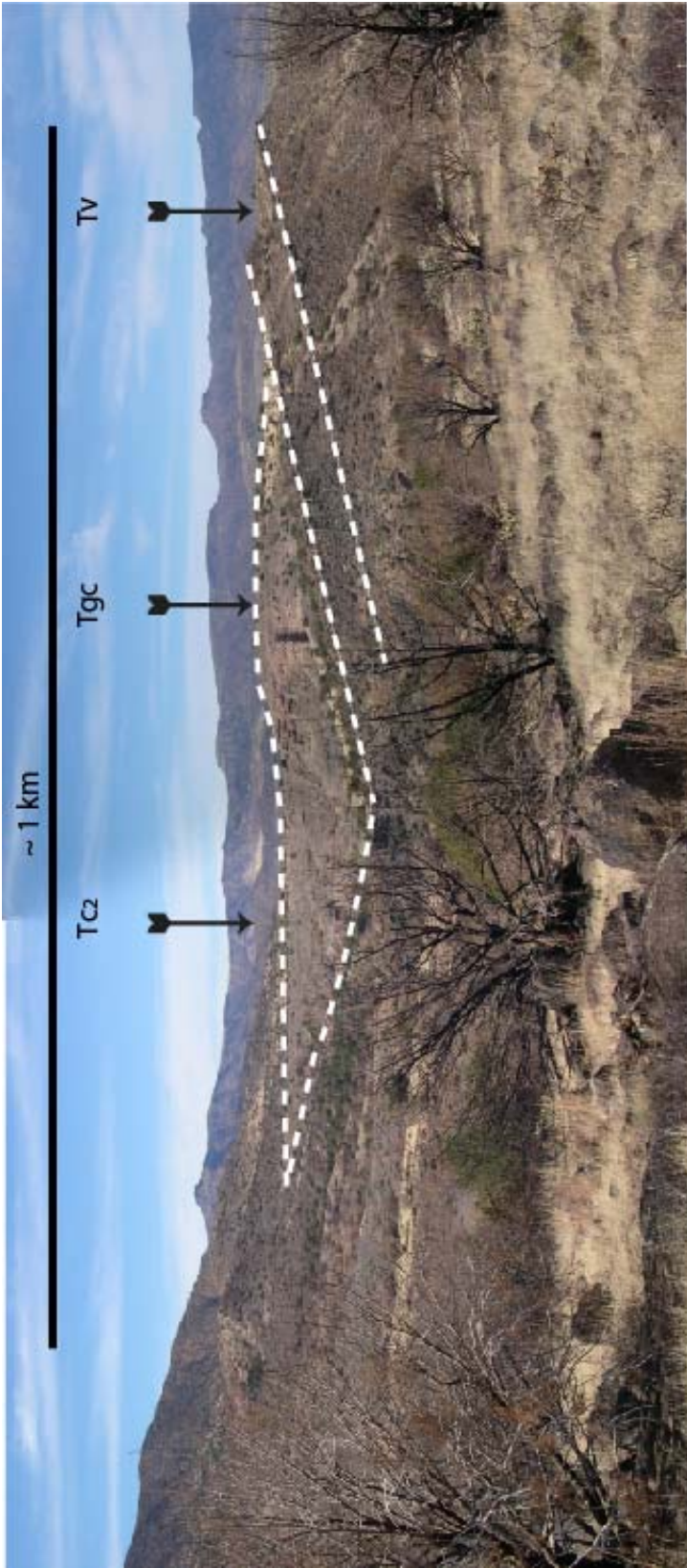


**Figure 17. Photograph of a well exposed angular unconformity in cross-section. Picture shows gently dipping volcanic unit (Tv) overlain by sub-horizontal basin fill, Tgc and Tgc. Tgc overlies Tc2 in the photograph. Tv is dipping to the southwest approximately 15°. Photograph looking north.**

lying nature. It should be noted that this unit was distinguished strictly on the presence of granite clasts. Brand (2005) discusses a similar sequence of evolving basin fill material; however, he lumped both volcanic-rich and granite-rich material into one unit.

*Tertiary plug and dome (Tp, Td)*

One volcanic plug (Tp) and one volcanic dome (Td) are observed in the study area. Tp is located in far northeast corner of the field area, adjacent to the Verde River and is known as Squaw Butte (Plate 1). Reconnaissance mapping in this area confirmed the interpretation by Wrucke and Conway (1987) and description is deferred to their work, although it is worth noting they yielded a K-Ar of  $8.9 \pm 6$  Ma.

Td is located in the west-central portion of the study area, adjacent to the Mustang Hills. This unit is grey to black on weathered surfaces and a light tan on fresh. It erodes as a cliff or as steep slopes. Td is in sharp contact with Tv to the east and Xg to the west. The margins of this body consist of an up to 15 m wide zone of angular fragments and brecciated rock of the same composition. Away from this breccia zone and towards the interior of the body, Td becomes a vertically to sub-vertically flow banded unit with typical band widths of 2 to 4 cm. Bands are locally highly deformed illustrating a complex eruptive history. The overall composition of this unit, as seen in thin-section, is dominantly sanadine (85%) with sparse phenocrysts of hornblende all aligned and displaying a trachytic texture. Overall diameter of this body is approximately 1 km. It is dissected nearly 150 m by the ephemeral Brushy Creek. Figure 18 shows flow-banding



**Figure 18. Photographs of Tertiary dome (Td) showing contrasting differences between the flow-banded interior and brecciated margin, A) detail of crackle breccia. Hammer is 29 cm. Photograph looking 080°, and B) vertical flow bands near the center of the dome. Compass arm is pointing due north.**

as observed in the interior of this body and the brecciated rock as observed on the margins.

Based on the brecciated margins, that can be considered tensional crackle breccia (Laznicka, 1988) and the massive core with well developed flow banding, in addition to the abundant potassium feldspar and the localized extent, which is probably due to the viscosity of the magma (Sheridan, 1984), Td is interpreted as a hornblende-bearing rhyolite dome that post-dates the basaltic volcanics in the area. The fact that this body straddles the major northeast trending fault suggests the fault acted as a conduit for magma migration. To further constrain the relative timing, Td is subsequently offset by strike-slip faulting probably related to a second generation of faulting in the area (see Fault section).

### *Tertiary Dikes*

Eight mafic dikes have been identified in the study area. A swarm of five dikes is observed in the south-central portion of the study area (Plate 1) and three more near the Mustang Hills (Plate 1). Dikes range in thickness from 25 cm to 4 m, have linear exposure of 0.5 to 1 km, and generally strike northwest-southeast. Dikes are generally black to grey on weathered surfaces and black on fresh. These tabular bodies are typically more resistant to erosion than the surrounding rocks resulting in fin-like exposures. Composition in hand samples is difficult to discern as they are primarily aphanitic in texture; however, in thin-section phenocrysts of olivine + plagioclase +

pyroxene are present. Dikes were observed intruding units Tc<sub>2</sub> and Tv. Additionally, two dikes were observed in the immediate vicinity of well exposed faults in the study area. Dikes are typically vertical, with the exception of the dike south of Tangle Creek which dips approximately 55° to the northeast. Figure 19 is an exposure of a dike found in the Bloody Basin.

Relative timing of dike formation can be constrained to be younger than the deposition of Tc<sub>2</sub> based on the contact relationship. The fortuitous proximity of the two dikes to faults (discussed above) is probably related to the fact that fault-related fracturing acted as a conduit for ascending magma.

## **QUATERNARY UNITS**

### *Quaternary alluvium (Qa)*

The alluvium (Qa) mapped in the study area is reserved for modern and active stream channels (Plate 1). The materials that compose this unit are primarily poorly sorted sands, gravels, cobbles and boulders from local sources.

### *Quaternary Verde River Terrace (Qvrt)*

The Verde River terraces along the eastern boundary of the study area (Plate 1)



**Figure 19. Photograph of northwestern exposure of dike south of Tangle Creek. Dike is approximately 4 m wide and dipping approximately  $55^\circ$  to the northeast. Picture looking  $330^\circ$ .**

were mapped in a reconnaissance fashion. Terrace deposits have a range in clast size from silt and sand to gravel and cobble. Although terraces along the Verde River corridor can be mapped based on relative age, there was no attempt to do so for this study. Pearthree (1993) has reported an extensive study on the Verde River corridor from Sullivan Lake to Horseshoe Reservoir.

#### *Quaternary colluvium (Qc)*

Quaternary colluvium (Qc) was mapped in the south-central and west-central portions of the study area (Plate 1). Colluvium positionally overlies older basin fill deposits (Tc) and volcanics (Tv) and is found at the toe of steep gradients. This unit is composed of poorly sorted detritus ranging from fine-grained sands to large, 25 cm, angular boulders. Materials composing this unit are locally derived volcanic, granitic, and metamorphic detritus.

#### *Quaternary terrace (Qt)*

A Quaternary terrace (Qt) was mapped in one location along Red Creek, an active stream channel draining into the Verde River (Plate 1). This unit sits approximately 10 m above the modern stream and is composed of sub-rounded to sub-angular sands, gravels, and cobbles of primarily volcanic composition.

## **PETROGRAPHY OF MAP UNITS**

Thirty-two samples were collected for petrographic analysis and prepared for thin-sections by Quality Thin-Sections of Tucson. The main purpose of this method was to bolster mineral identification in hand samples as well as to aid in identifying compositions of aphanitic rocks, which precludes not only accurate mineral identification but can lead to erroneous interpretation.

Below are a selective group of detailed petrographic descriptions for the metamorphic and igneous units as well as one sedimentary unit (Tm). Table 1 (located at the end of the section) is a summary of 20 samples, including geologic unit, composition, and textures present. Table 1 also shows composition in primarily alkaline basalts, with primary phenocryst composition ranging from olivine-rich to plagioclase-rich in either an interlocking granular texture or more commonly a trachytic texture. Compositions for the basalts are all very similar with varying percentages of phenocrysts. Figure 20 is a map showing sample locations.

The name of the unit is first and the sample number follows. Interpretation follows description where appropriate.

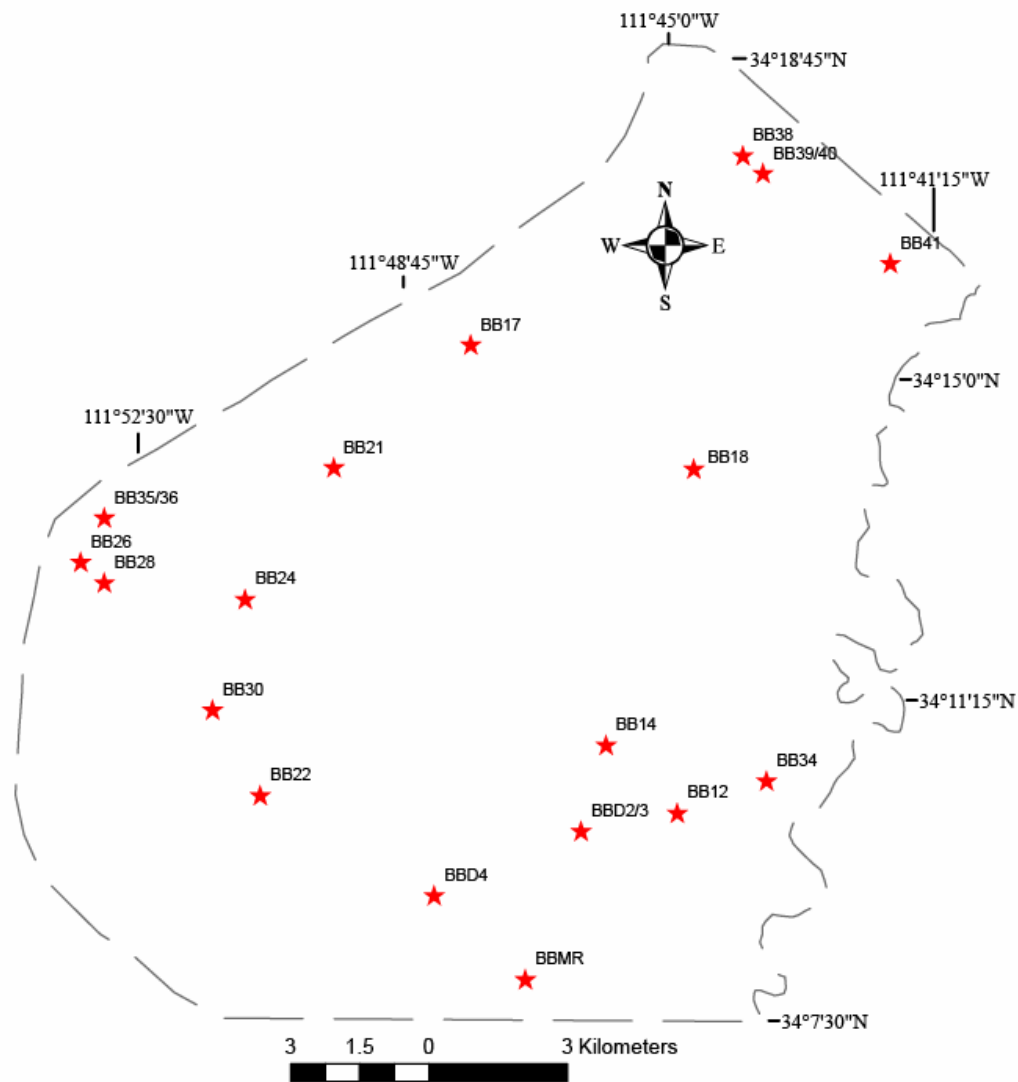


**Figure 20. Generalized map showing locations of samples collected for petrographic analysis in the study area.**

## PRECAMBRIAN UNITS

### *Precambrian chlorite-mica schist (Xcms) (BB22)*

The chlorite-mica schist consists of chlorite + muscovite + plagioclase + quartz. Chlorite makes up 30% of this unit and generally displays a corroded appearance, with irregular grain boundaries. Chlorite is observed with a distinctive green to pale green color in plain light and displays an undulatory extinction in polarized light. Oxide alteration on rims of phenocrysts and occasionally chlorite cores are replaced by the fine-grain mica, sericite. Muscovite composes up to 30% and generally has a corroded appearance, with local grains being subhedral to anhedral. Alteration to secondary sericite is not uncommon. Plagioclase is observed as less than 10% of composition and is generally corroded and fractured, with fractures filled with fine-grain sericite. Plagioclase, where present, can be identified by distinctive albite twinning. Quartz comprises roughly 30% of this unit and is observed as subhedral to corroded grains. Quartz grains display an undulatory extinction and locally contain opaque inclusions. Grain boundaries are generally curvy linear, and a weak suturing may be observed. The foliation of this unit is defined by the compositional layering of chlorite + muscovite + sericite and quartz. Local chlorite porphyroblasts have formed oblique to the main foliation. Figure 21 is a photomicrograph of this unit.

Based on the presence of chlorite + muscovite + plagioclase + quartz, this unit is interpreted to have been derived from argillaceous sandstone that underwent moderate

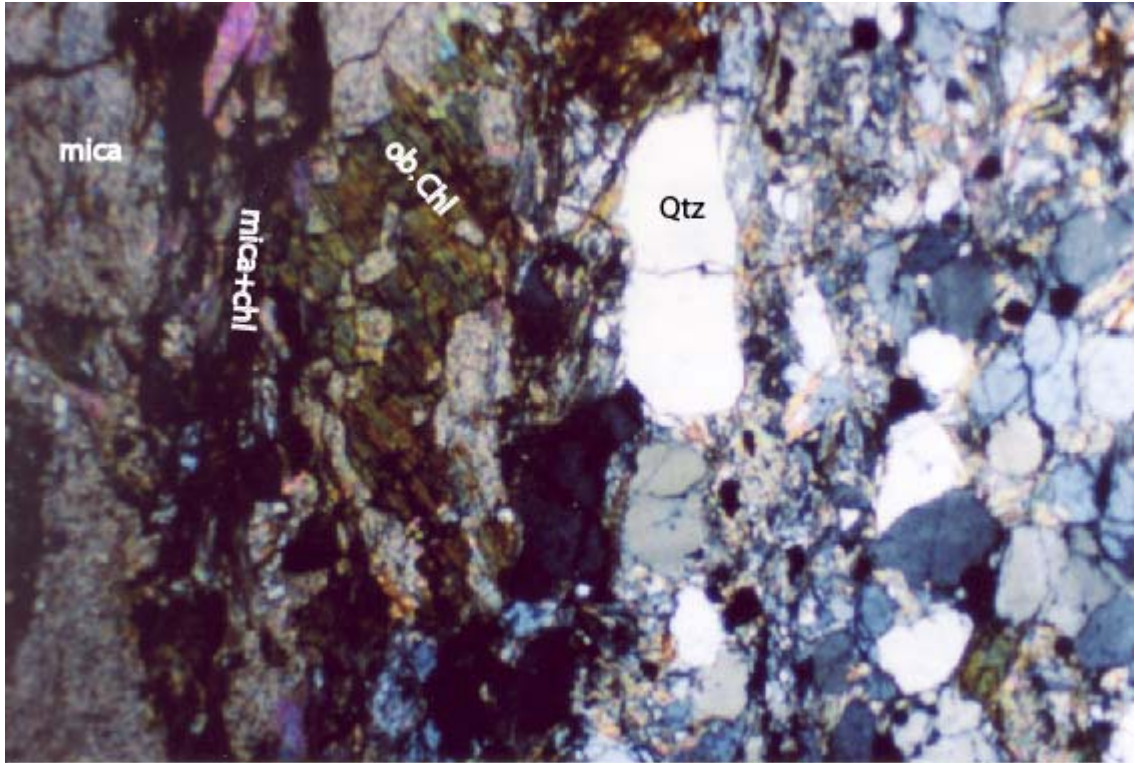


**Figure 21. Photomicrograph of Precambrian chlorite-muscovite schist (Xcms) showing moderate foliation development. Note chlorite (chl) + mica and quartz (Qtz) defines this foliation. Also note, oblique growth of chlorite porphyroblast (ob. chl). Crossed-polars, long dimension of photomicrograph is 5.5 mm. Sample BB22.**

greenschist facies metamorphism (Yardley, 1998). The presence of the oblique mineral growth of chlorite is probably the result of alteration of another mineral, such as biotite, having recrystallized subsequent to primary metamorphism.

*Precambrian granite (Xg) (BB28)*

The Precambrian granite is coarse grained and composed of potassium feldspar (microcline), quartz, plagioclase and a trace of biotite. Microcline composes 60% of this rock, is generally euhedral to subhedral and can be readily identified by a characteristic perthitic texture. Microcline grains commonly have a sieved appearance and may show some alteration to sericite. Grain boundaries are generally linear and display an interlocking texture. Plagioclase is readily identified by albite twinning and phenocrysts are generally euhedral or show a weak corrosion along grain boundaries. Quartz is generally corroded to subhedral, but interlocking, and typically possesses an undulatory extinction and sutured grain boundaries. In general, this unit is highly fractured with fractures typically filled with opaques. Figure 22 is a photomicrograph of granite from the study area.

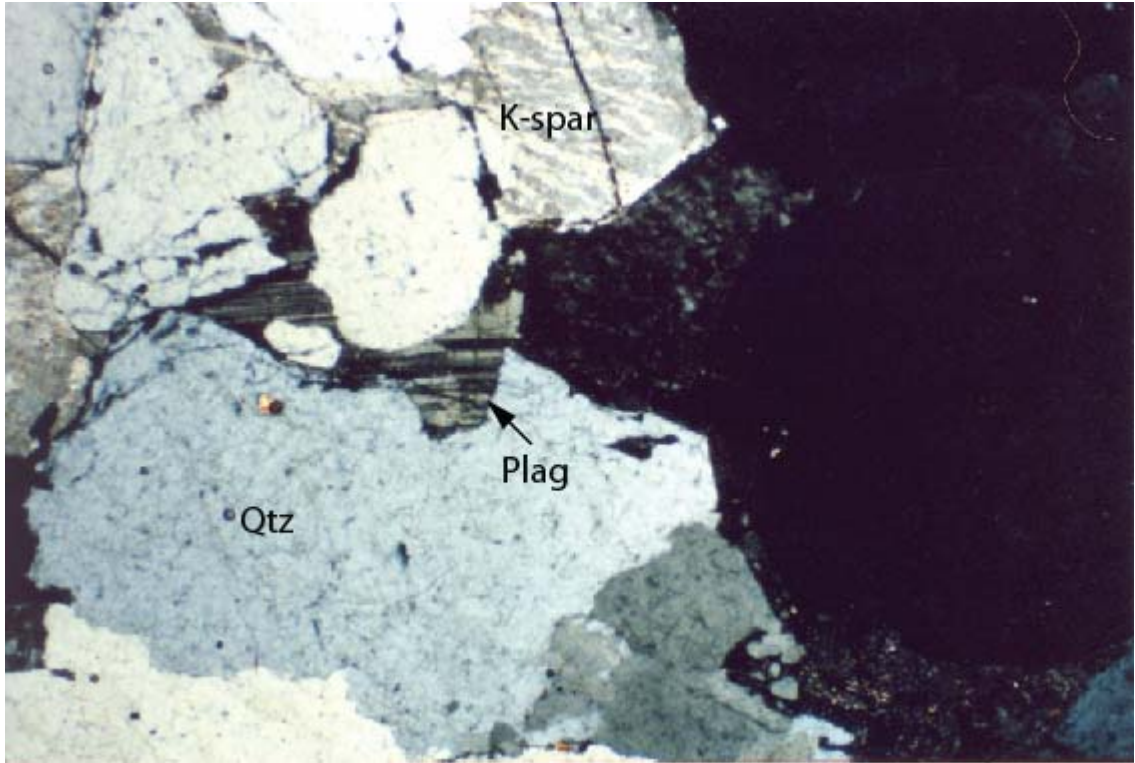


**Figure 22. Photomicrograph of Precambrian granite (Xg). K-spar (microcline) showing perthitic texture, plagioclase (Plag) identified by albite twinning, and quartz (Qtz). Crossed-polars, long dimension of photomicrograph is 5.5 mm. Sample BB28.**

## TERTIARY UNITS

*Tertiary volcanics (Tv) (BB:12,14,18,21,26,30,35,38,40)*

The volcanic rocks sampled from the Bloody Basin have an overall porphyritic texture with percentage of phenocrysts ranging from 5 to 60%. Samples are massive to highly vesicular, with vesicles locally filled with calcite. Phenocrysts are primarily olivine + plagioclase + clinopyroxene, with minor amounts of orthopyroxene. In general, composition of these rocks falls into an alkali basalt category.

Olivine is the most abundant mineral and can be up to 100% phenocryst content. Olivine is little to highly altered from rim alteration to fracture fill, to complete replacement of primary olivine by iddingsite. These phenocrysts are generally euhedral to subhedral. Plagioclase is also abundant and where olivine is in trace amounts plagioclase is the dominant species. Plagioclase phenocrysts are generally unaltered, and euhedral to subhedral, although local sericite replacement is observed in sieved phenocrysts. Plagioclase phenocrysts generally show twinning under Albite or Carlsbad twin laws. Plagioclase may also display local oscillatory zoning. Plagioclase content was determined to be between  $An_{30-40}$  using the *Michel-Levy Method* for plagioclase content (e.g. p. 272, Nesse, 1991). This plagioclase composition is consistent with McKee and Anderson (1971) were samples of Hickey basalt where determined to be composed primarily of labradorite by means of refractive indices. Pyroxene is generally euhedral to subhedral and is typically not as abundant as olivine and plagioclase, except

for BB12 and BB26, where pyroxene is between 60 and 90% of the phenocryst content (Table 1). Phenocrysts are locally concentrically zoned and may have a poikilitic appearance with inclusions of plagioclase or opaque minerals. Locally phenocrysts may also display exsolution lamellae.

Groundmass in these basalts typically includes plagioclase, olivine, pyroxene, and opaque minerals. At least one sample (BB21) has a microcrystalline groundmass. The texture of most samples is either an interlocking aggregate or highly to moderately trachytic (Figure 23), displaying primarily subparallel plagioclase laths, deflecting around and wrapping phenocrysts.

In general, composition of volcanics from the Bloody Basin is relatively similar and can be defined as alkaline to sub-alkaline (see Table 1). The dominant composition of phenocrysts from sample to sample varies somewhat, but is not enough to suggest individual and unique eruptive events. Groundmass textures do vary from trachytic to interlocking aggregate, but further sampling would be needed to show any consistency. Additionally, Leighty (1997) defined a middle-Miocene biotite-bearing alkaline basalt in the lower Red Creek area. BB12 was taken from the lower Red Creek and biotite is not observed in this sample. Sampling may be from different flows in the same area or because of the limited amount of biotite, it may just be that biotite was not in BB12. Also, McKee and Anderson (1971) conducted chemical analyses on samples taken from the Hickey basalt and found composition of volcanics to range from tholeiitic to alkalic basalt, as well as basanite. These basalt fields are consistent with compositions observed in the Bloody Basin.

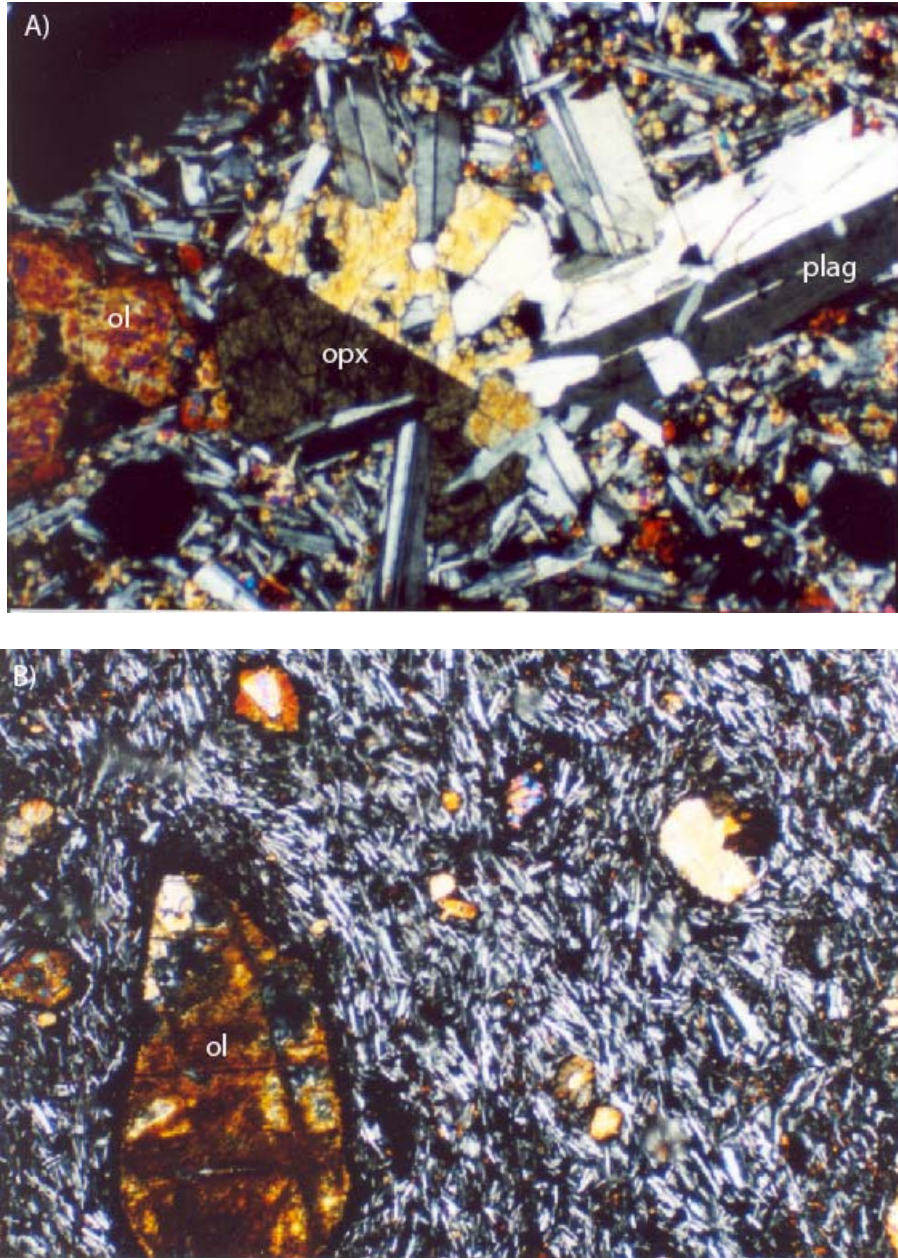


**Figure 23. Photomicrographs of two representative samples of Tertiary volcanics (Tv) in the Bloody Basin. A) interlocking aggregate of pyroxene (opx) showing Carlsbad twinning, plagioclase (plag) with distinctive albite twinning, olivine (ol) partially altered to iddingsite. Black holes are vesicles. Crossed polars, Sample BB18 and B) common trachytic texture in the Bloody Basin volcanics with subparallel microlites deflecting around olivine (ol) highly altered to iddingsite. Crossed polars, Sample BB35. Both photomicrographs have a long dimension of 2.8 mm.**

*Tertiary tuff (Tt) (BB34)*

BB34 is composed of approximately 40% fragmental phenocrysts in a dense, dark brown to black microcrystalline groundmass. Microscopically visible minerals are plagioclase, hornblende, and biotite. All plagioclase observed is either broken or fragmented and varies in size from 0.5 to 1 mm. Fragments display characteristic albite twinning and oscillatory zoning. Hornblende is observed as euhedral to fragmented and locally displays oxidized rims. Biotite is euhedral to fragmented and may contain opaque or plagioclase inclusions. Figure 24 is a photomicrograph of this unit.

The presence of primarily fragmented phenocrysts in a matrix of dense glass, accompanied by euhedral hornblende and biotite, is consistent with a volcanic tuff that underwent post-deposition mineral growth of euhedral hornblende and biotite.

*Tertiary mudrock (Tm) (BBMR)*

In hand sample this unit appears to be a fine-grained mudstone/siltstone; however in thin-section Tm is composed of poorly to moderately sorted regions composed of 60-70% sub-angular to sub-rounded silty detritus sharply separated from regions consisting of considerably less abundant silts (20-25%) but with similar angularity. Silt in both

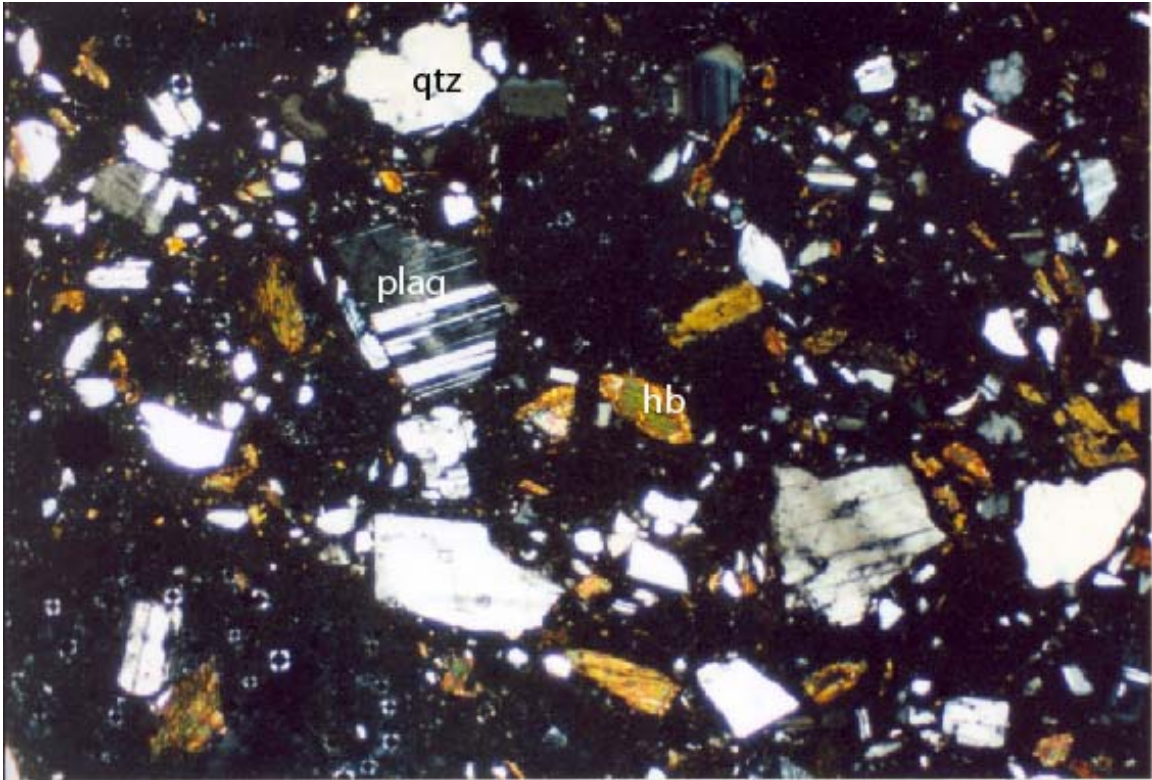


**Figure 24. Photomicrograph of Tertiary tuff (Tt) illustrating highly fractured and fragmented nature of this rock. Euhedral to subhedral hornblende (hb) is not uncommon, plagioclase (plag) and quartz (qtz), however, are commonly fractured. Crossed polars, long dimension of photomicrograph is 5.5 mm. Sample BB34.**

cases is roughly equal amounts of quartz, plagioclase, and clinopyroxene, with minor amounts of calcite. Also, in both cases, silt is in a black to dark brown volcanic glass. Figure 25 is a photomicrograph of Tm.

Confident interpretation as to the origin of this unit still remains ambiguous. However, one hypothesis that may explain the observation in terms of two separate and starkly contrasting silt percentages is reworked tuffaceous material. Rock fragments within this tuff may have been composed of high and low volumes of phenocrysts, allowing for the fortuitous deposition as now seen in thin-section.

#### *Tertiary dikes (BB:2,3,4)*

Three of the seven dikes observed in the Bloody Basin were sampled for thin-sections. These dikes all have a similar composition to each other as well as being consistent with overall composition of the volcanics in the study area. Dikes typically have an overall porphyritic texture with 15-20% phenocryst content in a trachytic groundmass. Phenocryst composition generally consists of olivine  $\pm$  plagioclase + clinopyroxene. Olivine is euhedral to subhedral and locally altered to iddingsite. Plagioclase is euhedral to subhedral and commonly displays oscillatory zoning. Plagioclase may be fractured and altered to sericite and also may contain opaque inclusions. Clinopyroxene is less abundant, is typically euhedral to subhedral, and locally displays twinning. The groundmass typically includes plagioclase, olivine,

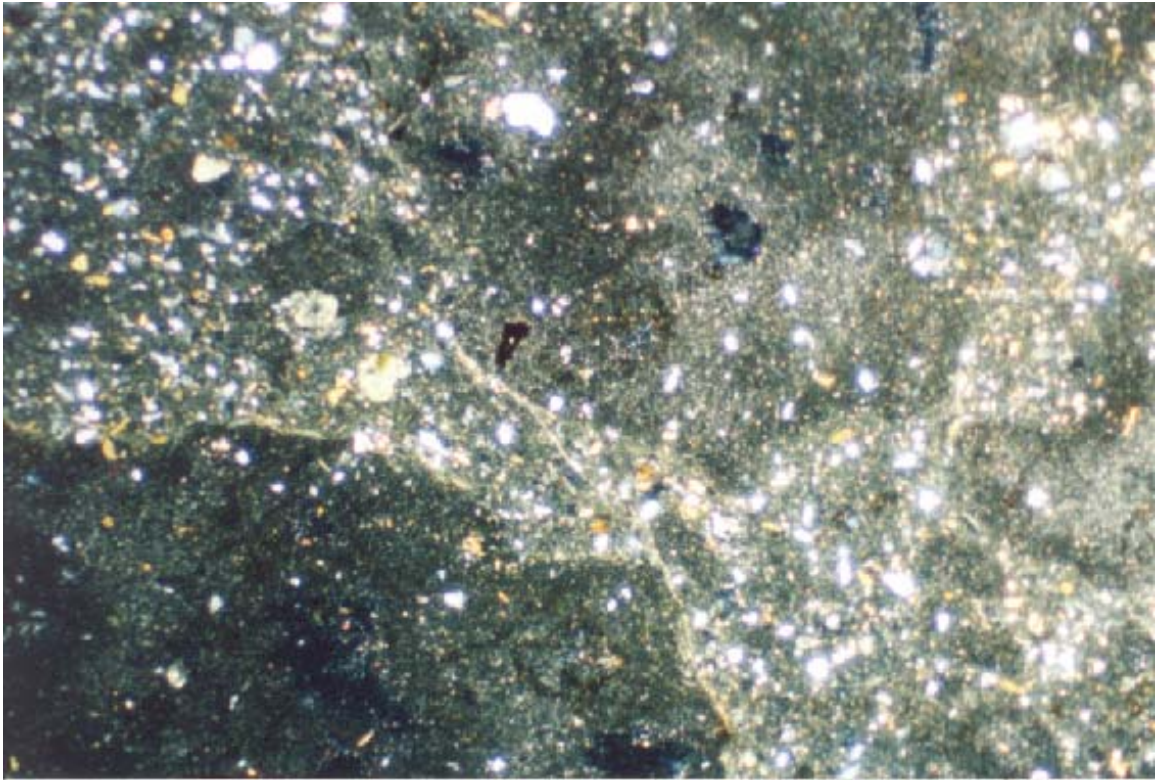


**Figure 25. Photomicrograph of Tertiary mudrock (Tm) illustrating zones of dominantly clastic fragments sharply separated by anastomosing boundaries from fine-grained microcrystalline areas. Bright ubiquitous objects are quartz fragments. Crossed polars, long dimension of photomicrograph is 5.5 mm. Sample BBMR.**

clinopyroxene, and opaques. The groundmass minerals are typically subparallel and deflect around the larger phenocrysts. Figure 26 is a photomicrograph of a dike south of Tangle Creek.

Leighty (1997) discusses dikes of similar composition and texture that he sampled in the Bloody Basin. Although locations of Leighty's (1997) samples are unknown, descriptions are consistent with the present study.

*Tertiary dome (Td) (BB24)*

The composition of Td consists of clinopyroxene, hornblende, and opaques, with a trace of quartz, in a dense and strongly aligned trachytic groundmass consisting of dense sanidine laths. Grains that comprise this rock are chiefly equigranular. Cpx is subhedral and lathlike. Hornblende is euhedral to subhedral. Opaque minerals are generally euhedral. Quartz phenocrysts are not common but when observed are subhedral to anhedral. Figure 27 is a photomicrograph of a sample from the dome.

The composition and strong trachytic texture are consistent with a hornblende-bearing rhyolite. Aside from the tuff discussed above, this is the only unit that contains hornblende.

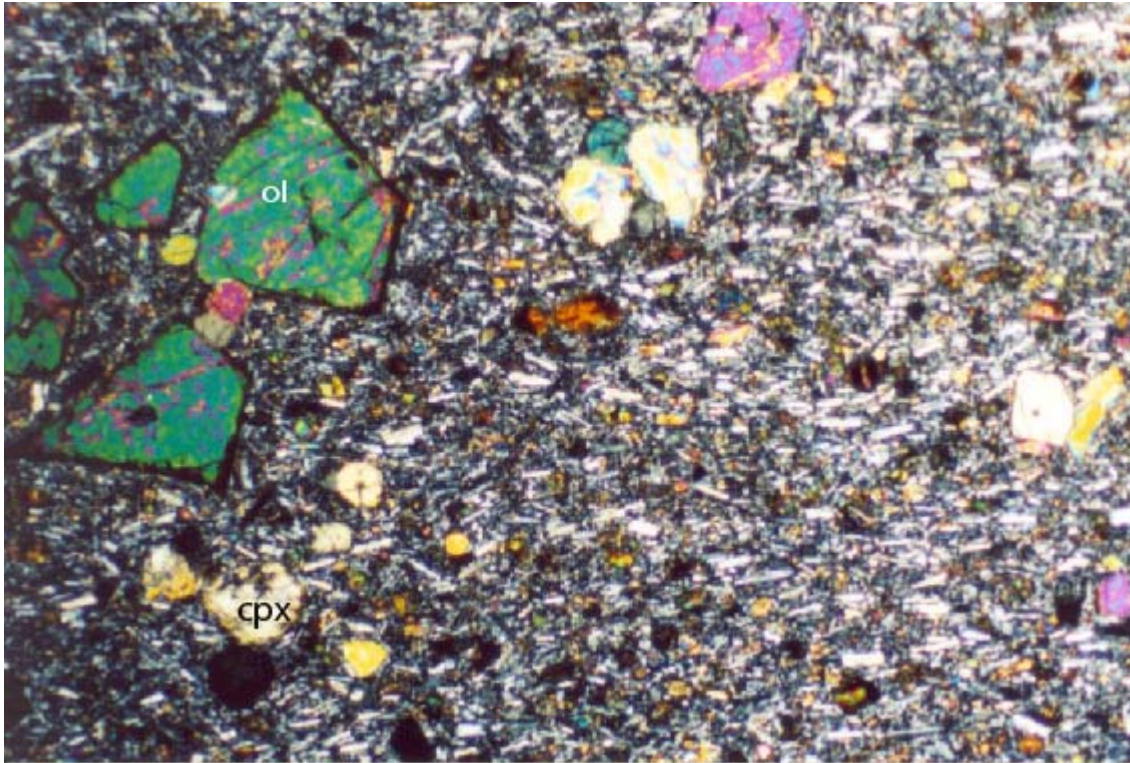


**Figure 26. Photomicrograph of representative dike in the Bloody Basin. Olivine (ol) is primarily fresh with rimmed alteration. Pyroxene (cpx) is partially corroded and shows concentric zoning. Note moderate trachytic texture shown by orientation of subparallel microlites. Crossed polars, long dimension of photomicrograph is 5.5 mm. Sample BBD4.**

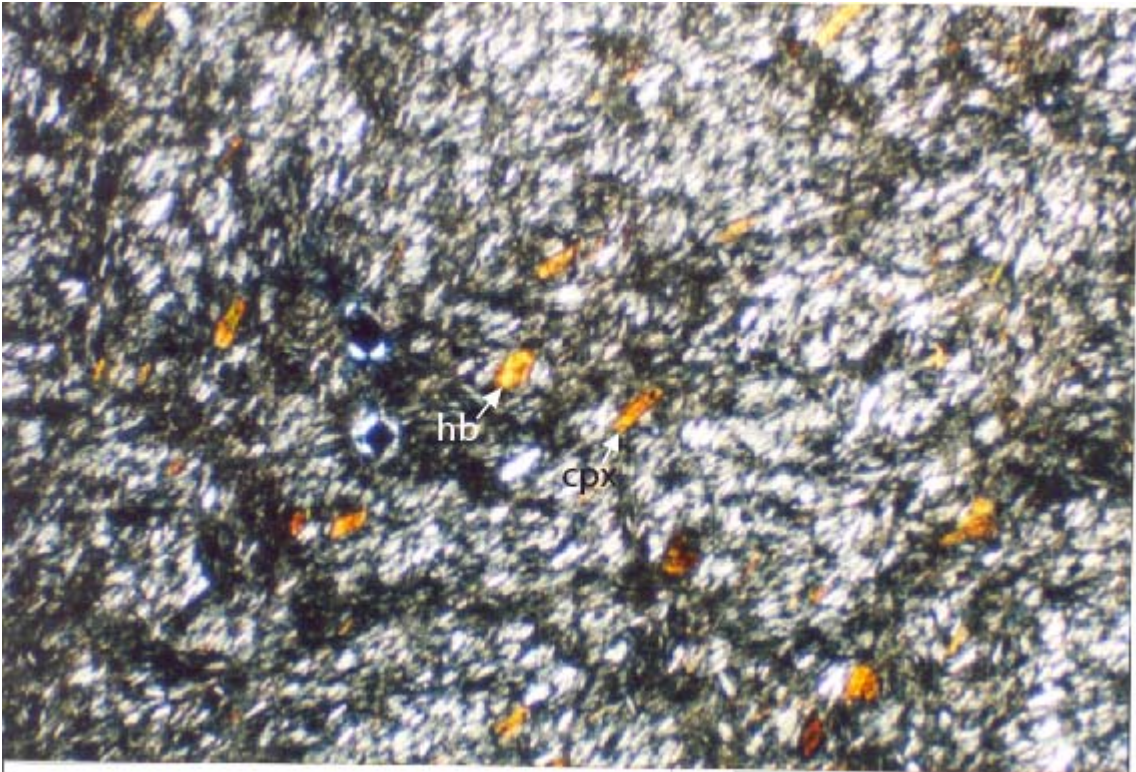


**Figure 27. Photomicrograph of Tertiary dome (Td) from the Bloody Basin. Microcrystalline sanidine displays trachytic texture. Hornblende (hb) and pyroxene (cpx) are commonly euhedral. Cross polars, long dimension of photomicrograph is 2.8 mm. Sample BB24.**

Sample	Unit	Phenocryst %	Phenocryst composition w/ relative abundance (%)	Groundmass	Texture	Rock Name
BB12	Tv	60	cpx (60) + ol (40) + plag (10)	Feld + cpx + ol + op	interlocking	Olivine Basalt
BB14	Tv	35	ol (100)	Feld (70) + ol (15) + op (15)	interlocking	Basanite
BB17	Qd	n/a	n/a	n/a	n/a	Quartz dike
BB18	Tv	30	Plag (60) + ol (15) + cpx (15)	cpx (60) + plag (30) + op (10)	interlocking	Andesite
BB21	Tv	5	Plag (80) + ol (20)	glass	none	Andesite
BB22	Xcms		Chl + musc + plag + qtz		foliation	Chlorite Schist
BB24	Tp <sub>2</sub>	< 1	n/a	k-spar (85) + hb (15)	trachytic	Alkali Trachyte
BB26	Tv	10	Cpx (90) + qtz (10)	Feld (60) + glass (30) + op (10)	trachytic	Quartz Tholeiite
BB28	Xg	n/a	k-spar (60) + qtz (40) + bio (<1)	n/a	coarse	Granite
BB30	Tv	50	Plag (90) + ol(10)	Plag (80)+ ol (10) + op (10)	trachytic	Andesite
BB34	Tt	35	Plag (70)+hb(20) + bio(10)	glass	fragmented	Crystal Tuff
BB35	Tv	15	Ol (70) + opx(20) + plag(10) +	Plag (80) + op (20)	trachytic	Olivine Basalt
BB36	Tv	n/a	n/a	n/a	welded	Tuff
BB38	Tv	30	Ol(60) + plag(40)	Plag(60) + ol(30) + op(10)	trachytic	Olivine basalt
BB39	Tv	25	Ol(80) + plag(20)	Plag(60) + op(30) + ol(10)	interlocking	Olivine Basalt
BB40	Tv	10	Ol(95) + qtz(<5)	Plag(60) + ol(20) + op(20)		Quartz Tholeiite
BB41	Tp <sub>1</sub>	50	Plag(70) + hb(30)	dense	Weak trachytic	Andesite Plug
BBD2/3	Dike	20	Ol(90) + cpx(10)	Plag (90)+ ol(10)	trachytic	Olivine Basalt
BBD4	Dike	15	Ol(70) + plag(20) + cpx(10)	Plag(50) + op(30) + ol(20)	trachytic	Olivine Basalt
BBMR	Tm	n/a	Qtz+plag+cpx+ca	glass	Poorly sorted	Mudstone

**Table 1. Summary table of petrographic analysis for rock units in the Bloody Basin. Igneous rock name is based on modal mineralogy after the classification scheme of the IUGS Subcommittee on the Systematics of Igneous Rocks.**

## **STRUCTURE**

Precambrian foliation development along with mesoscopic folding and major Tertiary fault block rotation with accompanying dike and dome emplacement characterize the major structural features of the Bloody Basin study area. Two Tertiary fault sets are identified in the study area with orthogonal orientation to one another. One set is related to northwest-southeast directed extension and the other is thought related to northeast-southwest directed extension with subsequent dike emplacement. In addition to the dominant Tertiary normal fault sets and dikes, minor strike slip-faulting with genetically related reverse movement has occurred in the Bloody Basin. This section provides details regarding these structures based on field observations and discusses timing where appropriate. Figure 28 is a general map of the structures and most locations discussed herein.

## **PRECAMBRIAN STRUCTURES**

The chlorite-muscovite schist (Xcms) has a highly corroded and weathered appearance and because of this characteristic, structures are difficult to decipher. A foliation, when present, is moderately to steeply dipping, and varies in strike from northwest to northeast, which are attitudes similar to other Precambrian terranes in Arizona (Rehrig et al., 1980). Mesoscopic folding is observed in well exposed road cuts

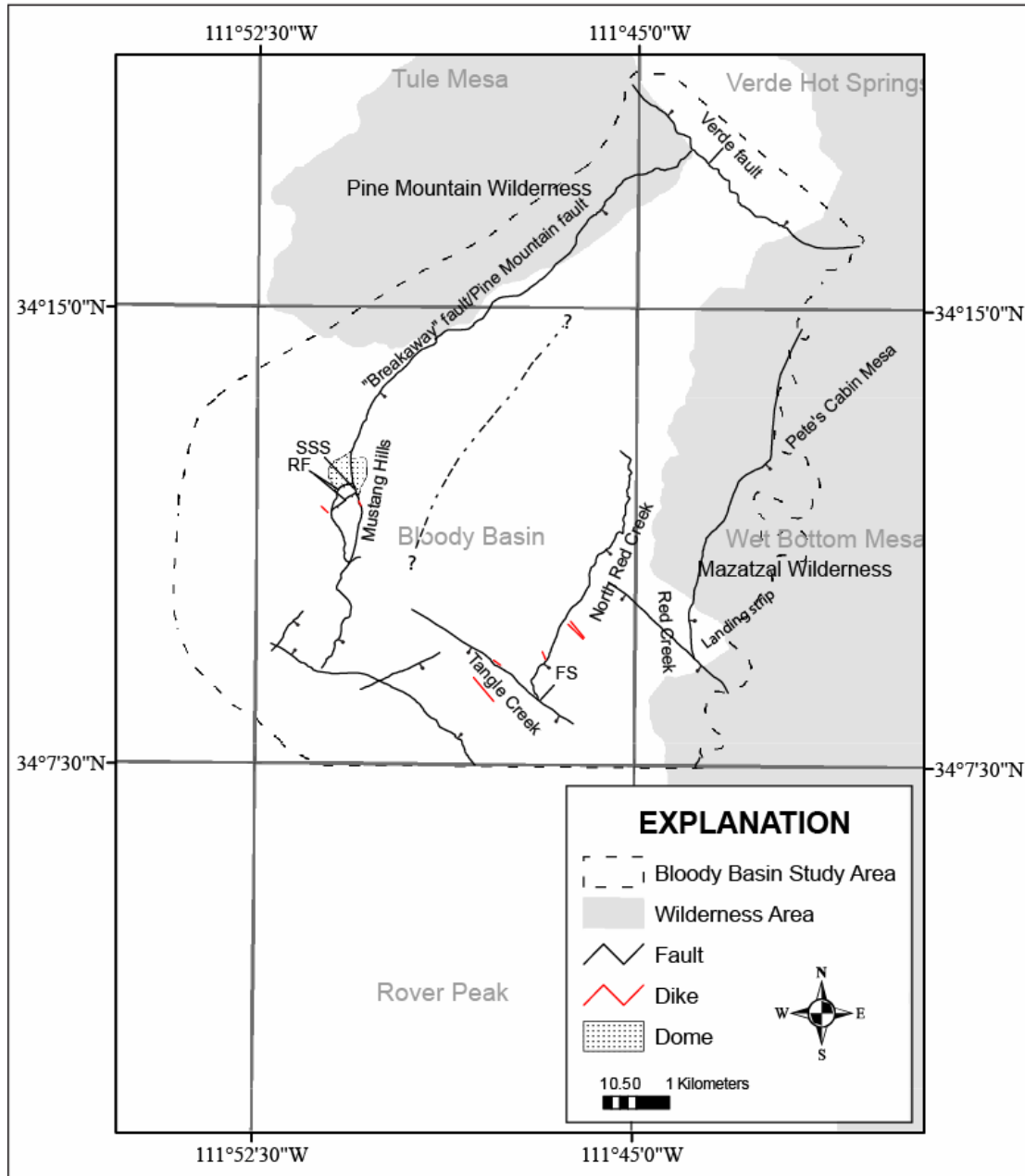


**Figure 28. Generalized map showing locations and structures discussed in this section. Normal faults are indicated by ball and stick on down-thrown side. Dashed and dotted line indicates inferred fault (see text for details). RF = Reverse fault (teeth on up-thrown side); SSS = Strike-slip segment; FS = Frog Springs. For further map details see Plate 1.**

along the Bloody Basin Road. Also observed are abundant northeast-striking, less than 1 m wide, weakly foliated quartz veins that are reduced mainly to piles of rubble.

The Precambrian granite (Xg) that has been correlated with the Verde River batholith (1700 Ma) contains randomly oriented dikes and sills of similar composition along with irregular fracture patterns. In addition to these features, in the extreme northeast corner of the study area, a previously mapped (Canney et al., 1967 and Wrucke and Conway, 1987) quartz vein described as a saddle reef deposit by Canney et al. (1967) was confirmed by field reconnaissance. This linear feature is approximately 2-3 m wide northeast-southwest-striking and exposed for nearly 5 km. It is noted that this body is not found beyond the cross-cutting Verde fault. In general, this coarse-grained granite does not display any structural grain such as the previously mentioned foliation, indicating a deformational event older than the intrusion.

## **TERTIARY STRUCTURES**

Evolution of Tertiary structures identified in the Bloody Basin area involved faulting, emplacement of basaltic dikes, and the emplacement of a hornblende-bearing rhyolite dome. As previously discussed, two distinct fault set orientations are recognized and are possibly unrelated, resulting from extensional events directed roughly orthogonal to each other. Northeast-striking faults are characterized by a series of tilted and moderately dissected fault blocks that display a synthetic normal fault block array indicating northwest-southeast directed extension. Block rotation related to this faulting

is responsible for moderately ( $10^{\circ}$ - $30^{\circ}$ ) northwest dipping strata that dominate the study area.

The second set of faults is oriented northwest-southeast, and is characterized by a series of moderate- to high-angle normal faults that show both northeast-and southwest-side-down motions indicating northeast-southwest extension. Local block rotation is responsible for gentle to moderate ( $10^{\circ}$ - $30^{\circ}$ ) southwesterly dipping strata. A southeasterly segment of the roughly 95 km trace of the northwest-striking Verde fault is associated with this second event and is within the extreme northeastern portion of the study area. In addition to the northwest-striking faults, a suite of dilatational dikes is associated with this second deformation event.

### **Northeast-Trending Faults**

The northeast-trending faults occur southeast of the southeast escarpment of the Pine Mountains Wilderness area (Plate 1; Figure 28). Strata are displaced down to the southeast along nearly parallel southeast dipping faults. Dip parallel separation along these faults, as measured in cross-section, varies from 730 to 1,200 m.

From northwest to southeast, the primary “breakaway” fault (Pine Mountain fault) (Figure 28) is traced along the southeast escarpment of the Pine Mountain Wilderness area (Plate 1). This fault has a roughly linear trace from the Mustang Hills, northeast to Skeleton Ridge (Plate 1), where it is intersected and truncated by the through going Verde fault. Because a large portion of this fault is concealed by Tertiary sediment (Tgc)

direct measurement of the attitude along this segment is difficult. However, the linear trace suggests a vertical to very steep dip (Figure 29A). South of the Mustang Hills, the trace of this fault abruptly changes to a nearly north-south strike (Plate 1). Dip along this section also appears nearly vertical based on the linear trace. Near Mud Springs Creek (Plate 1) the fault jogs to the southeast for a short distance before abruptly turning back to the south-southwest direction. The dip along this section changes from vertical to a moderate  $055^{\circ}$  to the southeast (Figure 29B). The fault appears to follow the attitude of the foliation of the metamorphic unit (Xcms) along this segment. This segment continues southwest to Cottonwood Springs where it is truncated by another northwest-striking fault (Figure 30). The trace of this fault is not observed southwest of the cross-cutting structure; however Brand (2005) mapped a similar striking fault in the Rover Peak quadrangle that would project to the north, suggesting a relationship between the two.

The primary faulting places younger Tertiary volcanics (Tv) against Precambrian granite (Xg). Block rotation responsible for dipping strata is evident in some locals (see Unit Description; Figure 13) which may indicate the fault flattens at depth.

Other details revealed by well exposed outcrops demonstrate dilatational and non-dilatational components of this fault. Figure 31 is an outcrop of the fault at the Marble Mine (Plate 1). A strong chaotic breccia, composed of angular volcanic clasts is within a tear drop shaped body (in map view) of primarily calcite/marble that is approximately 100 m wide and tapers southwest to thin ( $< 1$  m) veins in approximately 2 km. This segment of the fault is interpreted to have a large dilatational component resulting in the formation of this marbleized body. Figure 29B, demonstrates a largely non-dilatational

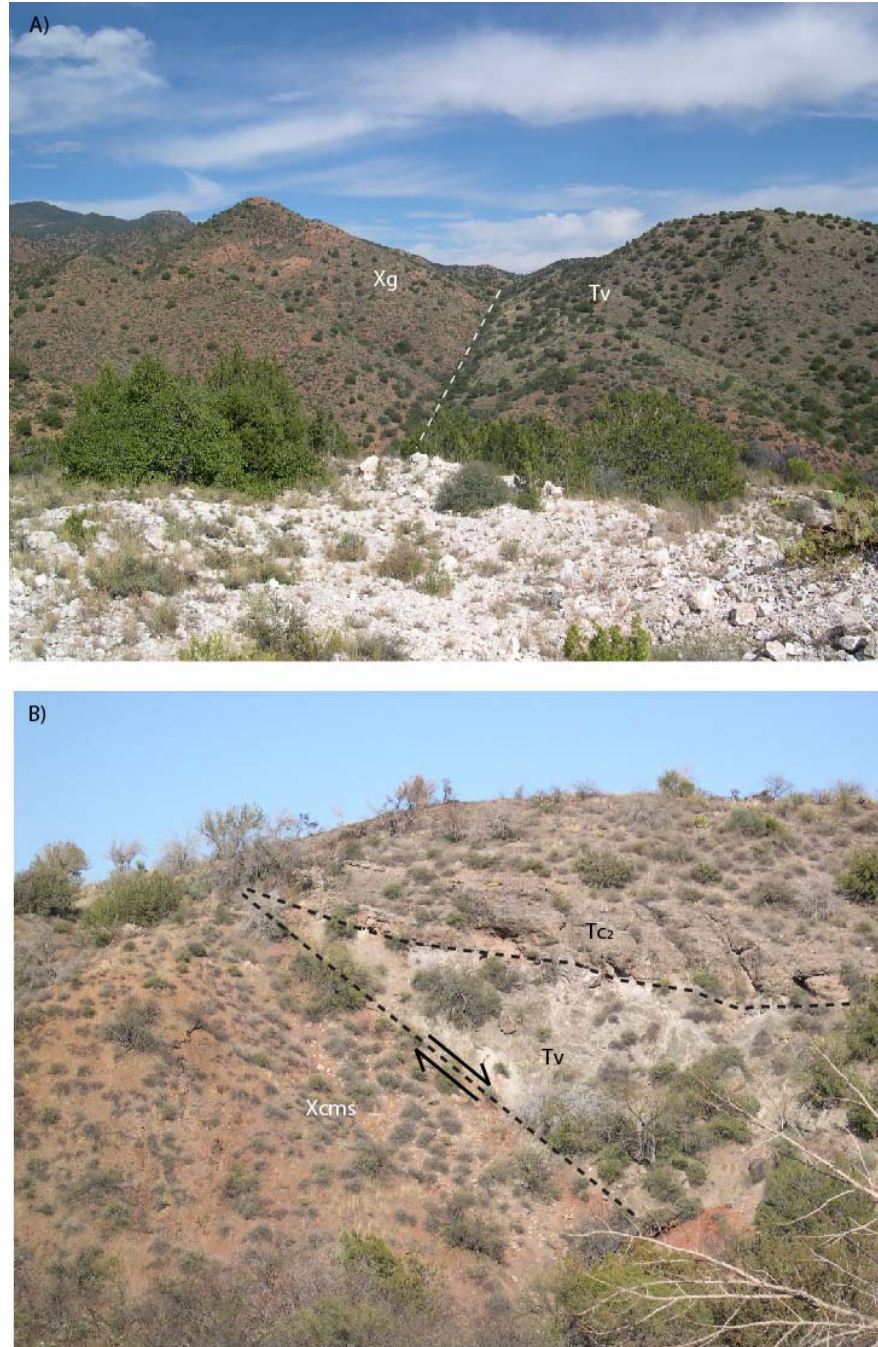


**Figure 29. Field photographs showing dip variability along the Pine Mountain fault. A) vertical trace of Pine Mountain fault looking northeast from Marble Mine (white rock in foreground) and B) trace of Pine Mountain fault dipping  $055^{\circ}$  to the east. Foliation within Xcms dips roughly  $060^{\circ}$  to the east. Picture looking north. See Unit Description section for details on symbols used.**



**Figure 30. Photograph showing the intersection of northeast-trending fault by a northwest-striking fault. The northeast-striking is demonstrated by the dashed white line and the northwest fault is coming out of the picture. Picture looking 270°.**



**Figure 31. Photograph of volcanic breccia within a marbled body along the Pine Mountain fault at Marble Mine. Pen for scale. Picture looking 180°.**

component, resulting in roughly 20 m of hanging wall brecciation. This sharp contact between the two units suggests lack of dilation at least in this setting. Additionally, a 5 m wide swath of gouge is present where the Tc<sub>2</sub> and Xcms are in fault contact (Plate 1). The difference in these characteristics shows the heterogeneity and probably differential movement along the fault as well as response to faulting of different lithologic bodies.

Studies on this fault have been documented by past workers. Canney et al. (1967) suggest that vertical displacement along this portion of the fault occurred along one large break. They go on to suggest that displacement along this fault to be at least 300 m based on topographic position of the Tertiary volcanics. If the same approach is taken in the Bloody Basin, similar displacement amounts, however actual displacement along this fault is probably much more than 300 m (Canney et al., 1967).

Elston (1984) and Canney et al. (1967) show the Pine Mountain fault as a zone and discuss a pair of faults along the Pine Mountain Wilderness margin. Elston (1984) shows a fault north of this study with strike-slip motion in undivided Precambrian rocks seemingly interpreted from a Skylab photograph of central Arizona. Canney et al. (1967) describe a similar fault with unknown sense of slip. Field reconnaissance southeast of Rugged Mesa (Plate 1) reveals a quite different interpretation from the Canney et al. (1967) map, which shows a fault separating two bodies of granite. The contact here is an unconformity with the unit Toc (see Unit Descriptions section) depositionally overlying Precambrian granite, and not fault related as they suggest.

Continuing to the east, toward the Verde River, a relatively short, but well exposed trace of a northeast-striking fault (Figure 32A) is observed in the North Red



**Figure 32. Well exposed North Red Creek fault in the east-central portion of the study area. A) excellent exposure of North Red Creek fault showing roughly 15 m tall fault scarp. Picture looking  $025^\circ$ , approximately along strike, and B) oblique striations along same fault further to the south near Dugan Rock Tank. Striations are oriented  $45^\circ \rightarrow 80^\circ$ . Picture looking  $290^\circ$**

Creek area (Plate 1). Measurements along this fault show a consistent northeast strike and dip to the southeast between  $55^{\circ}$ - $60^{\circ}$ . Lineations observed on the southern segment of this fault (Figure 32B), near Dugan Rock Tank, record left-lateral, oblique-slip motion. This fault appears to die out in the northeast and is truncated to the southwest by a northwest-striking fault near Frog Springs (Plate 1).

Previous work by Wrucke and Conway (1987) show the trace of this fault is inferred to continue beyond the intersection at Frog Springs. Detailed mapping of the area shows Quaternary cover south of Frog Springs to beyond the map area, which would conceal any trace likely to be found. Although likely that this fault continues to the southwest, it may also end at this location. The fault shown in Plate 1 and Figure 28 is therefore not traced beyond Frog Springs.

Continuing to the east, the third fault in this array roughly parallels the Verde River corridor (Plate 1) and is the western margin of a graben situated along the Verde River (see Wrucke and Conway, 1987). Available measurements along this fault show a consistent  $45^{\circ}$  dip to the southeast. Tertiary volcanics ( $T_v$ ) and sediments ( $T_{c1}$ ) dip moderately ( $15^{\circ}$ - $30^{\circ}$ ) west-northwest into Precambrian granite ( $X_g$ ). The dipping strata along this fault appear to become less steep to the northeast. Near the Landing Strip (Plate 1), dipping strata measure  $25^{\circ}$ - $30^{\circ}$  to the west-southwest and west-northwest, and on the western margin of Pete's Cabin Mesa to the northeast, dipping strata measure approximately  $15^{\circ}$ . This may reflect a change in fault geometry at depth. To the south, this fault is likely intersected by a northwest-striking fault concealed by Quaternary cover and to the northeast it probably intersects with the northwest-striking Verde fault as

suggested by Wrucke and Conway (1987) although the trace of the fault is difficult to decipher in this area.

A brief note on the inference of a fourth normal fault within this set (Figure 28). Under the Tertiary sedimentary cover in the central portion of the basin, there is believed to exist a fault that is similar in nature to those described above. The basis for this inference is shown well in cross-section (A-A'; Plate 1). The projection to the subsurface of the contact between Tv and Xg at the North Red Creek location, results in an unreasonable thickness of the Tertiary volcanics. With the inferred fault, a more reasonable approximation of the subsurface geometries is achieved. It is realized that only geometrical constraints in cross-section support this inference and that surface data for this fault is absent. However, it is not uncommon to have basin bounding faults covered by erosional processes as is a characteristic of the Basin and Range physiography (Shafiqullah et al., 1980).

Finally, Figure 33 is a stereogram of all measurements obtained along well exposed fault traces. The stereogram shows a cluster of poles to fault planes in the northwest, demonstrating the overall northeast-striking and steeply dipping attitude of this fault set. Also shown is the average strike and dip of the faults measured:  $033^{\circ}$  and  $57^{\circ}$  SE.

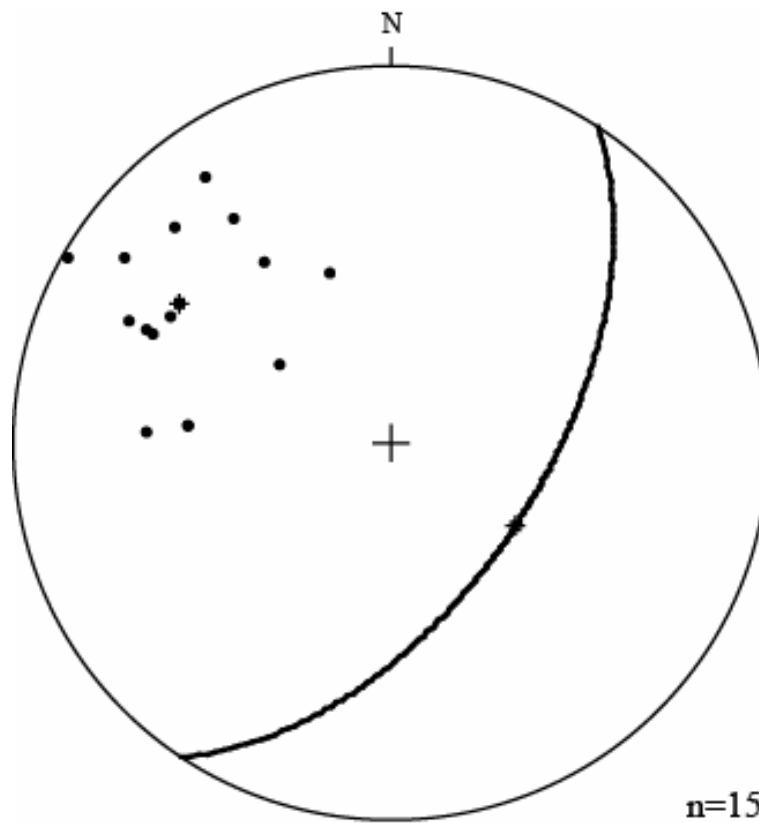


**Figure 33. Lower Hemisphere, equal area projection of fault data related to northeast-striking faults. Data shows a cluster of poles to planes in the northwest, indicating northeast-striking faults. Great circle represents average orientation of all northeast data:  $033^{\circ}; 57^{\circ}$  SE.**

### Amount of Northwest-Southeast Extension

Extension in the northwest-southeast direction was calculated to be 15% after the methods of Twiss and Moores (1992). This is in contrast to amount of extension by Brand (2005) which he estimated to be 8.5 - 10% of the for the Rover Peak area. However, this amount is within the estimates of extension for the Basin and Range province of 5 – 15% (see Thompson and Burke, 1974). Zoback et al., (1981) also suggest up to 23% extension in parts of the Basin and Range in north-central Nevada. The amount of extension calculated above may be an overestimate because of unknown geometries of faults at depth. If the faults at depth are made of multiple minor faults, than the estimate would be too high. Conversely, because the amount of total erosion is not known, and the Tc<sub>1</sub> marker horizon in one of the tilted blocks was removed, the estimate would be a minimum (Morley, 1996). This estimate is also based on the assumption of dip parallel movement along planar faults. The presence of lineations on a portion of the North Red Creek fault suggests some oblique movement has occurred.

### Timing of Northwest-Southeast Extension

Brand (2005) obtained an <sup>40</sup>Ar-<sup>39</sup>Ar date from tilted Hickey basalt in the Rover Peak area of 13.5 Ma and a younger age of flat-lying basalts at 6.4 Ma. With correlation of the volcanics to the north in the Bloody Basing, this loosely constrains the timing of

faulting in this area to between 13.5 and 6.4 Ma (see timing of northeast-southwest extension for additional constraints).

### **Northwest-Trending Faults**

The northwest-trending faults in the study area are a series of normal faults with down to the northeast and down to the southwest movement. Displacement along these faults is variable, and may be as little as 10's of meters (see B – B'; Plate 1) to as much as and probably more than 600 m on the Verde fault (Wrucke and Conway, 1987).

Beginning in the south of the study area, a high angle normal fault exists with down to the northeast motion. From the furthest southeastern position along the fault, heading northwest to Forest Service Road 24 (Plate 1) this fault has a consistent strike to the northwest and maintains a northeasterly dip of 55°-65°. A jog to the west in the fault trace occurs northwest of Forest Service Road 24, for a short distance before continuing strike to the northwest. This jog may be the result of a minor cross-cutting fault that displaces the trace of this fault to the southwest (Figure 34) along Forest Service Road 24. Tertiary volcanics and sediment northeast of this fault dip moderately (20°-30°) into the fault and appear to level off with closer proximity (Plate 1). The northwestern trace of this fault appears to terminate in the Hummingbird Spring area where it cuts across the main Pine Mountain fault (Plate 1). To the southeast this fault connects with a previously mapped fault by Brand (2005) where it maintains consistent strike before turning south near the Verde River.



**Figure 34. Photograph of northwest-striking fault being displaced by a minor northeast-striking fault along Forest Service Road 24. Displacement is less than 20 m as measured along strike of the cross-cutting fault. Lineations on cross-cutting fault of  $35^{\circ} \rightarrow 250^{\circ}$  are consistent with relative motion shown here. Photograph is looking  $320^{\circ}$ .**

Continuing to the north, another well exposed fault exists northeast of Tangle Creek (Plate 1; Figure 28) and appears to form the conjugate pair of the previously mentioned fault. Measurements along this fault reveal a northwest-southeast strike and dip to the southwest of  $65^{\circ}$ . Tertiary strata dip moderately away from the fault up to  $30^{\circ}$ , to the southwest. The trace of this fault becomes concealed to the northwest and southeast under Tertiary and Quaternary sediments (Plate 1). Figure 35 is a cross-section through the two previously discussed faults to demonstrate the geometry of the area.

Further to the northeast, a well exposed fault along Red Creek (Plate 1; Figure 28) also displays southwest-side-down motion. Direct measurement on this structure show a northwest-southeast strike, with a steep dip to the southwest at  $68^{\circ}$ . Striations observed on the polished Precambrian granite footwall (Figure 36) record nearly pure dip-slip motion. The trace of this fault probably continues northwest, beyond where it is currently mapped, based on the outcrop expression of the Precambrian granite to the northwest (Plate 1). However, fault recognition in these volcanics is often difficult precluding the ability to trace the faults extensively.

Wrucke and Conway (1987) show a trace of this fault continuing southeast across the Verde River with opposite side down motion. The reason for this is unclear, although it may have to do with some type of transfer boundary concealed under Quaternary sediment along the Verde River corridor.

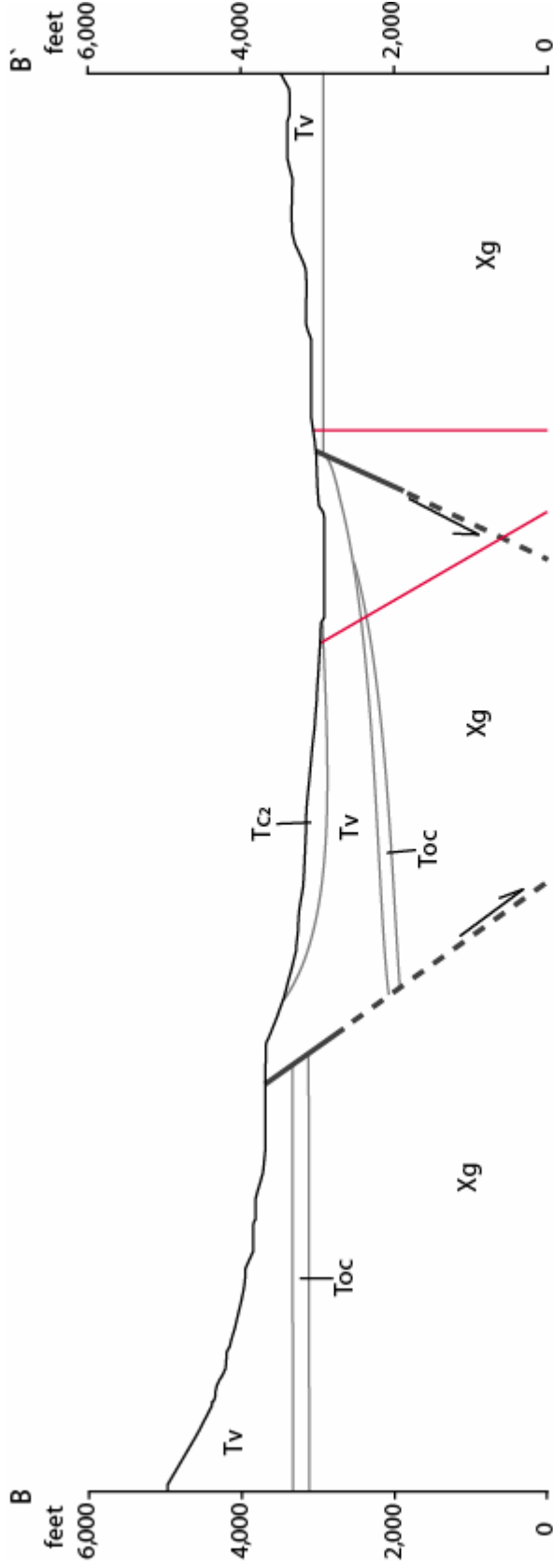


**Figure 35. Simplified cross-section B-B' showing geometries of conjugate faults. Red lines indicate dikes. See Unit Description for explanation on symbols used. Also see Plate 1 for location of cross-section. Cross-section has no exaggeration.**



**Figure 36. Mineral lineations on the Red Creek fault recording nearly dip-slip movement. Lineations are oriented 68→220°. Photograph looking 042°. Pencil for scale.**

### Verde Fault

In the far northeastern corner of the study area is a well exposed trace of the Verde fault readily identified (Figure 37) by a 10-15 m wide zone of gouge or the obvious juxtaposition of Tertiary volcanics on Precambrian granite . The well-known (Canney et al., 1967) Verde fault is a northwest-trending normal fault that is the eastern boundary of the uplifted Black Hills (Ransome, 1925; Anderson and Creasy, 1958) (Pine Mountain is the southern margin of the Black Hills). The Verde Valley to the east is the topographic expression of the down dropped block, which as Ransome (1925) and Elston (1984) describe is a Basin and Range structure that is located well within the Transition Zone. The Verde fault has been traced from near Bakers Pass north of Jerome (Anderson and Creasy, 1958) to the Mazatzal Wilderness area where it intersects the Deadman fault (Wrucke and Conway, 1987), a length of approximately 95 km. The Verde fault zone consist of up to 13 strands near the town of Jerome with primarily normal sense motion that have been down dropped progressively to the east. This zone eventually turns to a single strand 6.5 km south of 34° 15' in the Black Hills (Anderson and Creasy, 1958). Movement along the Verde fault has a protracted history, with vertical separation of up to 300 m during the Precambrian and 450 m of displacement occurring following the deposition of the Hickey basalt (Anderson and Creasy, 1958). In the Mazatzal Wilderness, Wrucke and Conway (1987) estimate about 600 m of displacement had occurred.

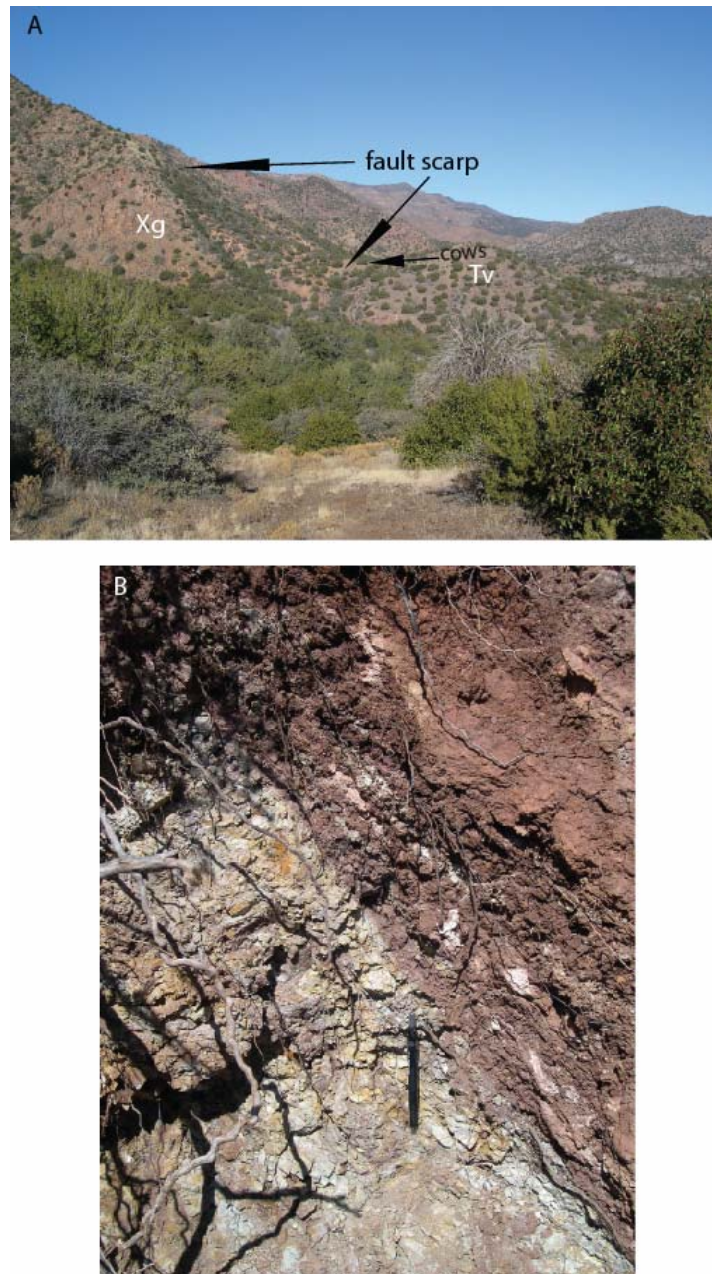


**Figure 37. Photographs showing exposures of Verde fault along the northeastern boundary of the study area. A) down to the northwest volcanics (Tv) against granite (Xg) footwall. Photo looking 330° (approximately along strike). Note cows for scale., and B) detail of Verde fault south of Squaw Butte (Plate 1). Gouge zone approximately 10 m wide in this area. Fault orientation is N 290° W; 55° NE. Pen for scale. Photo looking 290°.**

Dip along the Verde fault varies from 50°-70° to the northeast near Jerome to less than 45° northeast near Black Canyon. In the study area, the structure was measured as 45°-55° dipping to the northeast, with measurable strata dipping gently away from the fault approximately 15° to the northeast. Southeast of Squaw Butte, along the Verde River in the extreme northeast portion of the study area, the Verde fault cuts moderately tilted (55° N-NE) Precambrian bedding (Wrucke and Conway, 1987) (Figure 38).

The intersection of the Pine Mountain fault and the Verde fault (Plate 1) lacks strong evidence to trace the Pine Mountain fault beyond the Verde fault; however, a planar structural fabric exists within the volcanics on the north side of the Verde fault oriented roughly orthogonal to it. This fabric is sub-vertical, consistent with the northeast-trending fault. This feature could represent a trace of the northeast-striking Pine Mountain fault. However, the lack of abundant evidence to trace the Pine Mountain fault to the northeast across the Verde fault demonstrates the cross-cutting relationship of the Verde fault on the Pine Mountain fault.

Finally, Figure 39 is a stereogram of all measurements obtained along well exposed fault traces of northwest-trending structures. The stereogram shows a cluster of poles to fault planes in the southwest, demonstrating the overall northwest-striking and steeply dipping attitude of this fault set. Also shown is the average strike and dip of the faults measured: 302° and 60° NE.



**Figure 38. Steeply dipping Precambrian strata oriented  $290^{\circ}$ ,  $55^{\circ}$  NE. Trace of Verde fault in to the left of photograph where Tertiary volcanics are observed. Author for scale. Photo looking  $090^{\circ}$ .**

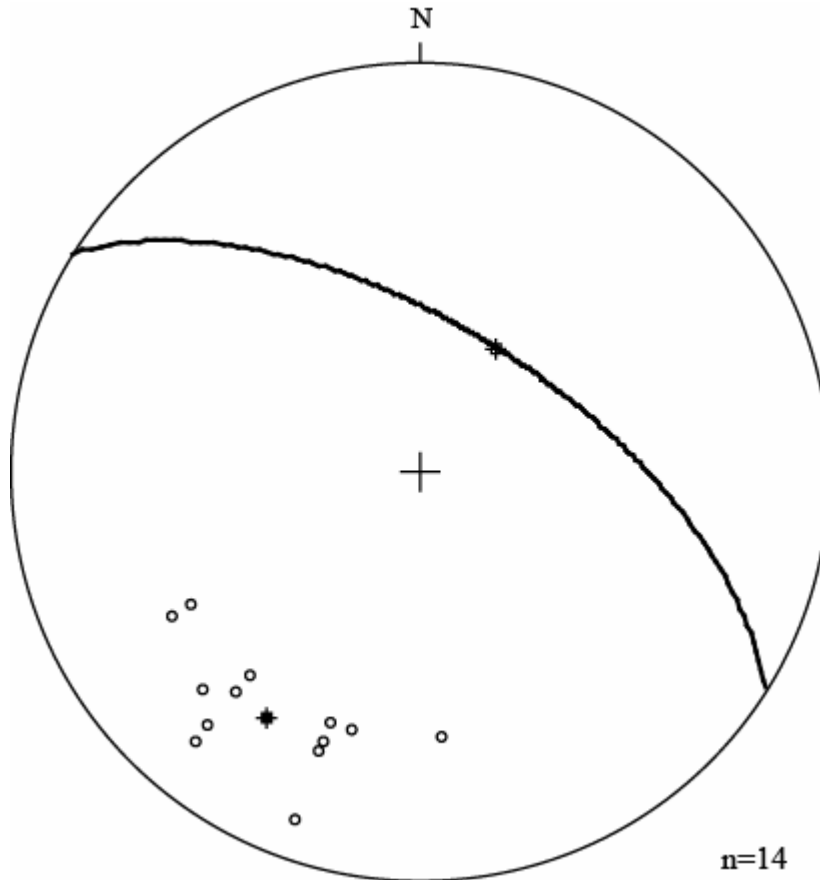


**Figure 39. Lower Hemisphere, equal area projection of fault data related to northwest-striking faults. Data shows a cluster of poles to planes in the southwest, indicating northwest-striking faults. Great circle represents average orientation of all northwest data:  $302^{\circ}$ ;  $60^{\circ}$  NW.**

### *Amount of Northeast-Southwest Extension*

The amount of extension for this direction was not calculated because the estimate would have required the assumption of largely unknown variables. There is a very lengthy span across the Tertiary volcanics in the central portion of the study (Plate 1) area where it would have to be assumed that this is a coherent block. The reality is that the volcanics had been rotated by previous extension making it improbable that this block remained coherent.

### *Timing of Northeast-Southwest Extension*

Timing of extension in this direction can be inferred based on the age of the Verde Formation which followed a major increment of block-faulting along the Verde fault in the Verde Valley (Bressler and Butler, 1978; Elston, 1984). It must also be assumed that by virtue of orientation all northwest-striking structures are related. So, if initial deposition of the Verde Formation occurred around 8 Ma (Bressler and Butler, 1977) a structural basin is suggested to already be in place to receive incoming detritus, constraining the initial movement on the fault; however deposition and faulting may have occurred simultaneously (Anderson and Creasy, 1958). This indicates that movement along the Verde fault may have started prior to 8 Ma in the Verde Valley, with continuation through to the Quaternary (Menges and Pearthree, 1983). It is not known whether movement along this fault in the Verde Valley was occurring at the same time as

the southern reaches, i.e., Pine Mountain area, however the amount of displacement that has occurred in this area and the fact that displacement along the Verde fault increases to the south from Jerome (p.81 Anderson and Creasy, 1958) suggests that the timing of initial movement can be extrapolated to the south. Elston (1984) also suggested initial movement along the Verde fault began around 8 Ma.

### **Reverse and Strike-Slip Faulting**

Two northeast-striking reverse faults are well exposed west of the Mustang Hills (Plate 1; Figure 28). These faults are parallel to one another, but largely different in angle of dip. The southern fault is a high angle structure that dips approximately  $70^\circ$  to the southeast. The northern fault dips moderately ( $45^\circ$ ) to the southeast. Vertical displacement on these faults is largely unknown, however based on the faulted units and outcrop exposure of Tertiary volcanics and Tertiary sedimentary rocks, displacement is thought to be minor compared to the adjacent high angle normal fault, (See cross-sections in Plate 1) i.e., if reverse faults had significant vertical movement, they would have likely exposed underlying basement rock.

A well exposed strike-slip fault (Figure 40A) is located west of the Mustang Hills. A sub-vertical, left-lateral strike-slip structure is observed displacing Tertiary strata. Movement along this fault was recorded by moderately ( $45^\circ$ ) north-dipping lineations on the plane of the exposed fault (Figure 40B), demonstrating a strike-slip sense of motion



**Figure 40. Photographs of strike-slip faulting in the Bloody Basin. A) on-strike exposure of the fault showing Tertiary dome (Td) on the left and Tertiary volcanics (Tv) on the right. Staff is 1.3 m. Photograph looking  $140^\circ$  and B) striations oriented  $45^\circ \rightarrow 345^\circ$  on Td side of fault record oblique slip motion. Photo looking  $145^\circ$ .**

with a dip-slip component. Total displacement in both the vertical and horizontal directions on this structure is also largely unknown, however based on outcrop exposure of the faulted rocks, net displacement could be from 1-2 hundred meters.

The development of the reverse faulting is thought to be the result of movement along the left-lateral strike slip fault. The bend in the fault would act as a restraining zone, providing appropriate conditions for the generation of reverse type faulting.

#### *Timing of Reverse and Strike-Slip Faulting*

Based on cross-cutting relationships, the timing of these structures succeeds evolution of the main Pine Mountain fault in the Bloody Basin, < 13.5 Ma. Additional constraints come from the inferred age of the rhyolite dome (discussed below) which could be as young as 8 Ma.

#### **Dikes**

Eight basaltic dikes were mapped in the study area. Dikes are generally vertical and range in thickness from 0.25 m to 4 m and have linear exposure of 0.5 to 1 km. Dikes intrude Tertiary volcanics and sediments and in at least two instances are coincident with faults, near Tear Springs and north of Tangle Creek. Figure 41 is a stereogram of orientations measured for dikes in the study area. The average trend of

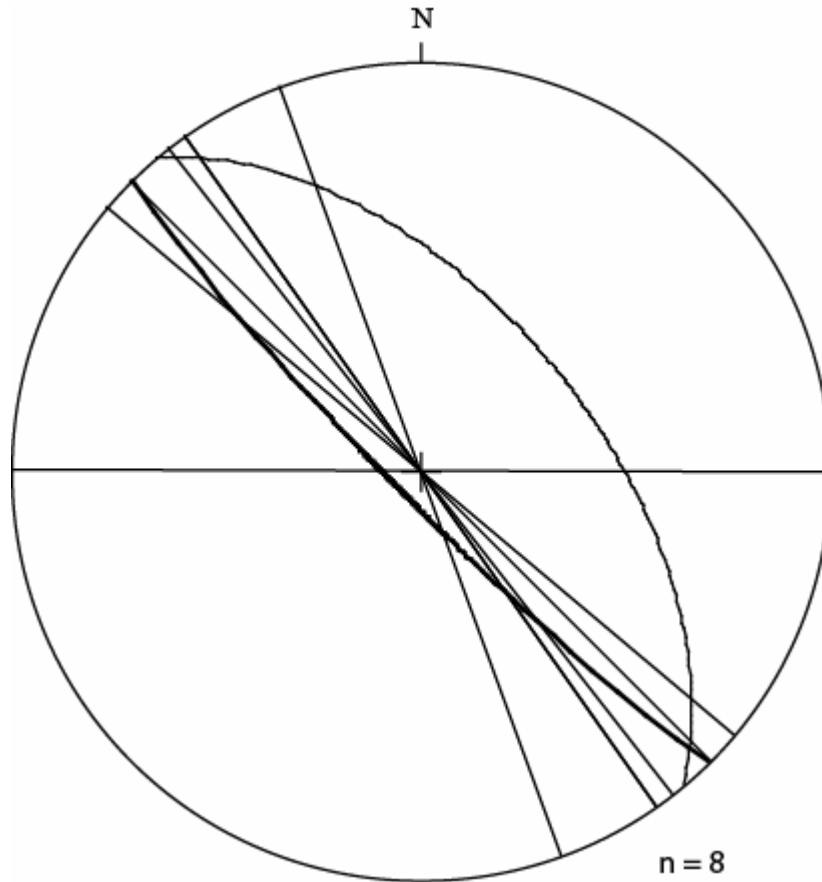


**Figure 41. Lower Hemisphere, equal area projection of dike orientation data. Data shows planes striking northwest-southeast, indicating northwest directed extension. Average orientation of all data: 315°.**

these dikes is  $315^\circ$ . These dikes are interpreted as Mode I structures, i.e. wholly dilatational (see Davis and Reynolds, 1996) and assuming they have not been rotated from original emplacement, the extensions direction required would be in the northeast-southwest direction. The average strike of the dikes mentioned above, coincides within  $15^\circ$  of the average northwest-striking faults.

#### Timing of Dike Emplacement

Dike emplacement is constrained by the fact they intrude Tertiary sediments and by the inference they are related to northeast –southwest extension, coeval with movement along the Verde fault, at least 8 Ma.

#### Dome

The Tertiary dome has a core with well developed flow banding, in some portions highly deformed by folding, grading outward to angular blocks and fragments of the same composition. Flow bands vary in orientation and can be nearly vertical to moderately dipping ( $30^\circ$ ). The steeper bands are generally toward the interior of the dome. This dome is centered on the through going northeast-striking Pine Mountain fault. Approximately 6.5 km to the northeast, in the Pine Mountain Wilderness, Canney et al. (1967), document at least three other such structures describing them as pluglike masses with similar weathering and composition as the dome observed in the Bloody

Basin. Their age assignment for the structures found in the Pine Mountain area, was Quaternary based on fresh appearance and similar structures found in the Verde Valley that penetrate the Verde Formation of 8 to 2.5 Ma (Bressler and Butler, 1977). If correlative, this age would suggest strike-slip faulting in the Bloody Basin would have to be younger than 8 Ma as this dome is offset by strike-slip faulting.

## DISCUSSION

### *Least Principal Stress Direction*

In the southwestern United States observations have been made concerning more than one orientation of Tertiary aged extensional features such as dikes and normal faults. These observations have led to studies conducted throughout the Basin and Range province to try and demonstrate that for example, suites of dikes oriented orthogonal to one another could be products of a reoriented least principal stress direction (see Rehrig and Heidrick, 1976). Determination of the least principal stress direction is applicable to features such as normal faults based on Anderson's theory of faulting (Anderson, 1951), where the least principal stress direction is orthogonal to the strike of the fault. This determination is equally applicable to extensional dikes known as Mode I (Twiss and Moores, 1992) features that require a local direction of least principal stress perpendicular to the strike of the planar body (Davis and Reynolds, 1996). Because the Bloody Basin contains more than one orientation of normal faults and Mode I features, it follows that there could be a manifestation here of a reoriented least principal stress direction displayed in late-Tertiary aged structures.

The orientation of the least principal stress direction from mid-Tertiary to present has been documented based on work conducted in Arizona and the southwest. Rehrig and Heidrick (1976) conducted a structural analysis of mid-Tertiary dikes, veins and stocks of Arizona and concluded a late Oligocene to Miocene regional  $\sigma_3$  stress orientation of  $\text{ENE} \pm 20^\circ$ . Zoback et al. (1981) also concluded this orientation for the

southern Basin and Range during mid- Miocene (20-10 Ma), citing trends of dike swarms, fault slip vectors, stratal tilts. Leighty (1997) discusses multiple least principal stress orientations for central Arizona: early Miocene (mid-Tertiary orogeny) → NE-SW directed extension; late-middle Miocene to late Miocene (Basin and Range Disturbance) → E-W directed extension; and late Miocene and younger (crustal buoyancy extension) → NE-SW directed extension. Currently, and broadly speaking, the least principal stress direction along the southwestern margin of the Colorado Plateau, i.e., the central Transition Zone, is directed northwest-southeast (Zoback and Zoback, 1989). Perpendicular to this direction and within the Colorado Plateau province is a northeast-southwest directed least principal stress field (Zoback and Zoback, 1989).

Studies that have focused on documenting manifestations of a varying least principal stress direction, such as the above fault and dike scenarios, have been ascribed to be the result of: 1) a reorientation of the least principal stress direction (Angelier et al., 1985) or 2) an interaction between more than one least principal stress direction, such as that between the Colorado Plateau and the Basin and Range provinces (Arabasz and Julander, 1986). Angelier et al. (1985) document multiple fault orientations in a study conducted near Hoover Dam and conclude the observed faults are the result of a reorientation of the least principal stress direction that occurred during the late Cenozoic. Conversely, studies conducted in the southeastern Transition Zone (see Aldrich and Laughlin, 1984) and in the seismically active western Transition Zone (see Arabasz and Julander, 1986) have concluded that varying orientation of extensional features are the

result of an interaction between least principal states of stress between the Colorado Plateau and the Basin and Range provinces.

In the Bloody Basin, the development of the northeast-trending structures (i.e. Pine Mountain fault) as well as the north-northeast-trending Verde River graben (Figure 42) (Wrucke and Conway, 1987), suggests extension occurred in a northwest-southeast direction. If timing of these northeast-trending structures is also considered ( $< 13.5$  Ma), one would expect that a similar orientation of structures would have developed due the bulk extension direction in place at this time in the southwest United States, which was E-W to ESE-WSW directed during the Basin and Range Disturbance (see Spencer and Reynolds, 1986, 1989). Based on the age of the tilted rocks in the Bloody Basin, timing of the northeast-trending structures is coeval with the Basin and Range Disturbance, but the extension direction required to produce these features is not entirely consistent with the Basin and Range directed extension. To account for this extension direction discrepancy, influences by preexisting structures (see Fault Orientations with Regional Considerations Section) may have played a role in the development of these normal faults precluding a required extension direction orthogonal to the strike of the fault.

If one considers the northwest-trending normal faults (i.e., Verde fault) and dikes in the Bloody Basin, the extension direction required to produce these features would presumably be northeast-southwest, nearly perpendicular to that described above. The northeast-southwest extension direction does not coincide with that of the bulk extension related to the Basin and Range Disturbance (discussed above). Additionally, because these features are thought to be distinctly younger (see next section) than the northeast-

trending structures, a timing discrepancy precludes their formation during the Basin and Range Disturbance. If the current direction of least principal stress is considered for the Colorado Plateau, then it could be asserted that the extension direction responsible for the Verde fault and other northwest-trending structures (i.e. dikes) in the Bloody Basin may have been influenced by the least principal stress that currently exists within the Colorado Plateau. This assertion is supported by the coincidence of the extension direction required for the development of the northwest-trending normal faults and the northwest-trending extensional dikes versus that of the current least principal stress of the Colorado Plateau, i.e., northeast-southwest directed. This is further supported by the fact that the Verde fault has had Quaternary movement along it (Menges and Pearthree, 1983) suggesting this least principal stress direction may still be in place.

Unlike studies showing the interaction of the states of stress between the Colorado Plateau and Basin and Range provinces (Aldrich and Laughlin, 1984) where it is shown that a zone of transition between the stress fields of both provinces reflects intermediate directions in terms of structural orientations, the Bloody Basin region may display a very discrete differentiation between past and present least principal stress directions in the Transition Zone.

*Fault orientation with Regional Considerations*

Studies conducted adjacent to the Bloody Basin (e.g. Brand, 2005; Wrucke and Conway, 1987; Canney et al., 1967) have resulted in differences of interpretation regarding the structural features observed, notably the orientation of faults. Wrucke and Conway (1987) suggest that fault geometries observed in the Mazatzal Wilderness are a result of contemporaneous formation, citing the fact that cross-cutting relationships are observed by all fault orientations. Also, the curving of faults from a northerly trend to a more northwesterly trend is observed, suggesting a continuum rather than a clear truncation or cross-cutting relationship. They go on to say, however, that north-trending structures are more commonly offset by the northwest-trending structures. Brand (2005) agreed with this interpretation using the Lime Creek fault and Horseshoe Dam fault as an example of a north-trending fault curving to the northwest, which intersects and cross-cuts a northeast-striking fault, and has resulted in the formation of rhomb-shaped fault blocks. Brand (2005) agrees with Leighty's (1997) interpretation that the north and northwest-trending structures are a result of an extensional continuum, rather than separate tectonic events. Work in the Bloody Basin shows an obvious trend of a set of faults to the northeast and a mutually orthogonal northwest -trending set (Plate 1). This relationship is consistent with the work by Canney et al. (1967) in the Pine Mountain Wilderness area, where their mapping also shows clear perpendicular sets of faults. They attribute these geometries to be the result of separate faulting events; however they do not clearly suggest a chronology of these events. Additionally to the south, Ferguson et al. (1998)

describe north-striking faults in the New River Mesa area that they interpret as the result of late-Miocene east-west extension (Basin and Range Disturbance) (see Leighty, 1997). They also describe a set of northwest-striking faults resulting from northeast-southwest oriented extension in the New River Mesa area that they suggest may have resulted from waning movements on the metamorphic core complex system to the south, block faulting of the Basin and Range Disturbance, or an even younger extensional event. Figure 42 is a simplified tectonic map of the region, including Pine Mountain Wilderness, Mazatzal Wilderness, Rover Peak quadrangle, New River Mesa quadrangle, Humboldt Mountain, and this study. The map demonstrates two orthogonal orientations of faulting throughout the region.

In the study area, four main criteria to evaluate the chronology of faulting and ultimately to support evidence for suggesting a reorientation of  $\sigma_3$  or an interaction of stress fields with a dominant direction prevailing are: 1) cross-cutting relationships at fault intersections, e.g., the Verde fault and Pine Mountain fault. Not only is the Pine Mountain fault truncated by the Verde fault, but also the southerly trace of this fault appears to be truncated by another northwest-striking fault (Plate 1). Additionally, based on field relations, other northeast-trending faults are truncated by these northwest-trending structures. The general northeast-southwest-trending Verde River graben (Wrucke and Conway, 1987) would require extension perpendicular to this overall direction, i.e., northwest-southeast directed. This structure is truncated by the through-going Verde fault (Figure 42); 2) orientation of Mode I fractures (dikes) are coincident with northwest-striking faults and they intrude basin fill thought related to the first

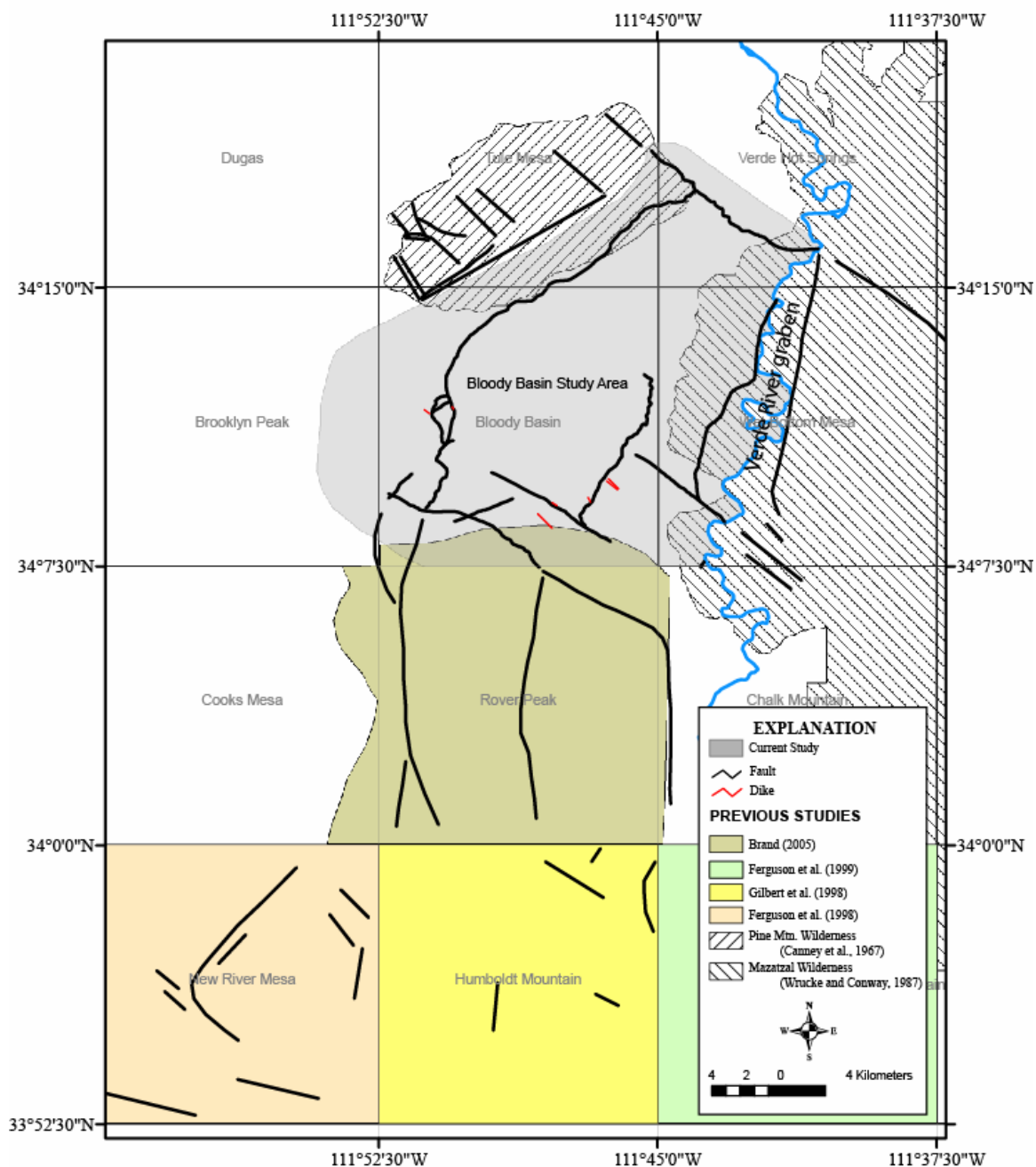


**Figure 42. Simplified tectonic map showing fault distributions in: Pine Mountain Wilderness, Mazatzal Wilderness, Rover Peak, New River Mesa, Humboldt Mountain, and the present study. A northwest-trending set of faults cross-cuts a northeast-trending set. Note the absence of northeast-trending faults beyond Pine Mountain Wilderness.**

extensional event. Assuming these dikes are Mode I fractures, a perpendicular orientation to the local direction of least principal stress is implied (Davis and Reynolds, 1996), i.e. northeast-southwest. Dike orientation and average strike of northwest-trending faults is within  $15^\circ$  (see Figures 41 and 39; respectively), by virtue of this similarity they are considered related and both types of structures are a result of northeast-southwest directed extension; 3) fault orientation data indicate a nearly  $90^\circ$  difference in dip direction of fault plane sets in the study area. Figure 43 shows combined fault plane data from the study area, and 4) the presence of the Verde River graben (Wrucke and Conway, 1987) supports a distinct extension direction from that responsible for the northwest-striking faults and dikes.

One question that remains unclear is the origin of the northeast-striking faults. Although evidence for these structures indicates formation in a northwest-southeast directed extensional regime, this fault orientation is anomalous in a more regional context. Review of the Arizona State geologic map (Reynolds, 1988) reveals a northeast-trending swath through this part of the Transition Zone that contains other northeast-trending faults southwest of the Bloody Basin. Northwest and southeast of this swath, faults are generally northwest-trending. One explanation for this anomalous fault orientation could be preexisting Precambrian structures that underlie the piles of volcanics in this area of the Transition Zone. Elston and Young (1991) report that many faults in Arizona have experienced episodes of reactivation and that the origin of these structures derives from Precambrian tectonic episodes. They go on to further say that these structures may have been reactivated during Neogene faulting. The dominant

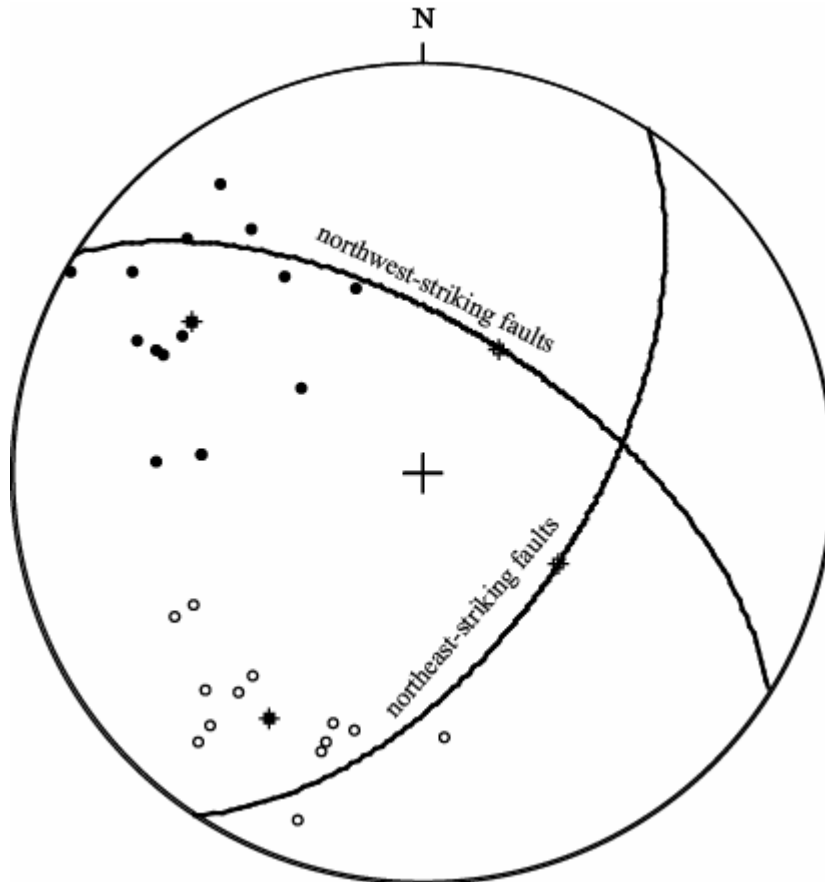


**Figure 43. Stereogram showing orthogonal orientation of fault plane data from the Bloody Basin. Solid circles are poles to planes of northeast-trending structures and open circles are poles to planes of northwest-trending structures. Average fault plane orientation for closed circles is:  $033^{\circ}$ ;  $57^{\circ}$  SE. Average fault plane orientation for open circles is:  $302^{\circ}$ ;  $60^{\circ}$  NW. The difference between strike of these two averages is:  $91^{\circ}$ .**

structural trends of Proterozoic rocks, as reported by Karlstrom et al. (1987), are north to northeast. Hendricks and Plescia (1991) report a series of northeast-trending positive magnetic anomalies across the Colorado Plateau that have been shown to originate in the Precambrian basement (Hedricks, 1974; Shoemaker et al., 1978; and Sumner, 1985). These anomalous ridges have also been related to major structural features (Shoemaker et al., 1978) with origination occurring during Precambrian tectonic episodes and later reactivated by Laramide and Basin and Range faulting events. Figure 44 is a simplified map of these northeast-trending lineaments across the Colorado Plateau. Hendricks and Plescia (1991) project the Holbrook lineament (Figure 44) southwestward across the Transition Zone, citing coincidence of the lineament with the vertical offset of the Moho described by Warren (1969). This projection centers on the Bloody Basin (Figure 44) and its boundaries are coincident with the absence of northeast-striking faults, northwest of the southeastern margin of Pine Mountain (Canney et al., 1967; Anderson and Creasy, 1958). This northeast orientation also wanes southeast of this projected lineament. It is reasonable to assert, based on its location and orientation, that the Holbrook lineament may be responsible for the observed orientations of the northeast-trending structures. These structures may be the result of reactivated preexisting Precambrian structures and because an existing weakness does not exist beyond this anomaly, northeast-trending structures are not observed. Pine Mountain may mark the northern boundary zone of this lineament.

Lastly, if the geographic position of the Bloody Basin is considered with other well developed structural basins in the Transition Zone, an elongate northwest-trend of

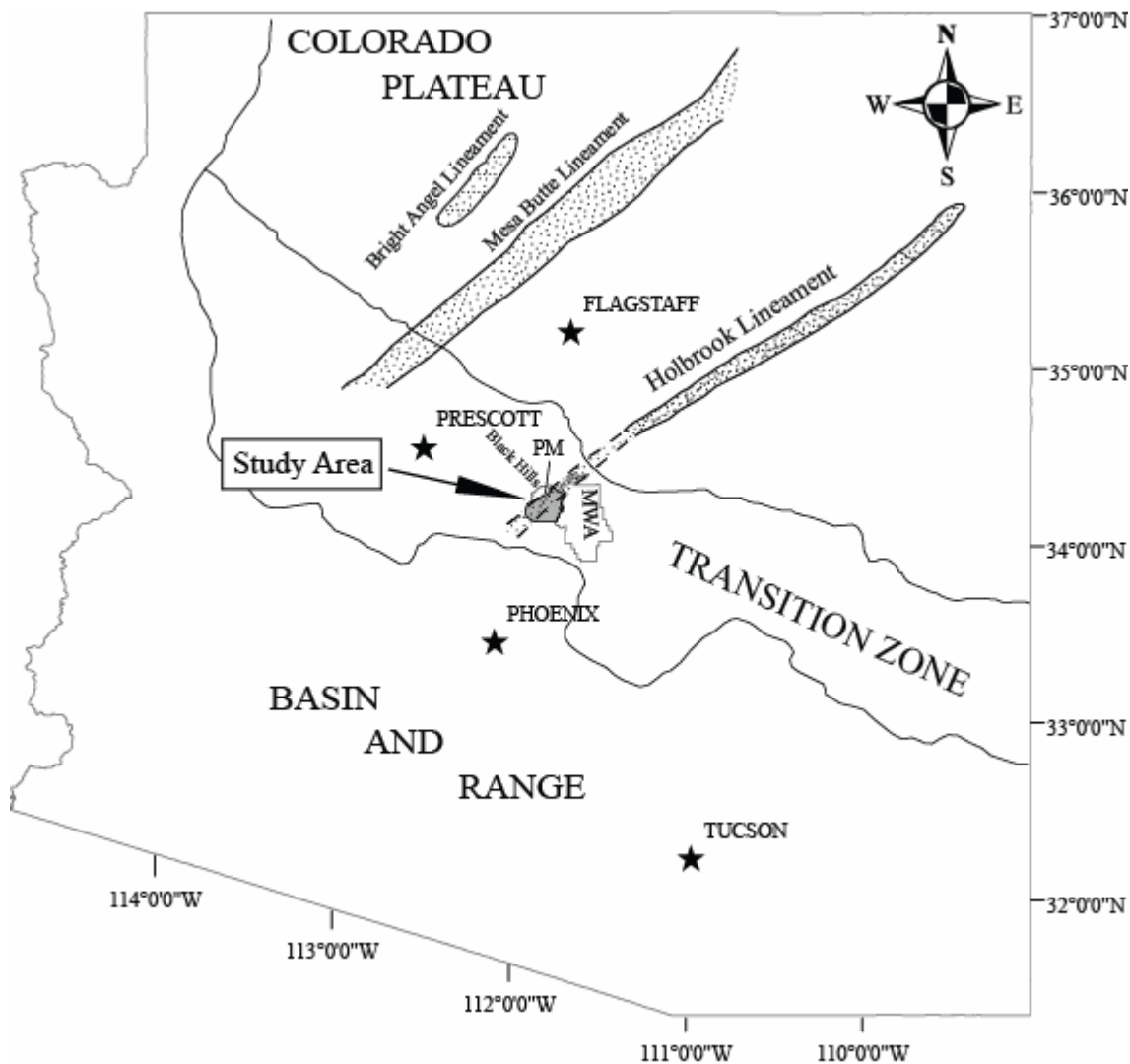


**Figure 44.** Map showing major northeast-trending positive magnetic anomalies that may be related to major Precambrian features (see text for details). The projection of the Holbrook lineament cuts across the southeast margin of the Pine Mountain Wilderness area, north of which, northeast-trending faults are not observed. Note this orientation of the Holbrook lineament coincides with normal faults in the Bloody Basin and vicinity. PM = Pine Mountain; MWA = Mazatzal Wilderness Area (modified from Hedrick and Plescia, 1991).

structures is apparent (Figure 45). In terms of aerial extent however, the Bloody Basin is comparatively smaller than these other Transition Zone basins. Timing of the depositional environments from the Payson-Tonto Basins to the Verde Basin reveals a northwest younging (see Figure 2 in Nations et al., 1982). Based on this trend, and the fact that the Bloody Basin is located between the Payson-Tonto and Verde Basins, there is a suggested link between all of these structures. Whether it is chronologic or genetic is unclear.

#### *Fault-block widths*

Two models have been proposed in the literature to explain Basin and Range structural development. One model is related to curved, downward flattening listric faults. The other model is related to horst and graben development (see p. 33 of Effimoff and Pinezich, 1986) above either plastically extending substrate or the result of fragmentation and segmentation into buoyant tectonic blocks. In the Bloody Basin study area, the western rim of the basin is a relatively flat-lying, thick sequence of Hickey basalt. Initial faulting occurs approximately 5 km east of the presumably retreated rim margin. Widths of fault blocks within the Bloody Basin are between 2 and 5.5 km. South of the Bloody Basin, in the Rover Peak area, major fault blocks are roughly 5 km wide (see Brand, 2005, Plate 2). The widths of the blocks in both areas are considerably less than the average crest to crest width of 30 km that is typical of Basin and Range structures (Stewart, 1998) that may sole into listric type faults.

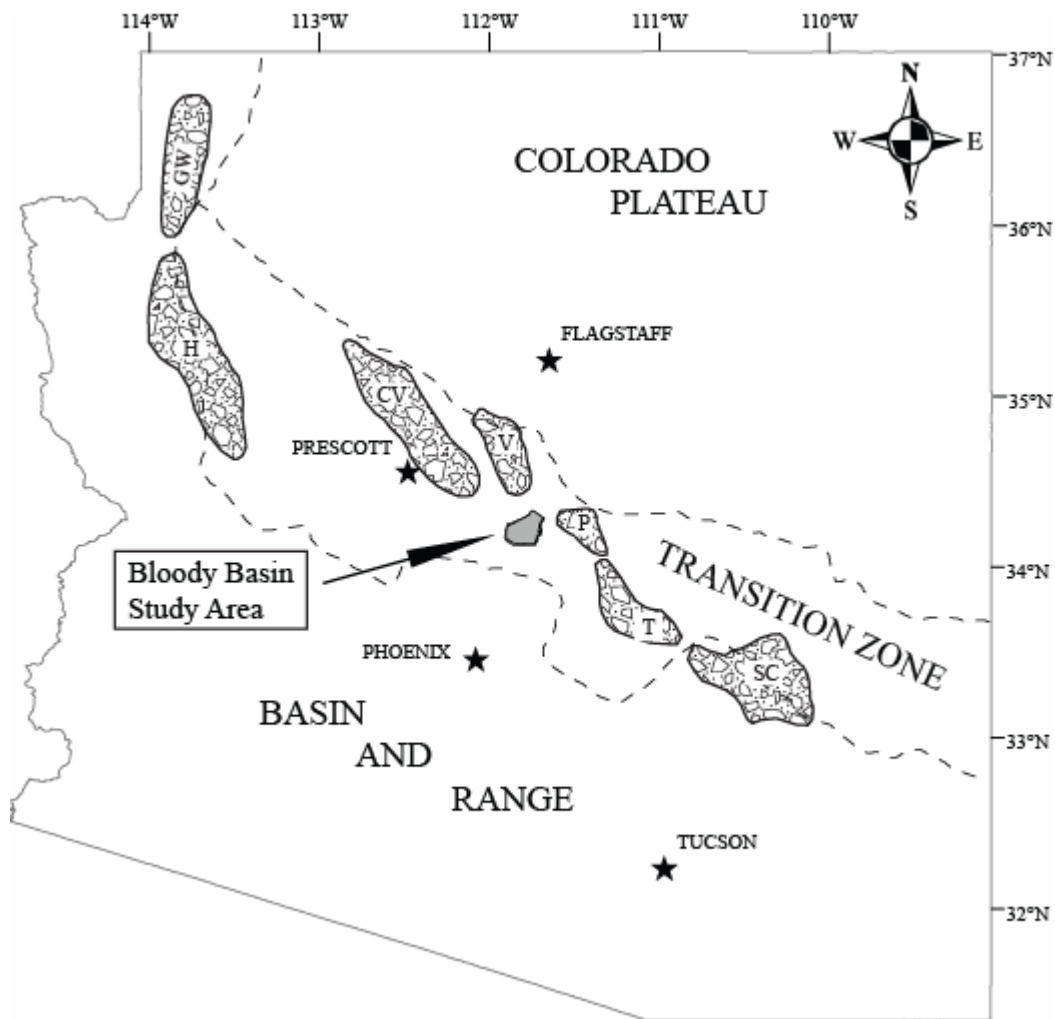


**Figure 45. Generalized map showing locations of major basins in the Transition Zone of Arizona. Note the northwest trend sub-parallel to the boundaries of the Transition Zone. GW = Grand Wash; H = Hualapai; CV = Chino Valley; V = Verde; P = Payson; T = Tonto; SC = San Carlos (modified from Nations et al., 1981).**

In terms of block rotation, rotating a relatively narrow (2-5 km) fault block to a depth of 10-15 km (brittle-ductile boundary) where a high-angle fault could sole out into a master listric fault seems unreasonable. In order to accommodate such movement, major dislocations of the block, either vertical or otherwise, would be required. These major dislocations would probably be manifested in surface expressions such as faulting, but such are not observed in the Bloody Basin. It is more likely that block faulting is of horst and graben type, which is observed in the Verde River corridor (see Verde River graben, Figure 42). To what depths faults continue is unclear, but it is suggested that a weak zone within basement material, possibly preexisting (see above), may be responsible for the narrow, moderately rotated blocks.

#### *Relations to Basin and Range Disturbance*

The timing of northwest-southeast directed extension is coeval with the Basin and Range Disturbance as indicated by the ages yielded from tilted Hickey basalts in the Cedar Mountains area (Brand, 2005). Timing of the northwest-trending structures are presumably younger than the Basin and Range Disturbance, especially considering the northwest-trending Verde fault has been active in the Quaternary Period (Menges and Pearthree, 1983). The uplifted Black Hills are a response to movement along the Verde fault, which has created a basin and range physiography and, as Ransome (1925; among others) puts it, this is a Basin and Range type structure that is impressed into the Transition Zone, but as indicated above the timing is not consistent with the Basin and

Range Disturbance. The style of faulting present in the Bloody Basin, i.e., high-angle normal faults with stratal rotations of up to  $30^\circ$ , is in contrast with the very little stratal rotation that is typically associated with Basin-Range tectonism (Stewart, 1998).

Additionally, if dip-slip displacement is considered a characteristic accompanying these high-angle faults, as Loring (1976) suggests, then the northeast-trending faults that are observed recording oblique movement (Figure 32) would not fit this dip-slip description. However, the younger northwest-trending faults that record dip-slip displacement (Figure 36) are consistent with this dip-slip quality. The magnitude of extension of the area does not quite compare to typical Basin-Range physiography in that high-angle normal faults are not concealed by deep alluvial basins, with up to 50 km separating ranges. The Bloody Basin contains basin-filled detritus, in some cases only locally, and fault bounded blocks are a maximum of 5 km apart.

### *Conclusions*

In terms of extensional faulting in the Bloody Basin, there exist manifestations of two separate deformational events. The first event, with northwest-southeast directed extension, resulted in a series of northeast-striking, high-angle normal faults with down-to-the-southeast motion. The orientation of these faults may be the result of the combination of extended crust and influence by pre-existing structures in Precambrian basement material. If these northeast-trending faults were influenced by preexisting structures such as the Holbrook lineament, then the resultant normal fault orientations

may not need a perpendicularly oriented least principal stress direction. This may be supported by the fact that lineations observed on these northeast-striking structures record oblique movement. Based on the timing of this first event ( $< 13.5$  Ma), extension was occurring in this portion of the Transition Zone during the Basin and Range Disturbance. This extension is manifested by: 1) northeast-trending, high-angle normal faults with moderate stratal rotation and 2) the presence of the north-northeast-trending Verde River graben.

The second event, with relative northeast-southwest directed extension, resulted in a series of northwest-striking normal faults and extensional dikes that cross-cut the preexisting northeast-striking structures. The orientation of these northwest-striking structures is not consistent with the bulk extension that occurred during the Basin and Range Disturbance and the timing of the Basin and Range Disturbance is presumably much older. Because the Verde fault has Quaternary movement along it and because of its proximity to the Colorado Plateau, the modern day least principal stress direction of the Colorado Plateau may be applied, which is northeast-southwest directed in this region. This least principal stress direction of the Colorado Plateau is consistent with that required for the development of the northwest-striking extensional features in the Bloody Basin. These northwest-striking extensional features may be a product of the coherent plateau extending away from its interior, in a fashion suggesting the margins of this massive block are being pulled away by an extending terrain. This type of mechanism and timing is also consistent with the crustal buoyancy deformation that Leighty (1997)

suggests for late-Miocene and younger that involved northeast-southwest directed extension.

Because of inconsistent styles and orientations of structures in the Bloody Basin area, a clear cut relationship to the Basin and Range Disturbance is difficult, albeit the timing of some fault orientations are coeval with that of the Basin and Range Disturbance. The relative least principal stress direction required to form the northeast-trending normal faults is not entirely consistent with that of the Basin and Range, however, the timing of these extensional events is consistent. It is suggested that a pulse of Basin and Range tectonism affected the area, but may have been influenced by preexisting basement structures. Because of the short duration of this extensional episode, highly extended terrain with deep alluvial valleys did not develop. Following this pulse of extension, the more dominant least principal stress direction of the Colorado Plateau region resulted in extension perpendicular to the previous northwest-southeast direction. Movement along the Verde fault ensued along with other subordinate and similarly oriented extensional features.

## **TERTIARY HISTORY**

Tertiary events of the Bloody Basin area can be dated from about 33-38 Ma based on the correlation by Elston (1984) of the Bloody Basin fanglomerate to a similar red fanglomerate in Cave Creek that underlies a tuff containing a fossil of early Oligocene age. By that time, Paleozoic sections of the area had been eroded away and the oldest Tertiary unit in the area, Bloody Basin fanglomerate, was filling fault related troughs (Elston, 1984) and/or irregular topography (Figure 46A and B). The deposition of this fanglomerate was probably in response to strong regional uplift (Elston, 1984) that may have resulted in an eastward thinning (see Figure 5) of this unit to unconformably overlie the widespread Precambrian Verde River batholith.

Following the formation of the Bloody Basin fanglomerate, up to 600 m of olivine-rich and alkaline basalt began to occupy the area around 15 Ma and continued through to at least 13 Ma (Figure 46C). During this interval, west-thinning accumulations of angular, coarse volcanic clastic material marked a period of locally derived deposition that may have been the result of local faulting in the area masked by subsequent lava flows. Also occurring during this period of active volcanism is the deposition of interbedded volcanoclastic sandstone layers and intermittent layers of pyroclastic tuffs. Additionally, local aqueous environments along the now southern edge of the current basin resulted in a relatively thin accumulation of fine-grained mudstone and siltstone.

Following the cessation of volcanism in the area (< 13 Ma), northwest-southeast directed extension produced a synthetic array of half grabens (Figure 46D), with

accompanying block rotation. Movement along these faults probably occurred until at least 8 Ma, but possibly later to allow for local accumulation of volcanoclastic basin fill to be shed into fault related half-grabens. Local accumulations of up to 100 m of chiefly volcanic-rich basin fill material were then capped by granite-rich detritus that records the footwall exposure of the Precambrian granite. Based on orientation, formation of the Verde River graben is coeval with this time frame.

Following the development of the northeast-striking faults and possibly subsequent to the primary basin filling event, emplacement of a viscous, rhyolite magma occurred along the Pine Mountain fault, and developed into a local dome-like mass west of the present day Mustang Hills.

Following the emplacement of the rhyolite dome, a reorientation of the least principal stress direction occurred. A northeast-southwest oriented, least principal stress direction began crustal rifting around ~ 8 Ma (Figure 46E), prior to the initial accumulation of the Verde Formation (Bressler and Bulter, 1977). Extension in this direction resulted in the formation of the Verde fault and other major northwest-striking faults that truncated and offset previously developed faults. Also occurring during this interval is the formation of minor strike-slip faulting along a reactivated, vertical Pine Mountain normal fault which was accompanied by reverse faulting, resulting in the offset of the rhyolite dome. This extensional interval is thought responsible for the current physiography between the topographically subdued Bloody Basin and the well exposed and elevated Cedar Mountain fault blocks to the south, in the Rover Peak quadrangle.

Northeast-southwest extension resulted in a thinned crust and allowed for magma migration along some already developed conduits, such as the fault north of Tangle Creek (Plate 1) and weak zones, and emplaced basaltic dikes into basin fill and volcanic flows (Figure 46F). Figure 46 is a diagrammatic summary of these events.

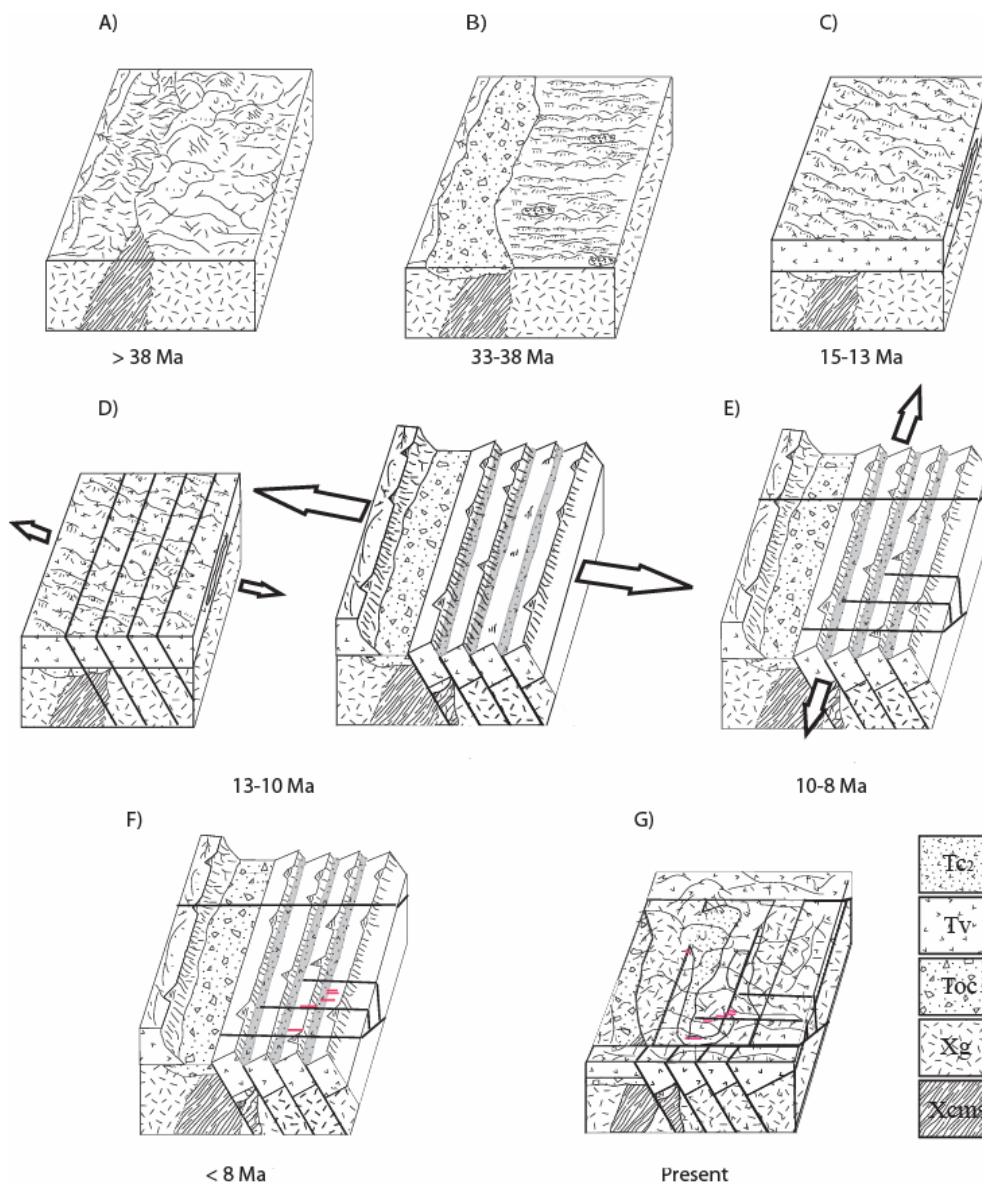


**Figure 46. Simplified, diagrammatic representation of the Tertiary history of the Bloody Basin. A) local basins and depressions developing during regional uplift, B) basins and depressions filled in with locally derived material, C) voluminous deposition of the Hickey basalt blankets the region and preserves older Tertiary conglomerate, D) northwest-southeast directed extension ensues, extending the terrain up to 15% with high-angle normal faults and results in the filling of half-grabens with fault related fill, E) northeast-southwest directed extension follows after a reorientation of the least principal stress field, F) dike emplacement results from over-thinned crust, and G) present day Bloody Basin configuration. Some details have been left out for clarity. See text for details on symbols used. Not to scale.**

## REFERENCES

- Anderson, E.M., 1951, The dynamics of faulting and dyke formation with application to Britain: Oliver and Boyd, Edinburgh, 206 p.
- Anderson, C.A., and Creasy, S.C., 1958, Geology and ore deposits of the Jerome area, Yavapai County, Arizona: U.S. Geological Survey Professional Paper 308, 185 p.
- Anderson, Phillip., 1989, Stratigraphic Framework, Volcanic-Plutonic Evolution, and Vertical Deformation of the Proterozoic Volcanic Belts of Arizona *in* Jenney, J.P. and Reynolds, S.J., Geologic Evolution of Arizona: Tucson, Arizona Geological Society Digest 17, p. 57-147
- Aldrich, M.J., and Laughlin, A.W., 1984, A Model for the Tectonic Development of the Southeastern Colorado Plateau Boundary, *Journal of Geophysical Research*, v. 89, no. B12, p. 10,207-10,218.
- Angelier, J., Colleta, B., and Anderson, R.E., 1985, Neogene paleostress changes in the Basin and Range: A case study at Hoover Dam, Nevada-Arizona, *Geological Society of America Bulletin*, v. 96, p. 347-361.
- Arabasz, W.J., and Julander, D.R., 1986, Geometry of seismically active faults and crustal deformation within the Basin and Range-Colorado Plateau transition in Utah, *Geological Society of America Special Paper* 208, p. 43-74.
- Brand, P., 2005, Tertiary Extension and Fault-Block Rotation in the Transition Zone, Cedar Mountains Area, Arizona, Masters Thesis, Arizona State University, 111 p.
- Bressler, S.L., and Fuller, R.F., 1977, Magnetostratigraphy of the Late Tertiary Verde Formation, central Arizona, *Earth and Planetary Science Letters*, no. 38, p. 319-330.
- Canney, F.C., Lehmbeck, W.L., Williams, F.E., 1967, Mineral Resources of the Pine Mountain Primitive Area, Arizona, *Geological Survey Bulletin* 1230-J, 45 p.
- Chase, C.G., J.A. Libarkin., and A.J. Sussman., 2002, Colorado Plateau: Geoid and Means of Isostatic Support, *International Geology Review*, v. 44, p. 575-587.
- Davis, G.H. and Reynolds, S.J., 1994, *Structural Geology of Rocks and Regions* (Textbook), 2<sup>nd</sup> ed., John Wiley and Sons, Inc., U.S.A., 776 p.
- Eberly, L.D. and Stanley, T.B., 1978, Cenozoic Stratigraphy and geologic history of southwestern Arizona, *Geological Society of American Bulletin*, v. 89, p. 921-940.

- Effimoff, E.B., and Pinezich, A.R., 1986, Tertiary structural development of selected basins: Basin and Range province, northeastern Nevada, *in* Mayer, L., eds., Extensional tectonics of the southwestern United States: Geological Society of America Special Paper 206, 59 p..
- Elston, D.P., 1984, Rocks, Landforms, and Landscape Development in central Arizona, *in* Smiley, T.L., Nations, J.D., Pewe, T.L., Schafer, J.P., eds., Landscapes of Arizona: The Geological Story, University Press of America, p. 151-173.
- Ferguson, C.A., Gilbert, W.G., and Leighty, R.S., 1998, Geologic map of the New River Mesa 7.5' quadrangle, Maricopa County, Arizona, Arizona Geological Survey, Open-File Report 98-12, 29 p., 3 sheets, scale 1:24,000.
- Ferguson, C.A., Gilbert, W.G., Skotnicki, S.J., Wrucke, C.T., and Conway, C.M., 1999, Geologic map of the Horseshoe Dam 7.5' quadrangle, Maricopa County, Arizona, Arizona Geological Survey, Open-File Report 99-15, 11 p., 1 sheet, scale 1:24,000.
- Gilbert, W.G., Ferguson, C.A., and Leighty, R.S., 1998, Geologic map of the Humboldt Mountain 7.5' quadrangle, Maricopa County, Arizona, Arizona Geological Survey, Open-File Report 98-11, 17 p., 3 sheets, scale 1:24,000.
- Gomez, E., 1979, Geology of the south-central part of the New River Mesa quadrangle, Cave Creek Area, Maricopa County, Arizona, United States Geological Survey, Open-File Report 79-1312, 156 p., 1 sheet, scale 1:12,000.
- Hendricks, J.D., 1974, Gravity measurements in the eastern part of the San Francisco volcanic field, Arizona, Geological Society of America, Abstract with Programs, v. 6, p. 446-447.
- Hendricks, J.D. and Plescia, J.B., 1991, A Review of the Regional Geophysics of the Arizona Transition Zone, *Journal of Geophysical Research*, v. 96, B7, p. 12,351-12,373.
- Karlstrom, K.E., Bowring, S.A., and Conway, C.M., 1987, Tectonic significance of an Early Proterozoic two-province boundary in central-Arizona, *Geological Society of America Bulletin*, v. 99, p. 529-538.
- Laznicka, P., 1988, Breccias and Coarse Conglomerates: Petrology, Environments, Associations, Ores, *Developments in Economic Geology*, 25, Elsevier, New York, 832 p.
- Leighty, R.S., 1997, Neogene tectonism and magmatism across the Basin and Range – Colorado Plateau Boundary, central Arizona, Ph.D dissertation, Arizona State University, 1019 p.

- Leighty, R.S., 1998, Tertiary volcanism, sedimentation, and extensional tectonism across the Basin and Range – Colorado Plateau boundary in central Arizona, *in*, Duebendorfer, E.M., eds, *Geologic Excursions in Northern and Central Arizona*, p. 59-95.
- Loring, A.K., 1976, The Age of Basin-Range Faulting in Arizona, *in* Wilt, J.C., and Jenney, J.P., eds., *Tectonic Digest: Arizona Geological Society Digest*, v. 10, p. 229-257.
- McKee, E.H., and Anderson, C.A., 1971, Age and chemistry of Tertiary volcanic rocks in north-central Arizona and relation of the rocks to the Colorado Plateaus: *Geological Society of America Bulletin*, v. 82, p. 2767-2782.
- Menges, C.M., and Pearthree, P.A., 1983, Map of neotectonic (latest Pliocene-Quaternary) deformation in Arizona: *Arizona Bureau of Geology and Mineral Technology, Open-File Report 83-22*, p.48.
- Menges, C.M., and Pearthree, P.A., 1989, Late Cenozoic Tectonism in Arizona and Its Impact on Regional Landscape Evolution, *in*, Jenney, J.P. and Reynolds, S.J., *Geologic Evolution of Arizona: Tucson, Arizona Geological Society Digest 17*, p. 649-680.
- Morley, C.K., 1996, Discussion of potential errors in fault heave methods for extensional estimates in rifts, with particular reference to fractal fault populations and inherited fabrics, *in*, Buchanan, P.G., and Nieuwland, D.A., eds., *Modern Developments in Structural Interpretation, Validation, and Modeling.*, *Geological Society Special Publication no. 99*, pp. 117-135.
- Nations, J.D., 1974, Paleontology, biostratigraphy, and paleoecology of the Verde Formation of Late Cenozoic age, north-central Arizona, *in* *Geology of Northern Arizona: Guidebook*, Rocky Mtn. Sec. Geol. Soc. Am. Meet., Flagstaff, Arizona, 611 p.
- Nations, J.D., Hevly, R.H., Blinn, D.W., and Landye, J.J., 1981, Paleontology, Paleoecology, and Depositional History of the Miocene-Pliocene Verde Formation, Yavapai County, Arizona., *Arizona Geological Society Digest*, v. 13, p. 133-149.
- Nations, J.D., Landye, J.J., and Hevly, R.H., 1982, Location and Chronology of Tertiary Sedimentary Deposits in Arizona: A Review, *in* Ingersoll, R.V. and Woodburne, M.O., eds., *Cenozoic Nonmarine Deposits of California and Arizona: Pacific Section, SEPM*, p. 122.
- Nesse, W.D., 1991, *Introduction to Optical Mineralogy*, 2<sup>nd</sup> ed.: New York, Oxford University Press, 335 p.

- Parsons, T., J. McCarthy, W.M. Kohler, C.J. Ammon, H.M. Benz, J.A. Hole, and E.E. Criley., 1996, Crustal structure of the Colorado Plateau, Arizona: Application of new long-offset seismic data analysis techniques, *J. Geophys. Res.*, v. 101, B5, 11,173-11,194.
- Pearthree, P.A., 1993, Geologic and Geomorphic Setting of the Verde River and Sullivan to Horseshoe Reservoir, Arizona Geological Survey, Open-File Report 93-4, 25 p.
- Ransome 1925, Basin and Range Structures at Jerome, Arizona, *Philosophical Transactions of the Royal Society of London*, v. 61, no. 1591, p. 659-660.
- Rehrig, W.A., and Heidrick, T.L., 1976, Regional tectonic stress during the Laramide and late-Tertiary intrusive periods, Basin and Range province, Arizona, *in* Wilt, J.C., and Jenney, J.P., eds., *Tectonic Digest: Arizona Geological Society Digest*, v. 10, p. 205-228.
- Rehrig, W.A., Shafiqullah, M., and Damon, P.E., 1980, Geochronology, Geology, and Listric Normal Faulting of the Vulture Mountains, Maricopa County, Arizona, *in*, Jenney, J.P., and Stone, C., eds., *Studies in Western Arizona: Arizona Geological Society Digest, Volume XII*, p. 89-110.
- Reynolds, S.J., 1988, A New Geologic Map of Arizona *in*, Jenney, J.P. and Reynolds, S.J., *Geologic Evolution of Arizona: Tucson, Arizona Geological Society Digest 17*, p. 863-866.
- Shafiqullah, M., Damon, P.E., Lynch, D.J., Reynolds, S.J., Rehrig, W.A., and Raymond, R.H., 1980, K-Ar Geochronology and Geologic History of Southwestern Arizona and Adjacent Areas, *in* Jenney, J.P., and Stone, C., eds., *Studies in Western Arizona: Arizona Geological Society Digest, Volume XII*, p. 201-260.
- Sheridan, M.F., 1984, Volcanic Landforms, *in* Smiley, T.L., Nations, J.D., Pewe, T.L., Schafer, J.P., eds., *Landscapes of Arizona: The Geological Story*, University Press of America, p. 79-109.
- Shoemaker, E.M., Squires, R.L., and Abrams, M.J., 1978, Bright Angel and Mesa Butte fault systems of northern Arizona, Cenozoic Tectonics and Regional Geophysics of the Western Cordillera, *in* Geological Society of America Memoirs, Smith, R.B., and Eaton, G.P., eds, no. 152, p. 341-367.
- Spencer, J.E. and Reynolds, S.J., 1986, Some Aspects of the middle Tertiary tectonics of Arizona and southeastern California, *in* Beatty, B., and Wilkinson, P.A.K., eds., *Frontiers in geology and ore deposits of Arizona and the Southwest: Arizona Geological Digest*, v. 16, p. 102-107.
- Spencer, J.E. and Reynolds, S.J., 1989., Middle Tertiary tectonics of Arizona and the

- Southwest, in Jenney, J.P., and Reynolds, S.J., eds., *Geological Evolution of Arizona: Arizona Geological Society Digest 17*, p. 539-555.
- Stewart, J.H., 1998, Regional characteristics, tilt domains, and extensional history of the late Cenozoic Basin and Range province, western North America, in *Faults, J.E., and Stewart, J.H., eds., Accommodation Zones and Transfer Zones: The Regional Segmentation of the Basin and Range Province: Boulder, Colorado, Geological Society of America Special Paper 323*, p.47- 74.
- Sumner, J.S., 1985, Crustal geology of Arizona as interpreted from magnetic, gravity, and geologic data, in *The Utility of Regional Gravity and Magnetic Anomaly Maps, Society of Exploration Geophysicists, Hinze, W.J. eds*, p. 164-180.
- Thompson, G.A., and Burke, D.B., 1974, Regional Geophysics of the Basin and Range Province, *Annual Review of Earth and Planetary Sciences*, v. 2, p. 213-238.
- Thompson, G.A., M.L. Zoback., 1979, Regional Geophysics of the Colorado Plateau, *Tectonophysics*, v. 61, p. 149-181.
- Twenter, F.R., and Metzger, D.G., 1963, Geology and Ground water in Verde Valley-the Mogollon Rim Region Arizona, *Geological Survey Bulletin 1177*, 132 p.
- Twiss, R.J. and Moores, E.M., 1992, *Structural Geology (Textbook)*, University of California at Davis, W.H. Freeman and Company, New York, 532 p.
- Warren, D.H., 1969, A Seismic-Refraction Survey of Crustal Structure in Central Arizona, *Geological Society of America Bulletin*, v. 80, p. 257-282.
- West, M., James, N., Baldrige, W.S., Wilson, D., Aster, R., Goa, W., and Grand, S., 2004, Crust and upper mantle shear wave structure of the southwest United States: Implications for rifting and support for high elevation, *J. of Geophys Res.*, 109, B03309, doi: 10.1029/2003JB002575.
- Wrucke, C.T., and Conway, C.M., 1987, *Geologic Map of the Mazatzal Wilderness and Contiguous Roadless Area, Gila, Maricopa, and Yavapai Counties, Arizona, United States Geological Survey, Open File Report 87-664*, 22 p., scale 1:48,000.
- Yardley, B.W.D, 1989, *An Introduction to Metamorphic Petrology*, Longman Group Limited., 248 p.
- Zoback, M.L., Anderson, R.E., and Thompson, G.A., 1981, Cainozoic evolution of the state of stress and style of tectonism of the Basin and Range Province of the western United States, *Philosophical Transactions of the Royal Society of London*, v. 300, no. 1454, p. 407-434.

Zoback, M.L. and Zoback, M.D., 1989, Tectonic stress field of the continental United States, *in* Pakiser, L.C., and Mooney, W.D., eds., Geophysical framework of the continental United States, Geological Society of America Memoir 172, p. 523-539.